Principles of the full-scale aerobic granular sludge process

van Dijk, E.J.H.

DOI
10.4233/uuid:132820aa-ec0e-40e5-92cf-9599a18579c0

Publication date
2022

Document Version
Final published version

Citation (APA)
van Dijk, E. J. H. (2022). *Principles of the full-scale aerobic granular sludge process*. [Dissertation (TU Delft), Delft University of Technology]. https://doi.org/10.4233/uuid:132820aa-ec0e-40e5-92cf-9599a18579c0

Important note
To cite this publication, please use the final published version (if applicable).
Please check the document version above.

Principles of the full-scale aerobic granular sludge process

Edward van Dijk

Principles of the full-scale aerobic granular sludge process

Principles of the full-scale aerobic granular sludge process

Proefschrift

ter verkrijging van de graad van doctor
aan de Technische Universiteit Delft,
op gezag van de Rector Magnificus prof. dr. ir. T.H.J.J. van der Hagen,
voorzitter van het College voor Promoties,
in het openbaar te verdedigen op vrijdag 11 november 2022 om 12:30 uur

door

Edward John Henrik VAN DIJK

Ingenieur Milieuhygiëne,
Landbouwuniversiteit Wageningen, Nederland,
geboren te Amersfoort, Nederland.

Dit proefschrift is goedgekeurd door de

promotor:	prof. dr. ir. M.C.M. van Loosdrecht
copromotor:	dr. ing. M. Pronk

Samenstelling promotiecommissie:

Rector Magnificus	voorzitter
prof. dr. ir. M.C.M. van Loosdrecht	Technische Universiteit Delft
dr. ing. M. Pronk	Technische Universiteit Delft
Onafhankelijke leden:	
prof. dr. ir. M.K. de Kreuk	Technische Universiteit Delft
prof. dr. E. Morgenroth	ETH Zürich
prof. dr. ir. C. Picioreanu	KAUST
prof. dr. A. Soares	Cranfield University
dr. ir. C. Haringa	Technische Universiteit Delft
prof. dr. D. Brdjanovic	Technische Universiteit Delft (reservelid)

Keywords:	aerobic granular sludge, mechanisms, settling, nitrous oxide, suspended solids, mathematical model, granulation
Printed by:	Proefschriftspecialist
Front & Back:	Photograph of the Prototype Nereda® in Utrecht, by Edward van Dijk

ISBN 978-94-6366-601-5

An electronic version of this dissertation is available at
https://repository.tudelft.nl/.

If you can't explain it to a six year old,
you don't understand it yourself

Albert Einstein

Contents

Summary

In this dissertation several principles of full-scale Aerobic Granular Sludge (AGS) were explored. In chapter 2 the main processes contributing to elevated effluent suspended solids in the full-scale aerobic granular sludge process were explored. The two most important processes were (1) rising of sludge due to degasification of nitrogen gas (produced by denitrification) and (2) wash-out of particles that intrinsically do not settle such as certain fats and foams. A mathematical model was made to describe the process of degasification of nitrogen gas during the feeding phase in an AGS reactor. The process of rising sludge due to degasification could be limited by stripping out the nitrogen gas before starting the settling phase in the process cycle. The wash-out of scum particles could be reduced by introducing a vertical scum baffle in front of the effluent weir, similar to weirs in traditional clarifiers. The Prototype Nereda® Utrecht was operated with a nitrogen stripping phase and scum baffles for 9 months at an average biomass concentration of $10\,g\,L^{-1}$ and an average granulation grade of 84 %. In this period the influent suspended solids concentration was $230 \pm 118\,mg\,L^{-1}$, while the concentration of effluent suspended solids was $7.8 \pm 3.8\,mg\,L^{-1}$.

In chapter 3 the settling behaviour of AGS is discussed. The settling behaviour of AGS in full-scale reactors is different from the settling of flocculent activated sludge. Current activated sludge models lack the features to describe the segregation of granules based on size during the settling process. This segregation plays an important role in the granulation process, and therefore, a better understanding of the settling is essential. The goal of this study was to model and evaluate the segregation of different granule sizes during settling and feeding in full-scale aerobic granular sludge reactors. For this, the Patwardhan and Tien model was used. This model is an adaption of the Richardson and Zaki model, allowing for multiple classes of particles. To create the granular settling model, relevant parameters were identified using aerobic granular sludge from different full-scale Nereda® reactors. The settling properties of individual granules were measured, as was the bulk behaviour of granular sludge beds with uniform granular sludge particles. The obtained parameters were integrated in a model containing multiple granule classes, which was then validated for granular sludge settling in a full-scale Nereda® reactor. In practice a hydraulic selection pressure is used to select for granular sludge. Under the same hydraulic selection pressure, the model predicted that different stable granular size distributions can occur. This indicates that granular size distribution control would need a different mechanism then the hydraulic selection pressure alone. This model can be used to better understand and optimize operational parameters of AGS reactors that depend on granular sludge size, like biological nutrient removal. Furthermore, insights from this model can also be used in the development of continuously fed AGS systems.

Chapter 4 presents insights on nitrous oxide emissions from AGS. The nitrous oxides emission was measured over 7 months in the full-scale aerobic granular sludge plant in Dinxperlo, the Netherlands. Nitrous oxide concentrations were measured in the bulk liquid and the off-gas of the Nereda® reactor. Combined with the batch wise operation of the reactor, this gave a high information density and a better insight into nitrous oxide emission in general. The average emission factor was 0.33 % based on the total nitrogen concentration in the influent. The yearly average emission factor was estimated to be between 0.25 % and 0.30 % of the nitrogen load. The average emission factor is comparable to continuous activated sludge plants, and it is low compared to other sequencing batch systems. The variability in the emission factor increased when the reactor temperature was below 14 °C, showing higher emission factors during the winter period. A change in the process control in the winter period reduced the variability, reducing the emission factors to a level comparable to the summer period. Different process control might be necessary at high and low temperatures to obtain a consistently low nitrous oxide emission. Rainy weather conditions lowered the emission factor, both in the rainy weather batches and the subsequent dry weather flow batches. This was attributed to the first flush from the sewer at the start of rainy weather conditions, resulting in a temporarily increased sludge loading.

In chapter 5 a mathematical framework is presented to describe aerobic granulation based on 6 main mechanisms: microbial selection, selective wasting, maximizing transport of substrate into the biofilm, selective feeding, substrate type and breakage. A numerical model was developed using four main components; a 1D convection/dispersion model to describe the flow dynamics in a reactor, a reaction/diffusion model describing the essential conversions for granule growth, a setting model to track granules during settling and feeding, and a population model containing up to 100.000 clusters of granules to model the stochastic behaviour of the granulation process. With this approach the model can explain the dynamics of the granulation process observed in practice. This includes the presence of a lag phase and a granulation phase. Selective feeding was identified as an important mechanism that was not yet reported in literature. When aerobic granules are grown from activated sludge flocs, a lag phase occurs, in which few granules are formed, followed by a granulation phase in which granules rapidly appear. The ratio of granule forming to non-granule forming substrate together with the feast/famine ratio determine if the transition from the lag phase to the granulation phase is successful. The efficiency of selective wasting and selective feeding both determine the rate of this transition. Breakup of large granules into smaller well settling particles was shown to be an important source of new granules. The granulation process was found to be the combined result of all 6 mechanisms and if conditions for one are not optimal, other mechanisms can, to some extent, compensate. This model provides a theoretical framework to analyse the different relevant mechanisms for aerobic granular sludge formation and can form the basis for a comprehensive model that includes detailed nutrient removal aspects.

This dissertation is finalized in chapter 6 with an outlook on future developments in AGS technology.

Samenvatting

In dit proefschrift zijn diverse eigenschappen van full-scale aeroob korrelslib (AGS) onderzocht. Hoofdstuk 2 gaat over de processen die leiden tot verhoogde zwevende concentraties in het effluent van het aeroob korrelslibproces. De hoofdoorzaken zijn (1) opdrijven van slib door stikstofgasproductie (door denitrificatie) en (2) uitspoeling van drijvende deeltjes, zoals schuim en bepaalde vetten. Ontgassing van stikstofgas tijdens de voedingsfase is beschreven met een wiskundig model. Opdrijven van slib door ontgassing kan worden beperkt door het stikstofgas voor de bezinkingsfase uit het water te strippen. Uitspoeling van drijvend materiaal kan worden verminderd door plaatsing van een verticaal duikschot voor de effluentgoot, vergelijkbaar met duikschotten in traditionele bezinktanks. Beide maatregelen zijn gedurende 9 maanden getest in het Prototype Nereda® Utrecht, bij een gemiddelde biomassaconcentratie van $10\,g\,L^{-1}$ en een gemiddeld korrelgehalte van 84 %. In deze periode was de zwevende stof concentratie in het influent $230 \pm 118\,mg\,L^{-1}$ en de zwevende stof concentratie in het effluent $7.8 \pm 3.8\,mg\,L^{-1}$.

Hoofdstuk 3 gaat over bezinking van aeroob korrelslib. Het bezinkgedrag van aeroob korrelslib verschilt van normaal actief slib. De huidige actiefslib modellen kunnen de segregatie van korrels op basis van grootte tijdens het bezinkingsproces niet goed beschrijven. Deze segregatie speelt een belangrijke rol in het korrelvormingsproces en daarom is een beter begrip van de bezinking essentieel. Het doel van deze studie was het modelleren en evalueren van de bezinking van verschillende korrelgroottes tijdens bezinken en voeden in full-scale AGS-reactoren. Hiervoor werd het Patwardhan en Tien model gebruikt. Dit model is een aanpassing van het Richardson en Zaki-model, waardoor gebruik van meerdere deeltjesklassen mogelijk is. Voor de bouw van het model werden de meest relevante parameters geïdentificeerd met behulp van aeroob korrelslib van verschillende full-scale Nereda®-reactoren. De bezinkingseigenschappen van afzonderlijke korrels werden gemeten, evenals het bezinkgedrag van een korrelbed met uniforme korrelslibdeeltjes. De verkregen parameters werden gecombineerd in een model met meerdere deeltjesklassen, dat vervolgens werd gevalideerd door een experiment in een full-scale Nereda®-reactor. In de praktijk wordt een hydraulische selectiedruk gebruikt voor selectieve spui van korrelslib. Het model voorspelt dat verschillende stabiele korrelgrootteverdelingen kunnen optreden bij een gelijke selectiedruk. Hieruit blijkt dat voor de sturing van de korrelgrootteverdeling hydraulische selectiedruk alleen niet voldoende is. Het model kan gebruikt worden om operationele parameters van AGS-reactoren, die beïnvloed worden door de korrelgrootteverdeling, beter te begrijpen en te optimaliseren. Denk bijvoorbeeld aan biologische nutriëntenverwijdering. Verder kunnen inzichten uit dit model gebruikt worden bij de ontwikkeling van continu gevoede AGS-systemen.

Hoofdstuk 4 draait om lachgasemissies vanuit het AGS-proces. Deze emissie is

over een periode van 7 maanden gemeten in de Nereda® installatie in Dinxperlo. Lachgas werd gemeten in de waterfase en in het afgas van de Nereda®-reactor. Door de batchgewijze werking van de reactor werd veel informatie verkregen, alsook een beter inzicht in de lachgasemissie in het algemeen. De gemiddelde emissiefactor was 0.33 % (als fractie van de totale stikstofconcentratie in het influent). De jaargemiddelde emissiefactor ligt naar schatting tussen 0.25 % en 0.30 %. De gemiddelde emissiefactor was vergelijkbaar met conventionele actiefslibinstallaties, en is laag in vergelijking met andere SBR-systemen. Bij een reactortemperatuur lager dan 14 °C nam de variabiliteit van de emissiefactor toe, resulterend in hogere emissiefactoren tijdens de winterperiode. Een wijziging in de procesregeling tijdens de winterperiode verminderde de variabiliteit, waardoor de emissiefactoren werden teruggebracht tot een niveau vergelijkbaar met de zomerperiode. Mogelijk zijn verschillende procesregelingen nodig bij hoge en lage temperaturen voor een constant lage lachgasemissie. Regenweer verlaagde de emissiefactor, ook in batches die volgden op de regenweergebeurtenis. Dit wordt toegeschreven aan de first-flush uit het riool bij het begin van de neerslaggebeurtenis, wat leidt tot een tijdelijke verhoging van de slibbelasting.

In hoofdstuk 5 worden de mechanismen voor aerobe korrelvorming onderzocht. In dit hoofdstuk wordt een wiskundig raamwerk gepresenteerd om aerobe korrelvorming te beschrijven op basis van 6 hoofdmechanismen: microbiële selectie, selectieve spui, maximalisatie van transport van substraat de biofilm in, selectieve voeding, substraattype en opbreken van korrels. Het model bestaat uit vier hoofdcomponenten: een 1D convectie/dispersiemodel om de stroming in een reactor te beschrijven, een reactie/diffusiemodel dat de belangrijkste conversies voor korrelgroei beschrijft, een bezinkmodel om korrels te volgen tijdens bezinking en voeding, en een populatiemodel met tot wel 100.000 korrelclusters om het stochastische gedrag van het granulatieproces te modelleren. Met deze benadering kan het model de dynamiek van het granulatieproces, zoals we dit zien in de praktijk, verklaren. Selectieve voeding werd geïdentificeerd als een belangrijk mechanisme dat nog niet in de literatuur is beschreven. De groei van aerobe korrels uit actiefslibvlokken begint met een opstartfase, waarin schijnbaar weinig korrels worden gevormd. Deze fase wordt gevolgd door een granulatiefase waarin snel korrels verschijnen. De verhouding tussen korrelvormend en niet-korrelvormend substraat samen met de feast/famine ratio bepaalt of de overgang van de opstartfase naar de granulatiefase plaatsvindt. De spui-efficiëntie en selectieve voeding bepalen de snelheid van deze overgang. Het opbreken van grote korrels tot kleinere goed bezinkende deeltjes bleek een belangrijke bron voor nieuwe korrels. Het granulatieproces blijkt een gecombineerd resultaat van alle 6 mechanismen te zijn. Als de omstandigheden voor een van de mechanismen niet optimaal zijn, kunnen andere mechanismen hier tot op zekere hoogte voor compenseren. Het model biedt een theoretisch kader om de verschillende relevante mechanismen voor aerobe korrelvorming te analyseren en kan de basis vormen voor een meeromvattend model met meer gedetailleerde aspecten zoals van nutriëntverwijdering. Deze dissertatie wordt afgesloten in hoofdstuk 6 met een blik op toekomstige ontwikkelingen in AGS-technologie.

An unexpected journey

This story starts in the year 2012. I had been working in the hydraulics department of DHV for 13 years, I had done some really nice projects, had been a project leader, and had decided I would never want to be a boss or do project management. I basically had no specific plans for the rest of my career. I found myself in a meeting with Paul Janssen, who at the time was head of the process engineers, talking about an offer for the Dutch foundation for water education. The idea was to build a "flight simulator" for wastewater treatment plants - in the modern era we would call that a digital twin - and since I had already built something similar for the drinking water industry, we were discussing how to approach this proposal. The simulator was meant as a training tool in the HTAZ course. While working on the proposal, Paul told me that this course was actually mandatory for people in his department. He added that if I would follow this course, it would mean a possible ticket for me into his department. I was not completely sure if I was offended - I graduated from the Wageningen University as a wastewater engineer - or grateful for the opportunity given. I decided on the latter.

This course was given by water professionals from both Dutch water authorities and consultancy companies. One of the teachers was my colleague Helle van der Roest. His enthusiasm and endless energy made him an excellent teacher and I enjoyed his teachings. I graduated top of the class and, more importantly, impressed Helle. So, at the graduation party he asked me to join the "Nereda core team", a new team he was building with five or six experts from within the company to accelerate the Nereda® development. I had been involved in the development of Nereda® from the sideline from about 2006, since scale-up of the new technology was for some part a hydraulic question and I was in the hydraulics department. I had already been involved with measuring settling characteristics of the aerobic granular sludge in pilot reactors and the hydraulic design of the first full-scale reactor in Epe. But that did not make me a logical choice for this team, at least in my opinion, but Helle thought differently. So, I dropped all my projects and joined the team.

In the first year Helle continued his role as a teacher, and I learned a great deal on aerobic granular sludge. Slowly my role in the team started to change, while I was searching for the fundamentals of this new technology. The first version of the granulation model - which can be found in chapter 5 of this dissertation - was born early 2014. In this year I met Mario Pronk, who was finalizing his PhD research on aerobic granular sludge. We found that we think alike and immediately started working together, both being explorers of new knowledge. While I was diving more and more into research, the inevitable question started to pop up: why not start your own PhD research. For almost two years my standard answer was: I am busy as it is, I already have a job. Meanwhile I had started to go to the university one day

per week. DHV had become Royal HaskoningDHV and the new management had decided we would not have our own desk anymore, so I thought it was a good idea to partially move to the university. I was going there more often anyhow, because I was supervising some students doing their master thesis and I was having regular meetings at the university. Mario started to be more and more convincing about starting my own PhD research...

In November 2016 there was a formal state visit by the Belgian government to the Netherlands. In the signing ceremony we would sign a collaboration agreement between Ghent University, TU Delft and Royal HaskoningDHV. I was carpooling with René Noppeney - at that time the director responsible for Nereda® - and I told him about this idea of starting my PhD research. He was really enthusiastic and supportive about the idea. So, the next day I planned a meeting with Mark van Loosdrecht to discuss the possibilities.

It took about half a year to sort out all the contractual issues and in May 2017 I finally started my research. The idea was I would spend 1 day per week on the PhD research and for the rest I would continue my job as a researcher at RHDHV. That basically meant not much changed for me, because I had already been going to Delft once a week for more than a year and my job was already about research full-time. The challenge was in finding topics suitable for publication. My main topic was rather vague, because I had a long list of Nereda® related research topics I was working on and there was not much consistency in that list. So, in the beginning I always answered "Nereda" when people asked what my topic was, which most of the time led to a somewhat uncertain "OK". Later I changed it into "scale-up of AGS technology", which apparently was a much more acceptable research topic, although in reality it also did not quite cover it.

In the first year I discovered a few things about myself and the organization I was working for. I was very happy with my role as a PhD researcher. In retrospect that was primarily because I was intellectually challenged by the people in Environmental Biotechnology - the group of Mark van Loosdrecht. Not only Mark, but also my room mates Viktor, Jure and Morez played an important role in that. I also found that I had been quite naive about how the company would deal with my PhD research. There was a clear conflict between the commercial interest of the company and my own ambition to play in the Champions League. I needed to carefully pick my topics to be able to publish them. In my first year the TU Delft also organized the IWA Biofilm conference, and I was asked by Merle de Kreuk to be one of the keynote speakers. I think that was the first time it really felt I was part of the Champions League...

After this first year I just continued. The research topics kept popping up and I think only a small part found its path into this dissertation. While I am writing this preface, I still have not decided on the title - I think that is inherent to the path I took. Still, I am very proud of this book and that I finalized this journey I started, contributing to the deeper understanding of aerobic granular sludge technology.

1

Introduction

There's still much to do;
still so much to learn.
Mr. La Forge - engage!

Captain Jean-Luc Picard

1

1.1. A brief history

Edward Ardern and William T. Lockett are widely recognized as the inventors of the activated sludge process [1]. Their discovery was that the retention of sludge in a reactor greatly improved the reaction rates in the nitrification process [2]. The set-up they used in their experiments was very similar to what we use today for research of Aerobic Granular Sludge (AGS). They would fill a bottle of 2.4 L, with biomass and influent. Then after aerating the bottle for multiple hours, the mixture was allowed to settle and the clear effluent was decanted. The biomass was retained in the bottle and fed the next batch of influent. They found that sludge retention was an important mechanism for *activating* the sludge. Looking back, they came surprisingly close to the invention of Aerobic Granular Sludge (AGS), but history tells us that it took more than 80 years for this fact to happen [3, 4]. The main reason for this might be the absence of automated valves that made the use of full-scale fill-and-draw batch systems almost impossible for many decades to come and for this reason the world moved towards continuous flow systems [1].

I will not try to cover the full history of aerobic granular sludge - others already did do a good job at this [5, 6]. But there are some key developments in wastewater treatment I need to address, that made the discovery of AGS possible. As the reader will notice, this dissertation is for a large part about the differences and similarities between conventional activated sludge and AGS. There are a few key mechanisms that are important for growing AGS, which are discussed in detail in chapter 5. One of the marker points in the history of *aerobic* granular sludge was the discovery of *anaerobic* granular sludge. In the early 1970's the Dutch sugar factor CSM worked together with the Landbouw Hogeschool Wageningen, to develop a compact solution for anaerobic treatment of wastewater from sugar beet processing. This led to the development of the Upflow Anaerobic Sludge Blanket reactor (UASB) [7]. In the decades after the discovery of anaerobic granular sludge the technology was rapidly adopted worldwide and new concepts like the Expanded Granular Sludge Bed and Internal Circulation reactors were introduced. Meanwhile the search for aerobic equivalents of these technologies started. First successes were made with biomass on carrier systems [8, 9]. In these biofilm suspended carrier systems similar physical properties were reached as we now know from AGS: terminal settling velocities of 50 $m\,h^{-1}$, volatile suspended solids of up to 40 $g\,L^{-1}$ and superficial velocities in the clarifier up to 30 $m\,h^{-1}$. In this same period researchers started to understand that the morphology of the aerobic biofilm resulted from a balance between biofilm loading rate and shear rate (or a balance between growth and detachment) [10]. Mathematical modelling also showed that a balance between substrate uptake rate and transport rate was necessary to form a smooth and stable biofilm [11]. If the substrate uptake rate is lower than the transport rate, this would lead to uniform bacterial growth throughout the biofilm, while the opposite case would lead to an unstable biofilm.

The first proof of concept of aerobic granulation was reported in 1998 [3, 4]. These granules were grown in an SBR with molasses as substrate and the SBR was operated completely aerobic, without an anaerobic feeding phase. Applying a selection pressure between 30 $m\,h^{-1}$ and 40 $m\,h^{-1}$ led to granules with an average

diameter of 2.35 mm and a terminal settling velocity of almost 40 m h^{-1}. Long term stability of the granules was found to be problematic, so further research was necessary. After this historic moment, the scientific world embraced the AGS technology and research really took off, as can be seen in figure 1.1, showing the increase of scientific publications on AGS over time.

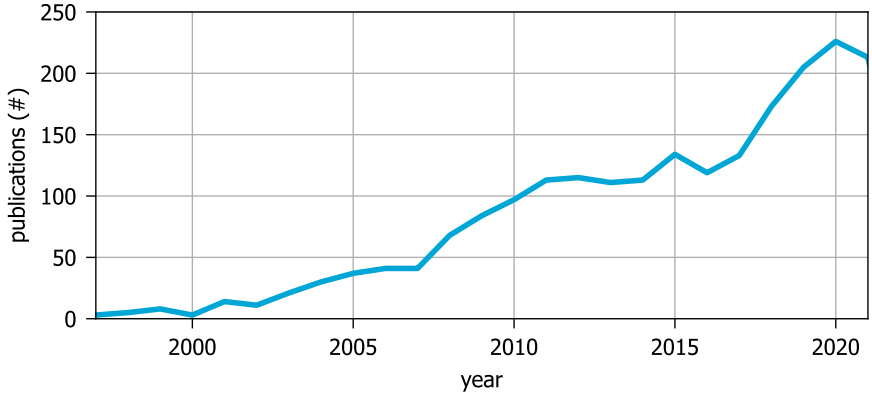

Figure 1.1: Yearly publications on aerobic granular sludge since the invention (1997-2021). Source data retrieved from https://www.scopus.com.

From research in the 2000's it was concluded that slower growing organisms will form granules more naturally than fast-growing organisms [12]. It was also recognized that the conversion of rapidly biodegradable substrates into slowly biodegradable stored substrates by applying an anaerobic feeding phase and an aerobic famine phase, greatly improved the granule stability and removed the need for high shear forces [13]. The feast and famine regime resulted in microbial selection of organisms capable of storing acetate as PHA, such as Phosphorus Accumulating Organisms (PAO) and Glycogen Accumulating Organisms (GAO). This approach effectively made the split between the transport of substrate into the biofilm and the growth of the biofilm, introducing a perfect balance between these two mechanisms. This step made the technology ready for adoption by the industry and shortly after this, in 2005 the first full scale application was built: a 250 m^3 d^{-1} Nereda® reactor at the Vika cheese factory in Ede, The Netherlands [14]. After this first market introduction, gradually more full-scale installations were built (see also the next section).

1

1.2. Benefits of AGS

So, what are the advantages of AGS over conventional activated sludge flocs? For a large part, AGS is similar to activated sludge. One can find the same species in an aerobic granule as in an activated sludge floc [15], although maybe in different ratios. Also, the species distribution is different in different granules sizes. It was shown by Ali *et al.* that for example, *Ca.* Accumulibacter phosphatis is more enriched in the largest granule sizes. This is to be expected because the current AGS reactors are fed from the bottom of the reactor, favouring the largest granule fraction with readily biodegradable substrates (see chapter 5), used by PAOs. Because of the similarities between granules and flocs, many processes will be similar. There are three major differences that make the use of AGS advantageous:

1. The good settling properties of AGS
2. The dense biomass and related biofilm properties
3. The production of biopolymers with special properties

The *settling properties* of AGS are very different from the settling properties of conventional activated sludge flocs (chapter 3). Activated sludge flocs will settle bulk-like, meaning the sludge bed will behave very much like one coherent entity, while AGS will settle as discrete particles. This results in a distinct separation between the sludge phase (the granules) and the water phase (outside the granules). Individual granules can settle with settling velocities up to 100 m h^{-1}, but in a sludge bed the actual settling velocity is (much) lower because of interactions between the granules. Nevertheless, the settling properties of an AGS sludge bed are much better than the settling properties of a bed with activated sludge flocs. Superficial flow velocities in an AGS reactor can be 5-10 times higher than in a secondary clarifier. As a result, the process of liquid/solid separation through gravity induced settling is much faster with AGS than with activated sludge flocs. In Conventional Activated Sludge (CAS) installations liquid/solid separation is typically done in a separate tank (secondary clarifier), or a separate phase in the case of a conventional SBR (settling and decanting phase), consuming a lot of surface area. In AGS the liquid/solid separation is started in a short settling phase at the end of the cycle, but mainly takes place during the simultaneous feeding of influent and decanting of effluent. As a result, the liquid/solid separation will only add about 10 % to the AGS reactor volume.

Aerobic granules grow in *dense aggregates*, with a typical biomass concentration of 35 kg m^{-3} to 50 kg m^{-3}. Because of voidage between granules, a settled sludge bed can have a concentration of 25 kg m^{-3}. A typical biomass concentration in an AGS reactor is 8 kg m^{-3}, but values over 15 kg m^{-3} can be reached in practice. This means the biomass concentration often is not the limiting factor in the AGS process. For example, a temperature drop will not decrease the nitrification rates of an AGS reactor as much as in a CAS system [16], because of an abundance of nitrifiers in the biomass. The thickness of the biofilm also allows for anoxic conditions in the centre of the granule during aeration, making it possible to nitrify and to denitrify during aeration. Activated sludge flocs are fully penetrated with

oxygen much quicker, often making it necessary to build separate denitrification tanks. With AGS denitrification can for a large part take place simultaneously [16]. It is therefore often not necessary to apply a denitrification phase, which is the CAS equivalent of not building a denitrification tank.

Recourse recovery is an important aspect in wastewater treatment nowadays. It was found that the extracellular polymeric matrix of AGS (Kaumera) can be recovered to produce novel materials. Although in activated sludge flocs similar polymers can be found, the gel-forming properties of polymers found in AGS form an interesting new resource. Low end application of these polymers can be found in agriculture (plant growth stimulant), but also potential high-end application such as flame retardants and high strength composite materials are already produced in the lab [6]. Research showed that about 25 % of the organic biomass of AGS consists of these polymers and can be used for all sorts of applications [17, 18]. So in the near future, wasting of biomass of an AGS reactor becomes harvesting of biomass. And this future is already here. The first full-scale recovery unit was built in Zutphen and opened in 2019. Here a dedicated Nereda® plant is built, treating wastewater from a dairy industry, with the sole purpose to produce AGS for polymer extraction.

1.3. Nereda technology

In this dissertation I often used data and biomass from pilot-scale and full-scale Nereda® reactors. Nereda® is the brand name of the aerobic granular sludge technology developed by Royal HaskoningDHV, which is also the company I was working for during the PhD research. After the first successful introduction in the dairy industry in 2005, several other industrial applications followed, as well as the first small municipal wastewater treatment plants. The next marker point in the history of Nereda® was the start-up of the first full-scale municipal plant in Epe, the Netherlands. The opening of the Nereda® plant in Epe generated a lot of national and international publicity, accelerating Nereda® development. Two years later, in the period 2013-2014, another 4 Nereda® plants were constructed in the Netherlands: Garmerwolde, Vroomshoop, Dinxperlo and the Prototype Nereda Utrecht (PNU). The Garmerwolde plant was a breakthrough in size. With a design capacity of 140 000 p.e. it was larger than all previous Nereda® plants combined and the first one larger than 100 000 p.e.. The PNU later became the primary research facility for municipal wastewater based aerobic granular sludge research and many of the experiments described in this dissertation were performed at this location. From this time forward more and more Nereda® plants were built, spanning over all continents (except Antarctica) - see figure 1.2.

A Nereda® reactor is a Sequencing Batch Reactor (SBR), in contrast to conventional continuous flow-through reactors with flocculent activated sludge. A mathematician would say that the difference between a SBR system and a flow through system is that the dimensions are interchanged. In a flow-through system the different process conditions (anaerobic, anoxic and aerobic) are separated in space and (more or less) constant over time. In an SBR system the process conditions are separated in time, but are applied in the same reactor. This is shown

1

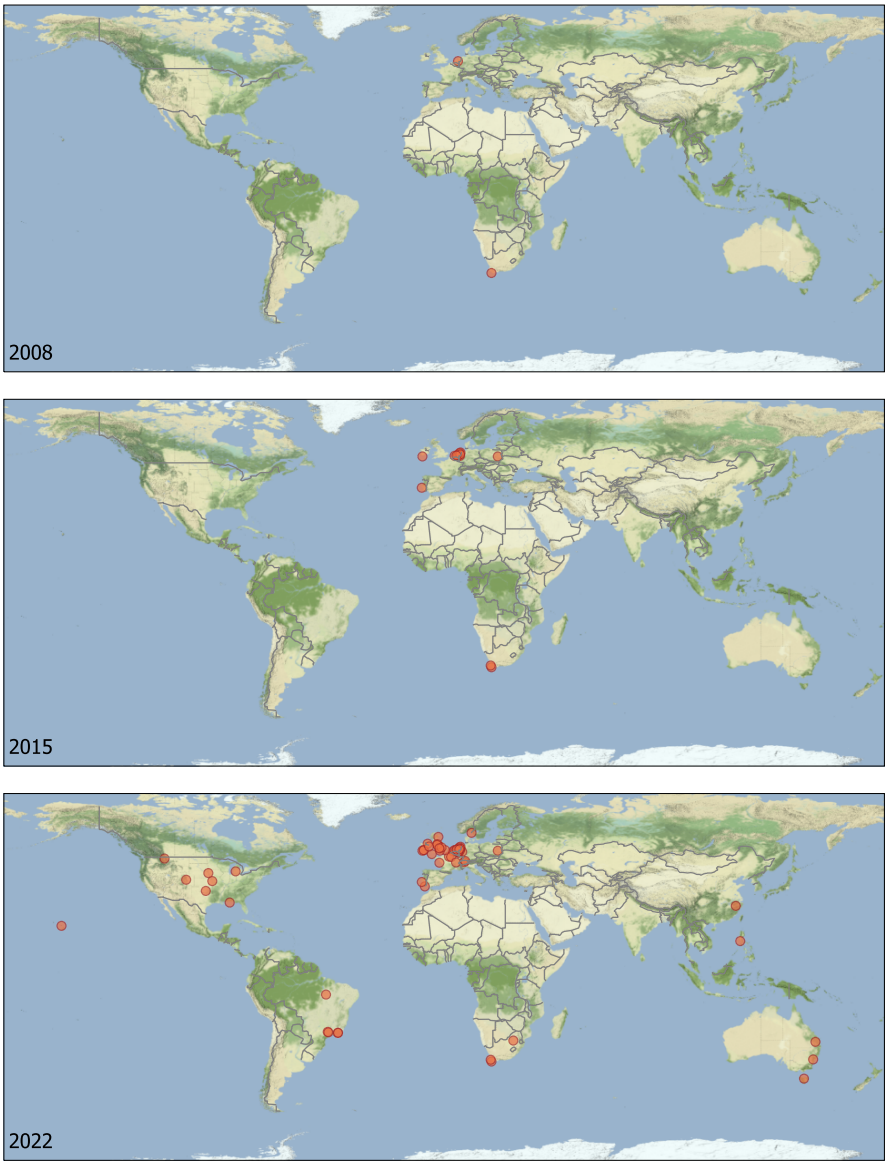

Figure 1.2: Full scale Nereda® plants over time; 6 in 2011 and 91 plants in operation or under construction in 2022.

in figure 1.3. Here the modified University of Capetown process (mUCT) process is compared with the Nereda® process. In the mUCT process biomass is recycled back to the anaerobic reactor, for fermentation and uptake of Volatile Fatty Acids (VFA) from the influent. In this anaerobic reactor, polyphosphate is degraded as an energy source for the uptake of VFAs. Then the biomass together with the influent, flows into the anoxic tanks for denitrification (and some phosphate uptake) and subsequently into the aerated reactors, for nitrification, phosphorus uptake and COD removal. Separation of the purified water and the biomass happens in the secondary clarifier. The thickened sludge is pumped back to the first anoxic tank. All of these process steps can be found in the Nereda® process. The anaerobic contact between biomass and influent happens when the reactor is fed from the bottom into the (settled) sludge bed. Because of the plug flow feeding, there is limited mixing of purified water from the previous batch and the influent, allowing for anaerobic conditions. After the feeding phase, the tank is aerated. The thickness of the granular biofilm allows for Simultaneous Nitrification and Denitrification (SND) and in many cases no separate anoxic phase is necessary. If necessary, a pre-denitrification or post-denitrification phase can be applied. The separation of the purified water and the granular sludge is done in the settling phase.

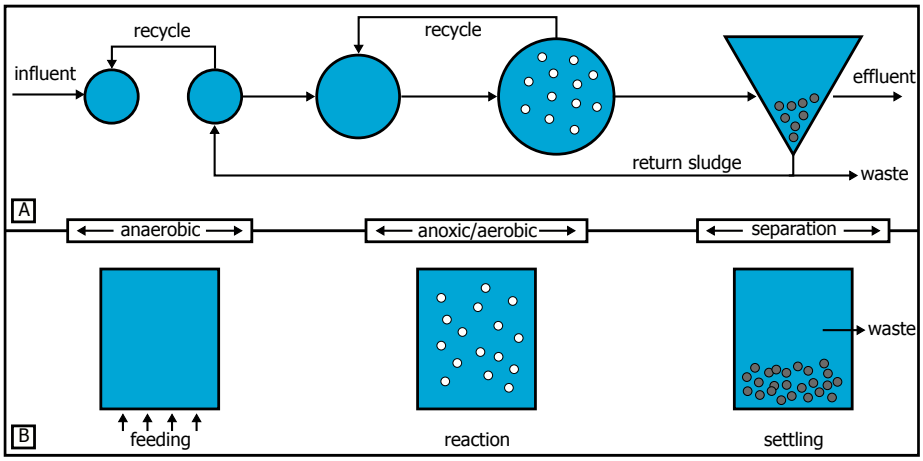

Figure 1.3: Comparison of a continuous flow-through system (A) with a sequencing batch system (B).

The Nereda cycle has three main phases, the feed and decant phase, the reaction phase and the settling and wasting phase. Feeding and settling happens simultaneous, as opposed to conventional SBR systems where feeding and decanting are separate phases. *Feeding and decanting* can be done simultaneously because of the advantageous settling behaviour of the AGS. At the superficial flow velocities applied in Nereda® (up to $5\,m\,h^{-1}$), conventional activated sludge would washout with the effluent. The settling properties of AGS (see chapter 3) allow for a good separation between biomass and purified water during the feeding phase. The plug flow feeding regime causes a limited contact between fresh influent and purified water from the previous batch, and at the same time ensures

good anaerobic contact between influent and the settled sludge bed. Readily biodegradable COD is taken up by the biomass, releasing phosphate in the process, because of the Enhanced Biological Phosphorus Removal (EBPR) process. In the *reaction phase*, aerobic and anoxic conversions take place. The reactor is aerated, and COD and ammonia are oxidized. Through the process of SND (part) of the nitrate formed is converted into nitrogen gas. Phosphorus is also removed because of the uptake of phosphate by the PAO. For extra nitrate reduction sometimes pre- or post-denitrification phases are added to the reaction phase. More advanced methods for optimizing SND are also available [19]. The *settling and wasting* phase often starts with a short period of aeration to strip dissolved nitrogen gas from the water phase (chapter 2). This aeration also mixes the biomass in the reactor. After a short settling period (depending on the applied selection pressure), the top of the sludge bed is wasted. Only the top of the sludge bed is wasted, allowing for selectively discharging flocs and other bad settling sludge from the sludge bed (see also chapter 5). After this the cycle starts over with simultaneous feeding and decanting.

Most Nereda® plants have 2 or more reactors. This is because most plants must take in wastewater continuously. In the reaction phase, and the settling and wasting phase, a reactor cannot receive influent. To overcome this problem, multiple reactors can be scheduled is such a way, that 1 reactor is always available to receive influent. This method of scheduling relates the feeding time to the number of reactors and the time available for reaction and settling. With only 2 reactors the feeding time will become equal to the time for reaction and settling, making the reactors relatively inefficient. With 3 or more reactors this is less of a problem. A solution for this inefficiency is application of an influent buffer. This allows for an interruption of the continuous feeding and an efficient reactor scheduling, also with 1 or 2 reactors available [6]. Under Dry Weather Flow (DWF) a different scheduling is used than under Rainy Weather Flow (RWF). Under dry weather conditions the scheduling is defined by the conversion rates, while under rain weather conditions the hydraulics (maximum batch size and up-flow velocity) determine the phase times. An example of different scheduling between DWF and RWF is shown in figure 1.4.

1.4. Nereda plants used in this research

In this dissertation measurements have been done on different locations, with sludge from multiple Nereda® reactors (see table 1.1).

The Nereda® in Garmerwolde is a municipal wastewater treatment plant, owned by the Dutch district water authority Noorderzijlvest and is operated since 2013. It consists of 2 Nereda® reactors and an influent buffer and it has a design capacity of 140 000 p.e..

Utrecht has two Nereda® plants, the full-scale of Utrecht and the PNU. The full-scale installation is a municipal wastewater treatment plant, owned by the Dutch district water authority Hoogheemraadschap de Stichtse Rijnlanden (HDSR) and it is operated since 2018. It has a design capacity of 430 000 p.e. and it consists of 6 Nereda® reactors and an influent buffer, each of 12 000 m^3.

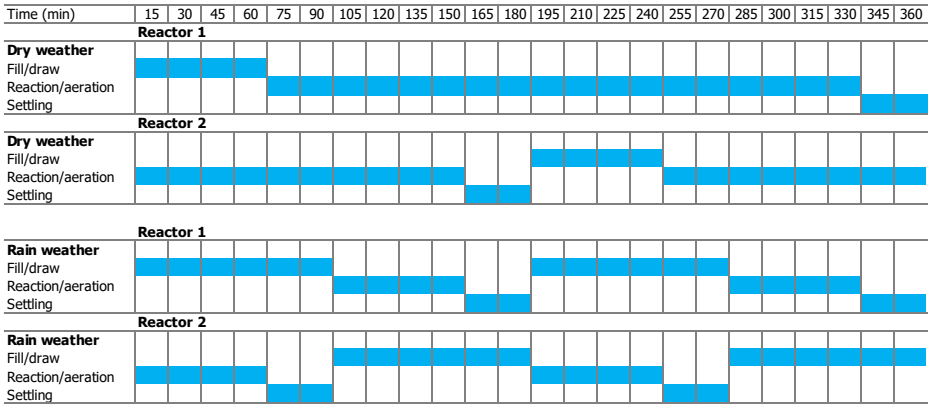

Figure 1.4: Example of a cycle of a Nereda® plant with an influent buffer for storage of influent between feeding phases during DWF. Continuous feed during RWF conditions.

The Prototype Nereda® Utrecht is a municipal wastewater treatment plant, owned by the Dutch district water authority HDSR and it is operated since 2013. It consists of 1 Nereda® reactor of 1000 m^3 and is operated at variable sludge loading rates. Since 2016 it is used as a facility for full-scale AGS research by Royal HaskoningDHV (RHDHV).

The Nereda® plant in Dinxperlo has 3 reactors and a small influent buffer. It is owned by the Dutch district water authority Waterschap Rijn en IJssel. The plant was designed for 15 730 p.e..

In Vroomshoop the first hybrid Nereda® reactor was build. It is owned by the Dutch district water authority Waterschap Vechtstromen and it is in operation since 2013. In the hybrid concept, AGS waste sludge is spilled into the nearby CAS plant. This is done to improve the sludge characteristics of the CAS system. The Nereda® plant in Vroomshoop consists of 1 reactor and an influent buffer.

The Nereda® plant in Epe was the first full-scale municipal AGS plant in the Netherlands. It is owned by the Dutch district water authority Waterschap Vallei en Veluwe and it is in operation since 2011. For the large part it receives domestic wastewater, but a considerable part of the influent comes also from slaughterhouses.

Table 1.1: Overview of plants used in this dissertation.

plant	geohash	volume m^3	capacity p.e.	water authority
Prototype Nereda Utrecht	u178kq8	1000	-	De Stichtse Rijnlanden
Nereda Utrecht	u178knt	6 x 12 000	430 000	De Stichtse Rijnlanden
Nereda Garmerwolde	u1kwzvt	2 x 9500	140 000	Noorderzijlvest
Nereda Vroomshoop	u1kdm7s	1340	22 600	Vechtstromen
Nereda Dinxperlo	u1hwgpz	3 x 1250	15 730	Rijn en IJssel
Nereda Epe	u1k3b88	3 x 4500	53 500	Vallei en Veluwe

1.5. About this dissertation

Aerobic granular sludge technology is becoming a widely accepted technology for wastewater treatment. Although it is widely accepted and soon the 100th full-scale treatment plant will be built, there are still many discoveries to be made. Mechanisms and fundamentals that are common ground for flocculent activated sludge are still undiscovered lands for aerobic granular sludge. In this dissertation I aimed to fill in a few of the important knowledge gaps we face in design and operation of AGS technology.

In chapter 2 the topic of effluent suspended solids was explored. In the first 15 years of AGS development the amount of suspended solids in the effluent of AGS reactors received little attention. This is mainly because the process conditions and the hydraulics of lab scale reactors are very different from full-scale reactors and lab reactors are mainly designed for optimal biological conditions. In the first full-scale installations effluent suspended solids were not a topic, because it concerned industrial installations discharging effluent to the sewer. The first full-scale domestic AGS plant in the Netherlands was Epe, which due to discharge to a small river needed post-treatment (sand filtration) of the full flow, to remove all solids from the Nereda® effluent. Only when more full-scale installations were built did it become clear that the concentration of effluent suspended solids could become too high. It was shown that degasification of nitrogen gas and wash-out of bad settling particles were the major source for these elevated concentrations and it could be solved relatively easily. In this chapter the mechanisms behind the degasification of nitrogen gas were explored. It was shown that effluent suspended solid concentrations comparable with CAS could be achieved with an AGS reactor.

In chapter 3 the settling behaviour of AGS was explored. As described above, the advantageous settling characteristics of AGS are a fundamental part of the technology. In previous research it was shown that individual granules can settle very fast, but in practice it is not about individual granules, but about the behaviour of the sludge bed, with interactions between trillions of individual granules. The settling behaviour of activated sludge is well described with widely accepted mathematical models. These models generally describe the behaviour of the sludge bed based on 1 sludge phase and a bed going through regimes of particulate settling, zone settling and compression. In AGS the particle coherence is much more discrete, demanding a different mathematical approach to describe the settling behaviour. In this chapter this different approach was combined with validation based on full-scale measurements.

Nitrous oxide is a gas commonly emitted from wastewater treatment plants, as a side product from nitrogen removal. Since nitrous oxide is a strong greenhouse gas, emission from wastewater treatment plants contributes to global warming. A long-term measurement campaign was performed in a Nereda® reactor at the wastewater treatment plant in Dinxperlo. In chapter 4, the dynamics of nitrous oxide emissions are explored.

How do aerobic granules grow? That is the question asked in chapter 5. After more than 20 years of research we know how to grow granules, but we lack an in depth understanding of how they grow. In this chapter we proposed 6 fundamental

mechanisms leading to growth of aerobic granular sludge. A mathematical model was made to show the importance of the different mechanisms.

Where do we go from here? The journey of AGS is only starting. We will explore the future in chapter 6.

1

Bibliography

[1] D. Jenkins and J. Wanner, *Activated Sludge – 100 Years and Counting,* (2014).

[2] E. Adern and W. T. Lockett, *The oxidation of sewage without the aid of filters,* J. Soc. Chem. Ind. **33**, 523 (1914).

[3] E. Morgenroth, T. Sherden, M. C. M. van Loosdrecht, J. J. Heijnen, and P. A. Wilderer, *Aerobic granular sludge in a sequencing batch reactor,* Water Res. **31**, 3191 (1997).

[4] J. J. Heijnen and M. C. M. van Loosdrecht, *Method for acquiring grain-shaped growth of a microorganism in a reactor,* (1998).

[5] M. Pronk, *Aerobic Granular Sludge - Effect of Substrate on Granule Formation*, Ph.D. thesis, TU Delft (2016).

[6] M. Pronk, E. J. H. van Dijk, and M. C. M. van Loosdrecht, *Aerobic granular sludge,* in *Biol. Wastewater Treat. Princ. Model. Des.*, edited by G. Chen, G. A. Ekama, M. C. M. van Loosdrecht, and D. Brdjanovic (IWA Publishing, 2020) Chap. 11, pp. 497–516.

[7] G. Lettinga, A. G. N. Jansen, and P. Terpstra, *Anaerobe zuivering van bietsuikerafvalwater,* H2O , 530 (1975).

[8] J. J. Heijnen, A. Mulder, R. Weltevrede, P. H. Hols, and H. L. J. M. van Leeuwen, *Large-scale anaerobic/aerobic treatment of complex industrial wastewater using immobilized biomass in fluidized bed and air-lift suspension reactors,* Chem. Eng. Technol. **13**, 202 (1990).

[9] J. J. Heijnen, M. C. M. van Loosdrecht, R. Mulder, R. Weltevrede, and A. Mulder, *Development and scale-up of an aerobic biofilm air-lift suspension reactor,* Water Sci. Technol. **27**, 253 (1993).

[10] M. C. M. van Loosdrecht, D. Eikelboom, A. Gjaltema, A. Mulder, L. Tijhuis, and J. J. Heijnen, *Biofilm Structures,* Water Sci. Technol. **32**, 35 (1995).

[11] C. Picioreanu, M. C. M. van Loosdrecht, and J. J. Heijnen, *Mathematical modeling of biofilm structure with a hybrid differential- discrete cellular automaton approach,* Biotechnol. Bioeng. **58**, 101 (1998).

[12] A. M. P. Martins, J. J. Heijnen, and M. C. M. van Loosdrecht, *Bulking Sludge in Biological Nutrient Removal Systems,* Biotechnol. Bioeng. **86**, 125 (2004).

[13] M. K. de Kreuk and M. C. M. van Loosdrecht, *Selection of slow growing organisms as a means for improving aerobic granular sludge stability,* Water Sci. Technol. **49**, 9 (2004).

[14] A. Giesen, L. M. M. de Bruin, R. P. Niermans, and H. F. van der Roest, *Advancements in the application of aerobic granular biomass technology for sustainable treatment of wastewater,* Water Pract. Technol. **8**, 47 (2013).

[15] M. Ali, Z. Wang, K. W. Salam, A. R. Hari, M. Pronk, M. C. M. van Loosdrecht, and P. E. Saikaly, *Importance of species sorting and immigration on the bacterial assembly of different-sized aggregates in a full-scale Aerobic granular sludge plant,* Environ. Sci. Technol. **53**, 8291 (2019).

[16] M. K. de Kreuk, M. Pronk, and M. C. M. van Loosdrecht, *Formation of aerobic granules and conversion processes in an aerobic granular sludge reactor at moderate and low temperatures,* Water Res. **39**, 4476 (2005).

[17] M. Pronk, A. Giesen, A. Thompson, S. Robertson, and M. C. M. van Loosdrecht, *Aerobic granular biomass technology: advancements in design, applications and further developments,* Water Pract. Technol. **12**, 987 (2017).

[18] N. K. Kim, N. Mao, R. Lin, D. Bhattacharyya, M. C. M. van Loosdrecht, and Y. M. Lin, *Flame retardant property of flax fabrics coated by extracellular polymeric substances recovered from both activated sludge and aerobic granular sludge,* Water Res. **170**, 115344 (2020).

[19] E. J. H. van Dijk, K. M. van Schagen, and A. T. Oosterhoff, *Controlled Simultaneous Nitrification and Denitrification in Wastewater Treatment,* (2020).

2

Effluent suspended solids

The main processes contributing to elevated effluent suspended solids in the full-scale aerobic granular sludge process were studied. The two most important processes were (1) rising of sludge due to degasification of nitrogen gas (produced by denitrification) and (2) wash-out of particles that intrinsically do not settle such as certain fats and foams. A mathematical model was made to describe the process of degasification of nitrogen gas during the feeding phase in an AGS reactor. The process of rising sludge due to degasification could be limited by stripping out the nitrogen gas before starting the settling phase in the process cycle. The wash-out of scum particles could be reduced by introducing a vertical scum baffle in front of the effluent weir, similar to weirs in traditional clarifiers. The Prototype Nereda Utrecht was operated with a nitrogen stripping phase and scum baffles for 9 months at an average biomass concentration of 10 g L^{-1} and an average granulation grade of 84%. In this period the influent suspended solids concentration was 230 $\pm$ 118 mg L^{-1}, while the concentration of effluent suspended solids was 7.8 $\pm$ 3.8 mg L^{-1}.

Parts of this chapter have been published in Water Research **147**, 50-59 (2018) [1].

2

2.1. Introduction

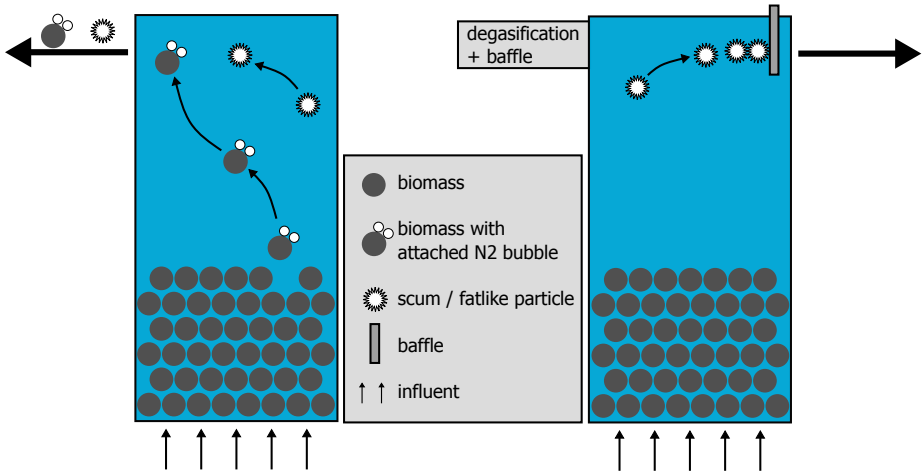

Figure 2.1: Graphical abstract.

If we look at the effluent quality of full-scale AGS reactors reported in literature, low effluent values for COD, total nitrogen and total phosphorus can be easily met, but average suspended solids effluent concentrations are relatively high with a range of 5 mg L^{-1} to 20 mg L^{-1} (see table 2.1).

Table 2.1: Reported effluent concentrations for different Nereda® plants.

Plant	COD mg L^{-1}	TN mg L^{-1}	NH_4^+-N mg L^{-1}	NO_3^+-N mg L^{-1}	TP mg L^{-1}	PO_4^{3-}-P mg L^{-1}	SS mg L^{-1}	Ref.
Epe			0.5	4		0.5	10-20	[2]
Dinxperlo			0.2	5		2	15-20	[2]
Gansbaai	40	<10	<1		3.2		<5	[3]
Garmerwolde	64	6.9	1.1		0.9	0.4	20	[4]
Ryki	45	5.60			0.85		13	[5]
Vroomshoop	55	7.2	1.4/3.0[1]	2.0	0.9	0.6	10	[5]

[1] summer/winter

Some reports indicate an increase in effluent suspended solids concentrations for AGS reactors with increasing granulation [6, 7]. In most laboratory studies the focus is on the granulation process and wasting of sludge for ease of operation is combined with decanting of the effluent [8]. As a result, biomass is present in the effluent of laboratory reactors. This poses no problem under laboratory conditions, but for the full-scale treatment of sewage the removal of suspended solids is an integral part of the purification process and is usually limited by law. Since hydraulics of laboratory and even pilot plant installations are not representative for full-scale conditions, effluent suspended solids can only effectively be studied at full-scale installations. In full-scale applications the effluent and sludge withdrawal are separated processes. This leads to relatively low suspended solids effluent

concentrations, certainly when compared to influent values [4]. Still, the reported average values of 5 mg L^{-1} to 20 mg L^{-1} are higher than usually reported for conventional activated sludge processes, which can be considerably lower than 10 mg L^{-1} [9].

Elevated levels of effluent suspended solids have been intensively studied over the last decades in conventional activated sludge systems. Commonly reported issues in these systems are bulking sludge and foam formation [10]. Another reported issue in secondary clarifiers is the rising of sludge due to denitrification [11]. Denitrification can lead to nitrogen bubble formation (degasification) if oversaturation of nitrogen gas in the liquid is reached. The bubbles attach to the sludge flocs which then rise towards the top of the clarifier and wash out with the effluent.

Sludge settling too fast, indicated by a low sludge volume index (SVI), is also reported to cause elevated levels of suspended solids in the effluent of conventional activated sludge systems, although this effect is doubted by others reporting a strong relation with the flocculator design [9, 12, 13]. Since reported SVI values for full-scale AGS reactors are generally low (35 mL g^{-1} to 70 mL g^{-1}) [2, 4] this might also be a potential cause of elevated levels of effluent suspended solids.

Besides a different sludge morphology and likely flocculation behaviour, current AGS plants according to the Nereda® concept deviate also in hydraulics from secondary settling tanks. Secondary clarifiers have typical superficial upflow velocities of 0.5 m h^{-1} to 1.0 m h^{-1}, while the complex flow in the clarifier is mainly caused by density currents [14]. For the Nereda® technology effluent results from pumping influent in the bottom of the granular bed. This generates an upward plug flow in the reactor with typical superficial velocities in the range of 2 m h^{-1} to 5 m h^{-1} through a granular bed with on top of that a layer of flocculent sludge. The relatively higher upflow velocities in Nereda® reactors might be responsible for the washout of floating sludge and fat-like particles. In contrast to conventional activated sludge systems, the mechanisms behind the formation and control of effluent suspended solids for full-scale aerobic granular sludge reactors are not yet fully understood.

The aim of this study was to evaluate the main processes leading to effluent suspended solids in full-scale AGS reactors, and investigate options to minimize effluent suspended solids. We focused on both removal of floating material and degasification of nitrogen gas. Full-scale experiments were performed in the PNU and a mathematical model was developed to describe the degasification of nitrogen gas during the operation of the aerobic granular sludge reactor.

2.2. Materials and methods

2.2.1. Description of the plant

Experiments were done in the Prototype Nereda Utrecht. The reactor has a footprint of 150 m^2 and a water depth of 7.00 m. The influent pumps have a total capacity of 900 m^3 h^{-1}. The influent is pumped directly from a main sewer line of the Overvecht district in Utrecht. The sewage consists mainly of domestic wastewater. Wastewater characteristics during this study are given in table 2.2. After screening by a 6 mm

perforated plate screen, the wastewater is directly pumped into the reactor. During the trial the reactor was operated at a MLSS concentration of 8 kg m^{-3} to 12 kg m^{-3}, a SVI5 of 34 mL g^{-1} to 57 mL g^{-1}, a SVI30 of 33 mL g^{-1} to 43 mL g^{-1}, a volumetric loading rate of 0.6 m^3 m^{-3} d^{-1} to 2.7 m^3 m^{-3} d^{-1} and an average sludge loading rate of 0.08 kg COD/kg MLSS/d. On average 84 % of the biomass present in the reactor was granulated during the experimental period (i.e. granule size larger than 0.2 mm). Average granule size distributions are shown in table 2.3. The reactor is equipped with two blowers each with a capacity of 400 m^3 h^{-1}. Air is supplied to the reactor using micro bubble diffusors evenly distributed on the floor of the tank.

Table 2.2: Influent characteristics of the PNU during the study.

Parameter	Average mg L^{-1}	Min mg L^{-1}	Max mg L^{-1}
COD	707.0	442.4	1007.5
N_{Kj}-N	64.0	35.0	81.7
NH_4^+-N	46.1	25.1	58.6
Total Phosphorus	8.9	5.3	11.8
PO_4^{3-}-P	5.6	3.2	8.2
Suspended solids	230.0	160.0	380.0

The reactor was operated with a normal Nereda® cycle as described in section 1.3. Process conditions were set to target full biological nitrogen and phosphorus removal. No possibilities for chemical dosing were present in the reactor. During the trial nitrogen removal was established by nitrification and denitrification.

The cycle time varied between 4 and 8 hours, with 1 hour of anaerobic feeding and simultaneous effluent withdrawal, a variable reaction phase and a phase for mixing, settling and decanting of sludge of 30 to 60 minutes.

The reaction phase was stopped when the set points, 2 mg L^{-1} and 3 mg L^{-1} for respectively ammonia and nitrate were reached. During the reaction phase the dissolved oxygen concentration was controlled in the range of 1.0 mg L^{-1} to 2.0 mg L^{-1}.

The plant is in operation since the 1st of April 2013. The reactor was started up without baffles in front of the overflow weir. On the 3rd of June 2015 vertical baffles were placed in front of the effluent weirs, to investigate the effect of scum baffles on the concentration of effluent suspended solids.

2.2.2. Online measurements

The reactor was equipped with probes for dissolved oxygen, redox potential, water level, temperature, turbidity, and nitrate. Ammonium and phosphate were continuously measured using a filter unit and auto sampling device (Hach Lange; Filtrax, Amtax and Phosphax). The filter unit was situated 0.5 meter below the water surface. Sampling was done at an interval of 5 minutes. A turbidity sensor (Hach Lange; Solitax) was present in the effluent gutter to observe the presence of suspended solids.

2.2.3. Sampling

Samples for analyses of influent and effluent were collected using refrigerated auto samplers, collecting flow proportional samples for both influent and effluent. Suspended solids concentrations of both influent and effluent were measured by filtering 1 L of sample with a glass fiber filter, which was dried at 105 °C until no weight change was measured.

Grab samples for Mixed Liquor Suspended Solids (MLSS) analyses were taken from the top of the reactor after at least 15 minutes of aeration at full capacity to ensure sufficiently mixed conditions.

2.2.4. Physical characteristics of the sludge

To determine the granule size distribution 1 L of sample was poured over a series of sieves with different mesh sizes (200 µm, 400 µm, 630 µm, 1000 µm and 2000 µm). These sieve fractions together with 100 mL of unsieved sludge were dried at 105 °C. The sludge volume index (SVI) was measured by pouring 1000 mL of mixed, undiluted sludge into a graduated measuring cylinder. The sludge volumes were measured after 5 and 30 minutes.

Table 2.3: Average granule size distribution of the sludge in the Prototype Nereda Utrecht.

sieve fraction µm	MLSS kg m^{-3}	granule fraction %
0 - 200	1.7	16 %
200 - 400	0.3	3 %
400 - 600	0.2	2 %
600 - 1000	0.4	4 %
1000 - 2000	3.2	31 %
>2000	4.6	44 %
Total	10.4	100 %

2.2.5. Microscopic analysis

A Leica Microsystems Ltd stereo zoom microscope (M205 FA) in combination with Leica Microsystems Qwin (V3.5.1) image analysis software was used to analyse the morphology of the sludge.

2.2.6. Modelling of N_2 stripping

A mathematical model was developed to calculate the concentrations of dissolved nitrogen gas in the reactor. The solubility of nitrogen gas in water, c_s, is dependent on the partial pressure of nitrogen gas in the gas phase, p, and is calculated using Henry's law:

$$c_s = M \cdot k_H \cdot p \tag{2.1}$$

Here k_H is the Henry's constant for the solubility of nitrogen gas in water and M is the molar mass of nitrogen gas. The Henry's constant is a decreasing function of temperature, meaning that the solubility of nitrogen gas in water decreases with an increasing temperature. The partial pressure of nitrogen in the gas phase is both

dependent on the gas fraction, f, and the pressure in the reactor, the latter being the sum of atmospheric pressure, p_{atm} and hydrostatic pressure:

$$p = f \cdot (p_{atm} + x \cdot \rho \cdot g) \tag{2.2}$$

Here x is the water depth, ρ is the mixture density and g is the gravitational acceleration.

The transfer of nitrogen gas between the air bubbles and the liquid is calculated by:

$$\frac{dc}{dt} = \alpha F \cdot (k_L a)_N \cdot (c_s - c) \tag{2.3}$$

Here c is the nitrogen gas concentration in the water phase, k_L is the mass transfer coefficient and a is the interfacial area of the gas bubbles. The subscripts O and N indicate the values for oxygen gas and nitrogen gas. The mass transfer rate is corrected for effects of wastewater contaminants, α, and fouling on the membrane aerators, F. The value of the product of k_L and a for oxygen transfer $(k_L a)_O$, is commonly measured during commissioning in full-scale wastewater treatment plants and depends on the temperature. For this study, a value of $(k_L a)_O$ including the effects of contaminants and fouling was used. For this, the values for α and F were set to 1.

This empirical value of $(k_L a)_O$ can be used to derive a value for nitrogen gas by using Higbie's penetration theory [15]. Based on this model the following relation between the $k_L a$ for oxygen gas and nitrogen gas and the diffusion coefficient for oxygen gas (D_O) and nitrogen gas (D_N) for can be derived:

$$\frac{(k_L a)_O}{(k_L a)_N} = \sqrt{\frac{D_O}{D_N}} \tag{2.4}$$

Both the diffusion coefficient and the Henry coefficient need to be corrected for temperature. For the diffusion coefficient this is based on the Stokes-Einstein equation [16]. In this equation the diffusion coefficient D is related to the temperature T and the dynamic viscosity μ_T:

$$D(T) = D_0 \frac{T}{T_0} \frac{\mu_0}{\mu_T} \tag{2.5}$$

The viscosity is also depending on temperature according to equation the Vogel-Fulcher-Tammann equation [17], in which parameters A, B and C are empirical parameters:

$$\mu(T) = \mathrm{e}^{A + \frac{B}{C+T}} \tag{2.6}$$

The Henry coefficient is corrected for temperature using the van 't Hoff equation [18], in which k_{H0} is the Henry coefficient at reference temperature, T_0 is the reference temperature and H_c is the temperature correction factor:

$$k_H\,(T) = k_{H0}\mathrm{e}^{-k_{Hc}(\frac{1}{T}-\frac{1}{T_0})} \tag{2.7}$$

The stripping of nitrogen gas is done by aeration of the reactor with fine bubble aeration. This leads to transport of dissolved nitrogen gas through the reactor. A simple axial dispersion model can be used to describe the liquid backmixing of dissolved nitrogen gas in the reactor [19], in which x is the water depth.

$$\frac{dc}{dt} = D_{ax,1}\frac{d^2c}{dx^2} \tag{2.8}$$

The axial dispersion coefficient, $D_{ax,1}$, is a lumped coefficient, containing the effect of both turbulent dispersion and global convective recirculation in the reactor. Molecular diffusion in this case is neglected due to an expected limited impact. A tracer experiment with ammonium was used to determine the value of $D_{ax,1}$.

To describe the transfer of nitrogen gas between the air bubbles and the water phase, equation 2.4 is substituted in equation 2.3. If this equation is combined with the transport of nitrogen gas in the water phase according equation 2.8 a description for the stripping of nitrogen in a 1D bubble column is constructed:

$$\frac{dc}{dt} = D_{ax,1}\frac{d^2c}{dx^2} + \alpha F\cdot(k_La)_O\sqrt{\frac{D_N}{D_O}}\cdot(c_s(x)-c) \tag{2.9}$$

The saturation concentration for nitrogen gas according to equation 2.1 can be combined with the actual concentration to calculate the nitrogen gas deficit in the bulk liquid, c_d.

$$c_d = c_s - c \tag{2.10}$$

When over-saturation occurs during aeration (i.e. the actual concentration c is higher than c_s at ambient pressure and temperature), it is assumed that N_2 gas bubbles are formed immediately and efficiently stripped out of the bulk liquid. This is modelled by artificially increasing the local k_La with an order of magnitude.

2.2.7. Modelling of mixing during imperfect plug flow feeding

During feeding the bulk liquid in the reactor is pushed up towards the top of the reactor where the overflow weirs are situated. To describe the transport of nitrogen gas during feeding, the same axial dispersion model of equation 2.8 is used with a different value for D_{ax}. Also an additional term is added to describe the transport of nitrogen gas through convection. Here, v is the upflow velocity of the liquid in the reactor. The value of $D_{ax,2}$ was experimentally established by measuring a step response curve with ammonium as a tracer.

$$\frac{dc}{dt} = D_{ax,2}\frac{d^2c}{dx^2} + v\frac{dc}{dx} \tag{2.11}$$

The influent is fed from the bottom of the reactor. It is assumed that the influent concentration of dissolved nitrogen is equal to the equilibrium concentration of

nitrogen gas at atmospheric pressure. During the feeding phase denitrification can take place. The denitrification rate depends on many parameters, but in this case a lumped specific denitrification rate, q, is used. The specific denitrification rate was measured in the reactor in the days before the experiment, by measuring the decrease of the nitrate concentration during an anoxic phase in the cycle. This rate is multiplied by the biomass concentration, c_X, which is a function of the reactor depth. The sludge bed is assumed to be in steady state and thus invariable in time. In the simulations it was assumed that the sludge bed occupies the lower 4 meters of the reactor and that the sludge is evenly distributed. We can then write equation 2.11 as follows:

$$\frac{dc}{dt} = D_{ax,2}\frac{d^2c}{dx^2} + v\frac{dc}{dx} + qc_X(x) \tag{2.12}$$

In this model the water in the reactor can get over-saturated with nitrogen gas. This means that the local concentration of nitrogen gas, c, becomes larger than the local saturation concentration according to equation 2.1. It is assumed that nitrogen gas bubbles are formed immediately after over-saturation. Most likely supersaturation of nitrogen gas can occur, but the effect is assumed to be limited [11].

All model parameters are given in table 2.4.

Table 2.4: Model parameters.

Parameter	Symbol	Value	Unit
Henry's constant for N_2 (25 °C)	k_h	6.4×10^{-6}	mol m^{-3} Pa^{-1}
Temperature coefficient N_2	k_{hc}	1300	K
Molar mass N_2	M	28	g mol^{-1}
Gas fraction of N_2 in air	f	0.78	-
Atmospheric pressure	p_{atm}	101,325	Pa
Density of water	ρ	1000	kg m^3
Gravity acceleration	g	9.81	m s^{-2}
Alpha factor	α	1	-
Fouling factor	F	1	-
Gas transfer rate for oxygen	$(k_La)_O$	5.5	h^{-1}
Diffusion coefficient O_2 (25 °C)	D_O	2.10×10^{-9}	m^2 s^{-1}
Diffusion coefficient N_2 (25 °C)	D_N	1.88×10^{-9}	m^2 s^{-1}
Empirical coefficient A	A	-10.6265	-
Empirical coefficient B	B	578.919	-
Empirical coefficient C	C	-137.546	-
Axial dispersion during aeration	$D_{ax,1}$	1.0×10^{-2}	m^2 s^{-1}
Axial dispersion during feeding	$D_{ax,2}$	1.0×10^{-4}	m^2 s^{-1}

2.3. Results

2.3.1. Reactor operation

The data were collected between June 2015 and May 2016. In this period the reactor was running stable and without interruption with average effluent values of COD of 41 mg L^{-1}, N_{kj}-N of 4.05 mg L^{-1}, NH_4^+-N of 1.29 mg L^{-1}, NO_3^--N of 3.72 mg L^{-1}, P_{tot} of 0.51 mg L^{-1} and PO_4^{3-}-P of 0.26 mg L^{-1}, showing a highly efficient N and P removal of respectively 94 % and 91 %. The average granule size

distribution is reported in table 2.3. The sludge in the reactor mainly consisted of smooth granules larger than 1 mm, which is also shown by the microscopic image of the sludge in figure 2.2A. The water temperature was in the range of 9 °C to 23 °C.

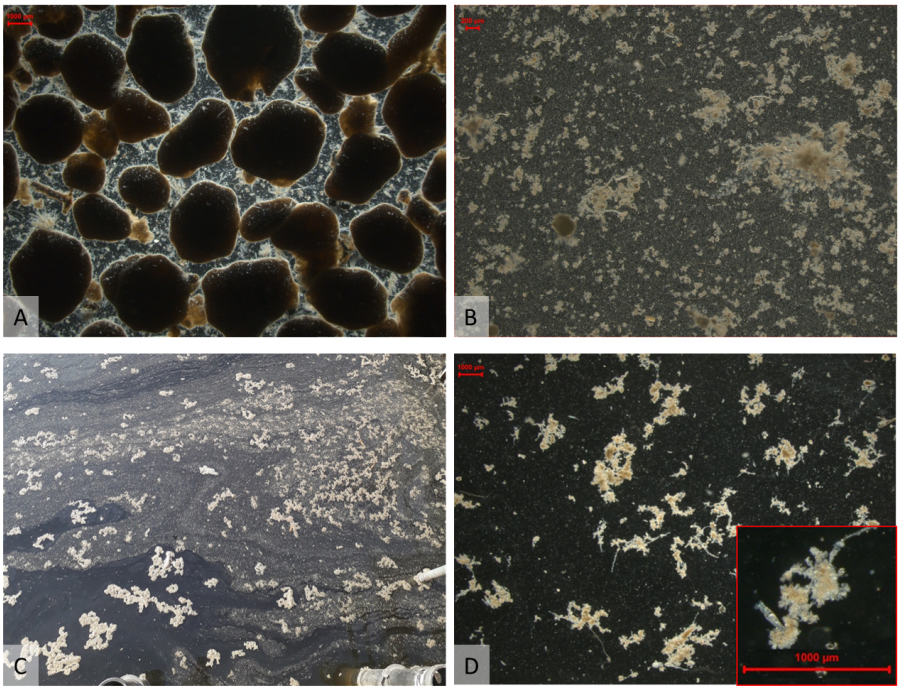

Figure 2.2: Biomass in the Prototype Nereda® Utrecht: (A) granules in the reactor, (B) light microscopic picture of effluent suspended solids, (C) scum on top of the reactor after installation of the baffles, (D) biomass from the top of the reactor.

2.3.2. Degasification of nitrogen gas

Due to denitrification and upward transport of liquid (decreasing local pressure) over-saturation of the water phase with nitrogen gas can occur, leading to gas bubble formation in the feeding/decanting period. To confirm that over-saturation of nitrogen gas is present during parts of the cycle an experiment was performed. Two comparable batches were fed to the reactor. The batch sizes are given as Volumetric Exchange Ratio (VER), which is the ratio between the batch size (f.e. 400 m^3) and the volume of the reactor (1000 m^3). Before the first batch (batch 1) the reactor was intensely aerated before feeding the reactor, while in the second batch (batch 2) this stripping phase was omitted. The gas stripping period was 30 minutes long, with an air flow of 800 $m^3\,h^{-1}$. This high value was chosen to strip a maximum amount of nitrogen gas. The process conditions in the two batches were comparable (batch 1: volumetric exchange ratio 40 %, nitrogen removed

in previous batch 13.8 mg L^{-1}, average temperature 13.6 °C; batch 2: volumetric exchange ratio 40 %, nitrogen removed in previous batch 13.9 mg L^{-1}, average temperature 13.5 °C). The effect of a stripping phase is clearly illustrated in figure 2.3, showing the effluent turbidity for both batches. Batch 1 showed an overall lower level effluent turbidity with a turbidity slightly decreasing over the batch, with an average value of 4.9 FNU. The turbidity in batch 2 was overall higher than in batch 1, with an average value of 21.0 FNU. At a volumetric exchange ratio of 30 % the effluent turbidity started to increase up to a value of 48.5 FNU at the end of batch 2. In figure 2.4 photographs recorded by a security camera are showing the gradual formation of a scum layer due to degasification during batch 2.

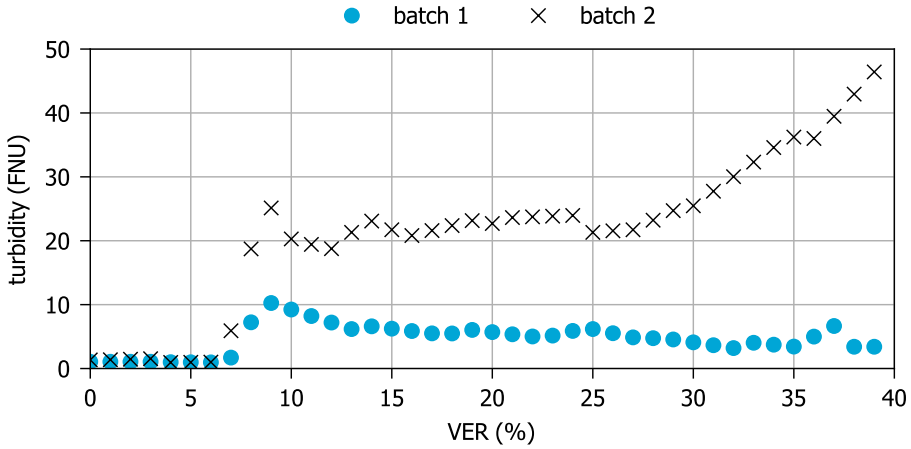

Figure 2.3: turbidity of the effluent in a batch with gas stripping (batch 1) and without gas stripping (batch 2).

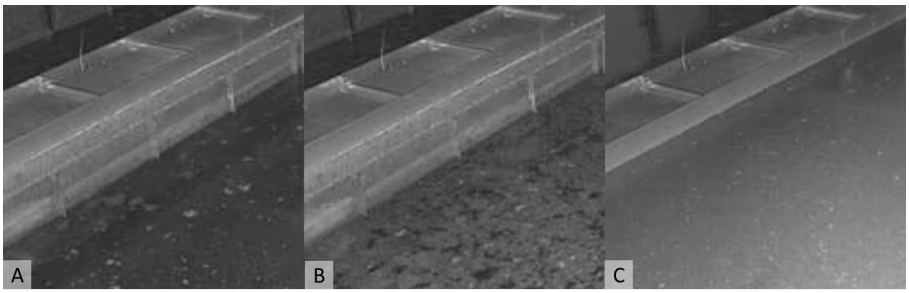

Figure 2.4: Degasification and the resulting floatation of biomass during feeding in a batch without stripping: (A) VER = 0 % (B) VER = 20 % (C) VER = 40 %.

2.3.3. Stripping of nitrogen gas

Dissolved nitrogen gas can be stripped out by aerating right before the feeding phase to prevent rising of biomass as is shown above. Equation 2.9, together with equation 2.1 and 2.2 for pressure correction, equation 2.5, equation 2.6 and equation 2.7 for temperature correction and equation 2.4 for the conversion of the k_La can be used to evaluate the effect of the stripping period on the dissolved N_2 concentration in the reactor.

In figure 2.5 the effect of stripping of an initially fully N_2 saturated situation in the reactor is shown at a temperature of 20 °C. The dissolved nitrogen gas concentration in the reactor (top at 0 m, bottom at 7 m) is shown. The figure shows three coloured zones: the blue zone marks the area where the nitrogen gas concentration is lower than the equilibrium concentration for air (i.e. no degasification expected). The grey zone marks the area where the nitrogen gas concentration is higher than the equilibrium concentration for pure nitrogen gas (i.e. degasification expected). The white zone marks the area where only a partial nitrogen gas deficit exists. The boundary between the blue area and the white area is calculated according to equation 2.1 and equation 2.2 with a gas fraction of nitrogen gas in air at ambient water pressure and temperature ($f = 78\,\%$). The boundary between the white and the grey area is calculated in a similar manner, but with pure nitrogen gas bubbles ($f = 100\,\%$).

The mixing of the reactor has a large impact on the effect of the stripping phase. Dissolved nitrogen gas is convectively transported through the reactor, leading to an over-saturated situation near the top of the reactor and an undersaturated situation near the bottom of the reactor. When the aeration continues, the nitrogen gas is slowly stripped out of the reactor and a N_2 deficit is created at the bottom of the tank. After 15 minutes, due to the mixing, the N_2 concentration near the bottom of the reactor is lower than the air equilibrium concentration at 7 meters water depth. However, near the top of the reactor the N_2 concentration is still over-saturated. Even after 60 minutes of aeration the nitrogen concentration is still at saturation concentration near the top of the reactor due to upmixing of dissolved N_2 gas. Note that for operational conditions over-saturation at the top of the reactor is not important since there is no sludge bed/blanket near the top of the reactor during effluent withdrawal.

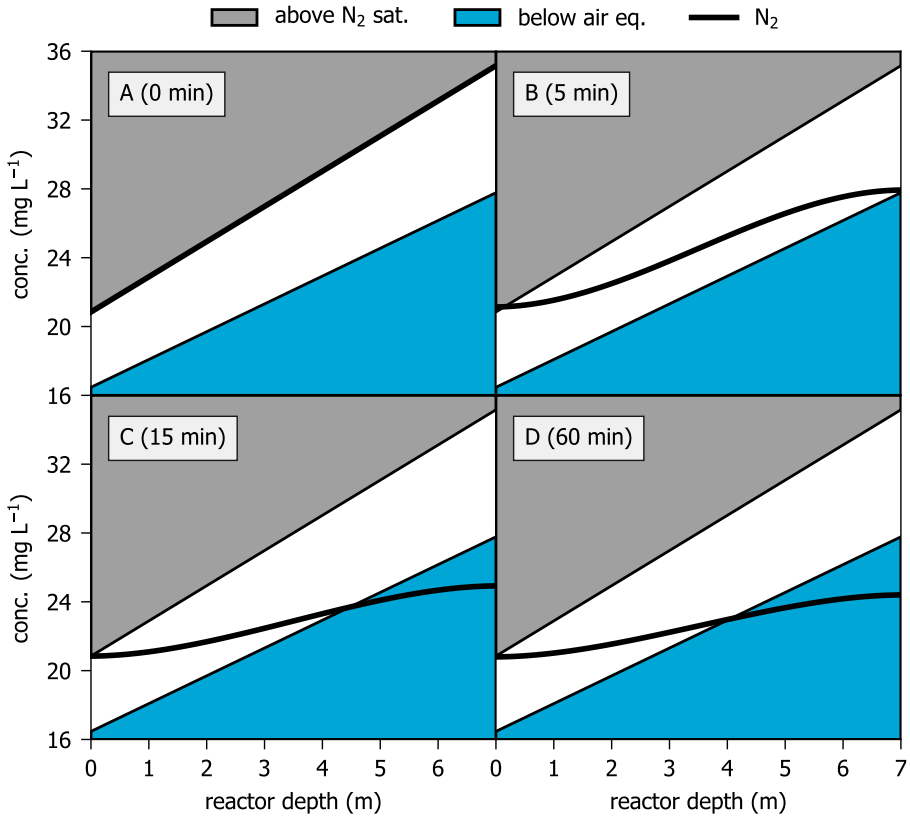

Figure 2.5: Stripping of N_2 gas from fully saturated situation (A) and after 5 minutes (B), 15 minutes (C) and 60 minutes of stripping (D) at 13.5 °C. Black solid line: the actual N_2 concentration, grey area: N_2 concentration above saturation, blue area: N_2 concentration below equilibrium with air, boundary between grey area and white area: N_2 concentration at equilibrium with pure nitrogen gas at ambient water pressure, boundary between blue area and white area: N_2 concentration at equilibrium with air at ambient water pressure.

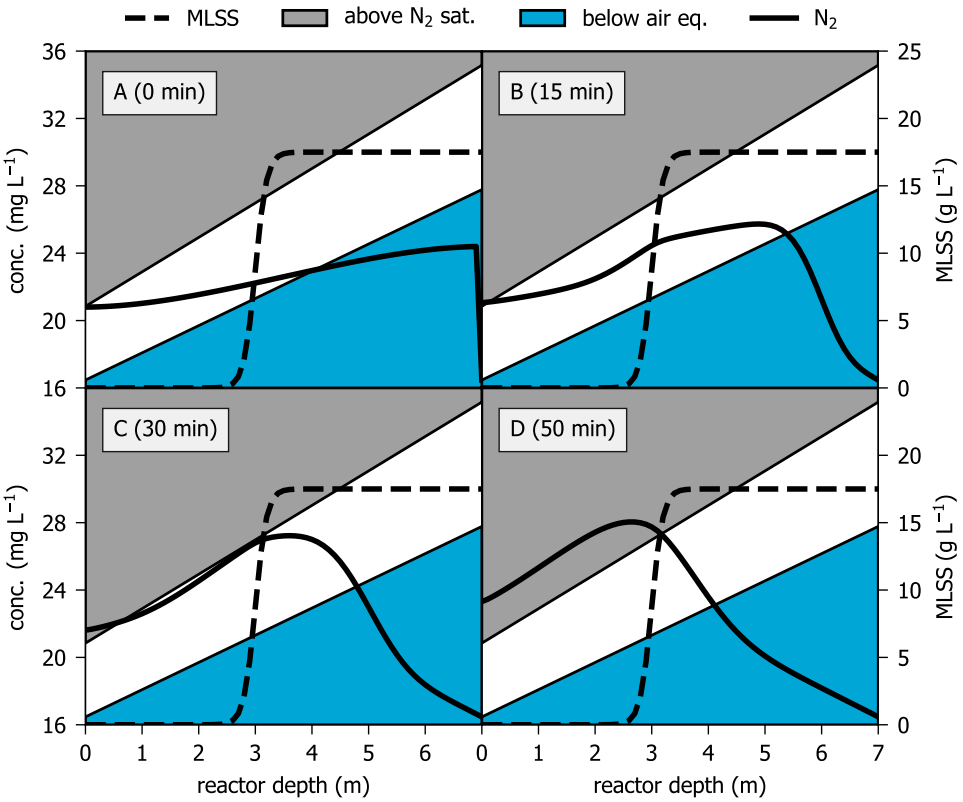

Figure 2.6: effect of feeding after a stripping phase on the dissolved nitrogen gas concentration from the start (A), after 15 minutes (B), after 30 minutes (C) and after 50 minutes (D). T = 13.5 °C, r = 0.25 mg g^{-1} h^{-1}. Black solid line: the actual N_2 concentration, black dashed line: biomass concentration, grey area: N_2 concentration above saturation, blue area: N_2 concentration below equilibrium with air, boundary between grey area and white area: N_2 concentration at equilibrium with pure nitrogen gas at ambient water pressure, boundary between blue area and white area: N_2 concentration at equilibrium with air at ambient water pressure.

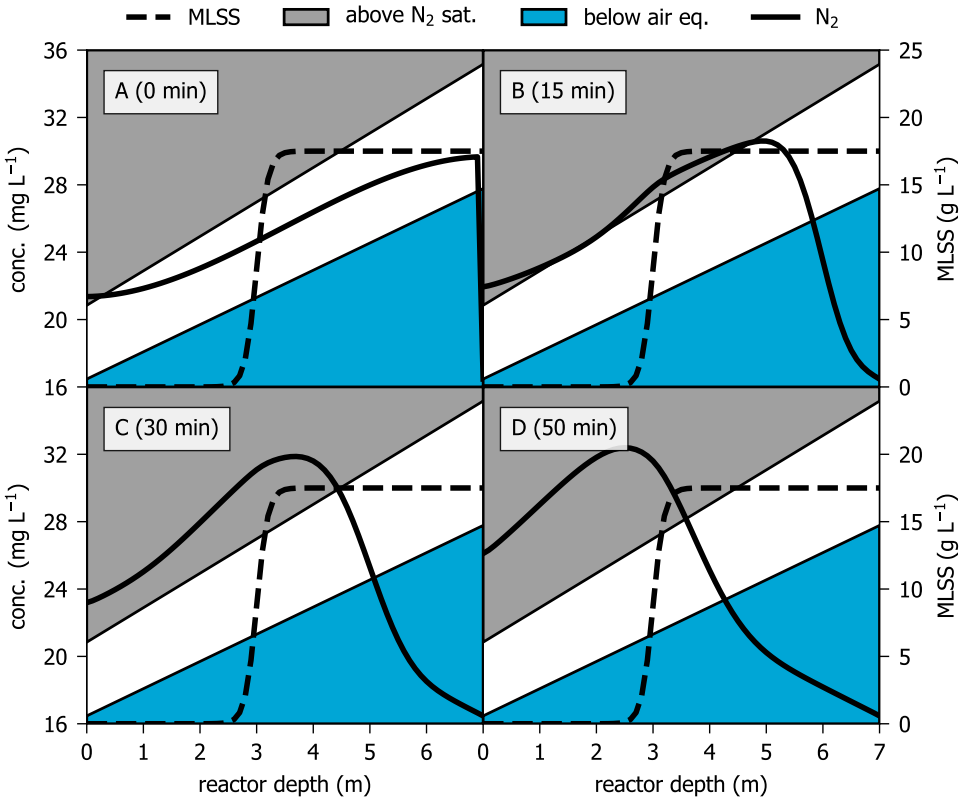

Figure 2.7: effect of feeding without a prior stripping phase on the dissolved nitrogen gas concentration from the start (A), after 15 minutes (B), after 30 minutes (C) and after 50 minutes (D). T = 13.5 °C, r = 0.25 mg g^{-1} h^{-1}. Black solid line: the actual N_2 concentration, black dashed line: biomass concentration, grey area: N_2 concentration above saturation, blue area: N_2 concentration below equilibrium with air, boundary between grey area and white area: N_2 concentration at equilibrium with pure nitrogen gas at ambient water pressure, boundary between blue area and white area: N_2 concentration at equilibrium with air at ambient water pressure.

2.3.4. Degasification during feeding

The effect of denitrification during feeding on degasification of nitrogen gas was also evaluated by extending the model according to equation 2.12. In figure 2.6 an example is shown for a batch comparable with the previously described batch 1 in which a stripping phase of 30 minutes is applied, with T = 13.5 °C, r = 0.25 mg g^{-1} h^{-1}.

The model shows limited over-saturation during the feeding period of 1 hour, but the over-saturation only occurs above the sludge blanket so rising of sludge due to bubble formation is not likely to happen.

If the stripping phase is reduced to 5 minutes, again with T = 13.5 °C, r = 0.25 mg g^{-1} h^{-1}, a situation comparable with the above described batch 2 experiment can be modelled. The results are shown in figure 2.7. The water in the vicinity of the sludge blanket is almost immediately slightly over-saturated with nitrogen gas. After 30 minutes the top of the sludge blanket is fully over-saturated with nitrogen gas, which most likely will lead to rising sludge as the escaping nitrogen bubbles get caught by small flocs near the supernatant - sludge interface.

2.3.5. Identification of suspended solids in the effluent

The suspended solids present in the effluent were examined under a stereo-zoom microscope to determine the characteristics and possible origin. Figure 2.2b and 2.2d show that the suspended solids in the effluent are small dense light brown flocs. No filamentous organisms like *Thiothrix* spp. or *Microthrix* spp. were observed that would normally be associated with bad settling sludge (figure 2.2d). It was also observed that after light shaking of the sample flask the suspended solids quickly settled to the bottom indicating that the suspended solids were able to settle well.

2.3.6. Effect of the vertical baffle

During the first experimental period (between April 2013 and May 2015) the average suspended solids effluent concentration was 30 mg L^{-1} with a 50-percentile value of 19.8 mg L^{-1}. In the same period, many values below 10 mg L^{-1} were also recorded with a 25-percentile value of 9.3 mg L^{-1}. On the 3rd of June 2015 vertical baffles were installed in front of the overflow weirs. Composite samples of the effluent of the reactor were taken in the period immediately before and after the baffles were installed; i.e. under similar operational and sludge characteristics. Figure 2.8 shows the effluent suspended solids in this period. In the period immediately before installation of the baffles the average effluent suspended solids concentration was 23 mg L^{-1}, which is 10 % of the influent suspended solids concentration. In the period directly after installation of the baffles only 1 sample was above 10 mg L^{-1} with a total average of 7.2 mg L^{-1}. In the period June 2015 to May 2016, 175 composite influent and effluent samples were taken by the local water authority. The suspended solids concentration in the influent was 230 ± 118 mg L^{-1} and the concentration of effluent suspended solids was 7.8 ± 3.8 mg L^{-1} with a 95-percentile value of 13.6 mg L^{-1}. The average removal efficiency of suspended solids was 97 %.

After installation of the baffles a thin layer of scum was present in most batches during feeding (figure 2.2c), but in this period no built up of scum was observed. The thin layer of scum always disappeared in the first few minutes of the reaction phase of the cycle.

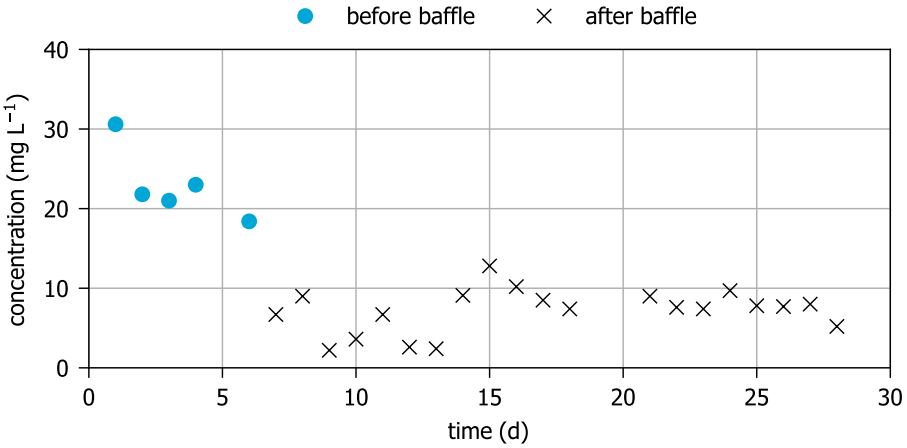

Figure 2.8: Suspended solids concentration in the effluent before and after installation of vertical baffle in front of the overflow weirs.

2.4. Discussion

2.4.1. Comparison with floc systems

In this study we examined the main processes for production of effluent suspended solids in full-scale aerobic granular sludge reactors. The problem of rising sludge is known from both continuously fed activated sludge systems [11] as from sequencing batch reactors [20]. Comparison of the flow patterns in a secondary clarifier and the AGS reactor reveals some important differences (figure 2.9). The outflow from an aeration tank towards a secondary clarifier generally flows over a weir making the water pressure almost atmospheric and generating a lot of turbulence. This is an effective way to remove at least part of the dissolved nitrogen gas. Subsequently, the water from the aeration tank flows into the secondary clarifier through the centre well where the water pressure is close to atmospheric pressure again. In the clarifier the flow splits into effluent and return sludge. The return sludge is removed from the bottom of the clarifier. During dry weather conditions a limited amount of sludge is present in the clarifier and this sludge will be near the bottom of the clarifier at a water pressure well above atmospheric pressure. If the water pressure increases at higher water depth, automatically the nitrogen gas deficit increases. Thus, if nitrogen gas is formed in a clarifier due to denitrification this will mainly take place at the bottom of the clarifier, where a relatively high nitrogen gas deficit is present. This is probably why degasification in a clarifier is not a very common problem and is only known from high loaded

systems at high temperatures with high denitrification rates [21] or when the inflow to the clarifier is not degassed at an overflow weir. In the AGS reactor the influent is fed from the bottom of the reactor, pushing the with nitrogen gas saturated water in the reactor upwards to lower water pressure. This process is comparable with the process occurring in a sequencing batch reactor, where degasification can occur while decanting the effluent and thereby decreasing the water pressure. Thus, while feeding the reactor, the upwards moving liquid gets a lower saturation concentration for nitrogen gas, while in a clarifier it gets increased. In the AGS reactor during feeding, denitrification of remaining nitrate on storage polymers by GAO and PAO like organisms, built up in previous cycles, can occur [22]. The combination of a lower nitrogen gas deficit due to pressure decrease and a higher denitrification potential make the AGS reactor more susceptible for degasification of nitrogen gas in comparison to a clarifier. Therefore, washout of suspended solids due to degasification of nitrogen gas is less common in clarifiers than in AGS reactors.

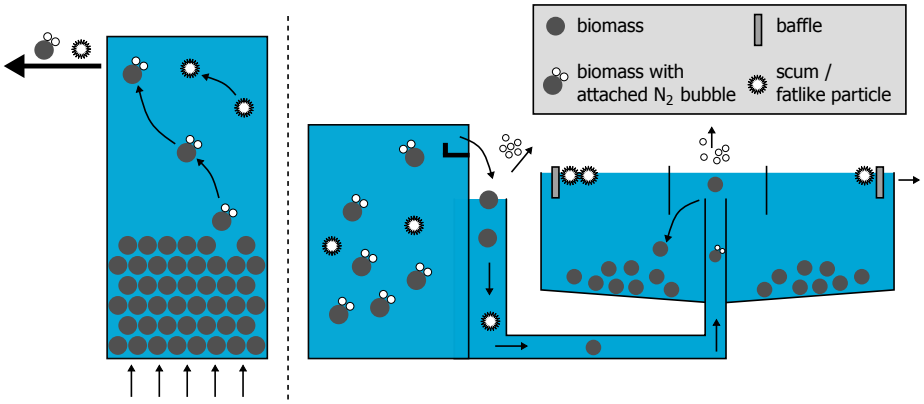

Figure 2.9: Comparison of flow in an AGS reactor (left) and flow in a conventional aeration tank and clarifier (right).

2.4.2. Effect of N_2 stripping

Rising of sludge due to degasification of dissolved N_2 gas can cause elevated levels of suspended solids in the effluent of activated sludge and AGS plants. Experimentally it was shown that a nitrogen gas stripping phase just before the influent feeding phase was effective to prevent rising of sludge in the AGS process. The developed mathematical model shows that a limited amount of N_2 gas deficit can be reached by applying a stripping phase. When the water is pushed up during the feeding phase almost immediate over-saturation occurs when no stripping phase is applied.

The model presented by Henze et al. [11] only showed a steady state N_2 gas deficit in an unmixed situation. This model was extended to show the effect of non-steady state aeration and feeding. A convection/dispersion term was added to the model to describe both mixing due to aeration of the reactor and the plug flow behaviour of the AGS reactor during feeding. The model shows that

the local dissolved N_2 gas concentration changes over time and depth of the reactor. The maximum deficit for N_2 gas depends highly on the temperature, as do the denitrification rates. The model can easily be extended to calculate the risk of rising sludge based on temperature, batch size and aeration history of the reactor. Denitrification rates increase with temperature and the N_2 gas deficit will decrease with temperature. At temperatures above 20 °C the need for a stripping phase increases. It should be realized that for the denitrification during the settling/feeding phase mainly residual COD from the previous cycles is used. The COD containing influent is replacing the nitrate containing liquid in the reactor. Therefore, influent COD and nitrate will only mix after the feeding phase when the aeration is switched on.

2.4.3. Effect of the scum baffle

Introduction of the vertical scum baffles in front of the effluent weir lowered the effluent suspended solids concentration from 23 mg L^{-1} to 7 mg L^{-1}. Analyses of the suspended solids in the effluent before installation of the baffles did not show any significant presence of granules or filamentous bacteria. Microscopic analyses only revealed the presence of small sludge flocs. The thin layer of sludge present on the surface of the reactor during feeding, observed after installation of the baffles apparently was the result of the blocking of wash-out of floating sludge by the baffles. The same effect is known from clarifiers in activated sludge systems [23].

It was shown that at a MLSS concentration of 10.1 g L^{-1} and an influent suspended solids of 230 mg L^{-1} an effluent suspended solids concentration below 10 mg L^{-1} was obtained over long-term operation. The flocs present in the layer on top of the reactor are assumed to be grown in the reactor. Apparently, not all biomass grown in the reactor is granular. The flocculent mass likely consists of non-biodegradable inert COD from the influent and detached biomass from the granules. This is also shown by the fractionation of the sludge showing an average 16 % of mass smaller than 200 µm.

The influent of the reactor contained an average of 230 mg L^{-1} of TSS after screening. Since the only pre-treatment of the reactor was a 6 mm perforated plate screen, some floating material from the sewerage will end up in the reactor. Although the influent consists merely of domestic wastewater, the sewage of the Overvecht district is known to contain relatively large fraction of fat. Some fatlike particles were observed in the reactor, but in the period of 10 months in which the experiment was run, no build-up of scum or fat on the reactor was observed. Apparently, the fat particles were converted or removed with the excess sludge.

The reported values of effluent suspended solids of 20 mg L^{-1} for the Garmerwolde plant [4] are comparable with the levels measured in this study before installation of the vertical baffles in front of the effluent weirs. Since the Garmerwolde plant mainly treats domestic sewage and also the pre-treatment of the wastewater is comparable, these levels of effluent suspended solids are to be expected. Also reported values for other plants (table 2.1) were in the range of 10 mg L^{-1} to 20 mg L^{-1} and thus comparable with the values measured in this study before installation of the vertical baffle. This value is to be expected from

a full-scale aerobic granular sludge reactor on domestic wastewater if no baffle is present. The Gansbaai plant is the exception, with a value of 5 mg L^{-1}, but detailed information is not available. Baffles have proven to be an effective and economic way to keep effluent suspended solids below 10 mg L^{-1}, similar to well operated secondary clarifier effluents.

2.5. Conclusions

In this study, two main processes have been identified that can contribute to elevated suspended solids concentration in the effluent of the aerobic granular sludge process in practice. These processes also play an important role in suspended solids control in secondary clarifiers of activated sludge plants. Two solutions known from operation of secondary clarifiers could successfully be incorporated into the AGS process leading to low concentration of suspended solids in the effluent. The implementation of nitrogen stripping, before the settling period, avoids gas bubble formation during feeding and thus the floatation of lighter biomass. A mathematical model describing degasification was developed that explains the observations of higher suspended solids concentrations in the effluent when treating sewage. Introduction of a vertical baffle in front of the effluent weir showed to be an effective measure to keep floating sludge and fat-like particle in the reactor, resulting in an effluent suspended solids concentration lower than 10 mg L^{-1} with an average influent suspended solids concentration of 230 mg L^{-1}. This was achieved with high biomass concentrations (10 g L^{-1}) and a high granulation grade (84 %).

Bibliography

[1] E. J. H. van Dijk, M. Pronk, and M. C. M. van Loosdrecht, *Controlling effluent suspended solids in the aerobic granular sludge process,* Water Res. **147**, 50 (2018).

[2] H. F. van der Roest, L. M. M. de Bruin, G. Gademan, and F. Coelho, *Towards sustainable waste water treatment with Dutch Nereda® technology,* Water Pract. Technol. **6**, 1 (2011).

[3] A. Giesen, L. M. M. de Bruin, R. P. Niermans, and H. F. van der Roest, *Advancements in the application of aerobic granular biomass technology for sustainable treatment of wastewater,* Water Pract. Technol. **8**, 47 (2013).

[4] M. Pronk, M. K. de Kreuk, L. M. M. de Bruin, P. Kamminga, R. Kleerebezem, and M. C. M. van Loosdrecht, *Full scale performance of the aerobic granular sludge process for sewage treatment,* Water Res. **84**, 207 (2015).

[5] A. Giesen, M. C. M. van Loosdrecht, M. Pronk, S. Robertson, and A. Thompson, *WEFTEC 2016 - 89th Water Environ. Fed. Annu. Tech. Exhib. Conf.*, Vol. 3 (Water Environment Federation, 2016) pp. 1913–1923.

[6] Z. H. Li, T. Kuba, T. Kusuda, and X. C. Wang, *A comparative study on aerobic granular sludge and effluent suspended solids in a sequence batch reactor,* Environ. Eng. Sci. **25**, 577 (2008).

[7] T. Rocktäschel, C. Klarmann, J. Ochoa, P. Boisson, K. Sørensen, and H. Horn, *Influence of the granulation grade on the concentration of suspended solids in the effluent of a pilot scale sequencing batch reactor operated with aerobic granular sludge,* Sep. Purif. Technol. **142**, 234 (2015).

[8] M. K. de Kreuk, M. Pronk, and M. C. M. van Loosdrecht, *Formation of aerobic granules and conversion processes in an aerobic granular sludge reactor at moderate and low temperatures,* Water Res. **39**, 4476 (2005).

[9] D. S. Parker, D. J. Kinnear, and E. J. Wahlberg, *Review of Folklore in Design and Operation of Secondary Clarifiers,* J. Environ. Eng. **127**, 476 (2001).

[10] D. Jenkins, *Towards a comprehensive model of activated sludge bulking and foaming,* Water Sci. Technol. **25**, 215 (1992).

[11] M. Henze, R. Dupont, P. Grau, and A. de la Sota, *Rising sludge in secondary settlers due to denitrification,* Water Res. **27**, 231 (1993).

[12] D. S. Parker, R. Butler, R. Finger, R. Fisher, W. Fox, W. Kido, S. Merrill, G. Newman, R. Pope, J. Slapper, and E. Wahlberg, *Design and operations experience with flocculator-clarifiers in large plants,* Water Sci. Technol. **33**, 163 (1996).

[13] Z. Vitasovic, S. Zhou, J. McCorquodale, and K. Lingren, *Secondary clarifier analysis using data from the Clarifier Research Technical Committee protocol,* Water Environ. Res. **69**, 999 (1997).

[14] S. Zhou, J. A. McCorquodale, and Z. Vitasovic, *Influences of Density on Circular Clarifiers with Baffles,* J. Environ. Eng. **118**, 829 (1992).

[15] R. Higbie, *The rate of absorption of a pure gas into still liquid during short periods of exposure,* Inst. Chem. Eng. **35**, 36 (1935).

[16] A. Einstein, *Über die von der molekularkinetischen Theorie der Wärme geforderte Bewegung von in ruhenden Flüssigkeiten suspendierten Teilchen,* Ann. Phys. **322**, 549 (1905).

[17] L. Dagdug, *A theoretical framework for the Vogel-Fulcher-Tammann equation for covalent network glasses derived by the stochastic matrix method,* J. Phys. Condens. Matter **12**, 9573 (2000).

[18] M. J. H. van't Hoff, *Recl. des Trav. Chim. des Pays-Bas*, Vol. 3 (F. Muller & Co., Amsterdam, 1884) pp. 333–336.

[19] S. Degaleesan and M. P. Dudukovic, *Liquid backmixing in bubble columns and the axial dispersion coefficient,* AIChE J. **44**, 2369 (1998).

[20] J. A. Torà, J. A. Baeza, J. Carrera, and J. A. Oleszkiewicz, *Denitritation of a high-strength nitrite wastewater in a sequencing batch reactor using different organic carbon sources,* Chem. Eng. J. **172**, 994 (2011).

[21] M. Sarioglu and N. Horan, *An equation for the empirical design of anoxic zones used to eliminate rising sludges at nitrifying activated sludge plants,* Water Sci. Technol. **33**, 185 (1996).

[22] T. Kuba, E. Murnleitner, M. C. M. van Loosdrecht, and J. J. Heijnen, *A metabolic model for biological phosphorus removal by denitrifying organisms,* Biotechnol. Bioeng. **52**, 685 (1996).

[23] Metcalf & Eddy, *Wastewater Engineering: Treatment and Resource Recovery*, 5th ed. (McGraw-Hill, 2013) pp. 906–907.

3

Settling behaviour

The settling behaviour of AGS in full-scale reactors is different from the settling of flocculent activated sludge. Current activated sludge models lack the features to describe the segregation of granules based on size during the settling process. This segregation plays an important role in the granulation process, and therefore, a better understanding of the settling is essential. The goal of this study was to model and evaluate the segregation of different granule sizes during settling and feeding in full-scale aerobic granular sludge reactors. For this, the Patwardhan and Tien model was used. This model is an adaption of the Richardson and Zaki model, allowing for multiple classes of particles. To create the granular settling model, relevant parameters were identified using aerobic granular sludge from different full-scale Nereda® reactors. The settling properties of individual granules were measured, as was the bulk behaviour of granular sludge beds with uniform granular sludge particles. The obtained parameters were integrated in a model containing multiple granule classes, which was then validated for granular sludge settling in a full-scale Nereda® reactor. In practice a hydraulic selection pressure is used to select for granular sludge. Under the same hydraulic selection pressure, the model predicted that different stable granular size distributions can occur. This indicates that granular size distribution control would need a different mechanism then the hydraulic selection pressure alone. This model can be used to better understand and optimize operational parameters of AGS reactors that depend on granular sludge size, like biological nutrient removal. Furthermore, insights from this model can also be used in the development of continuously fed AGS systems.

Parts of this chapter have been published in Water Research **186**, (2020) [1].

3.1. Introduction

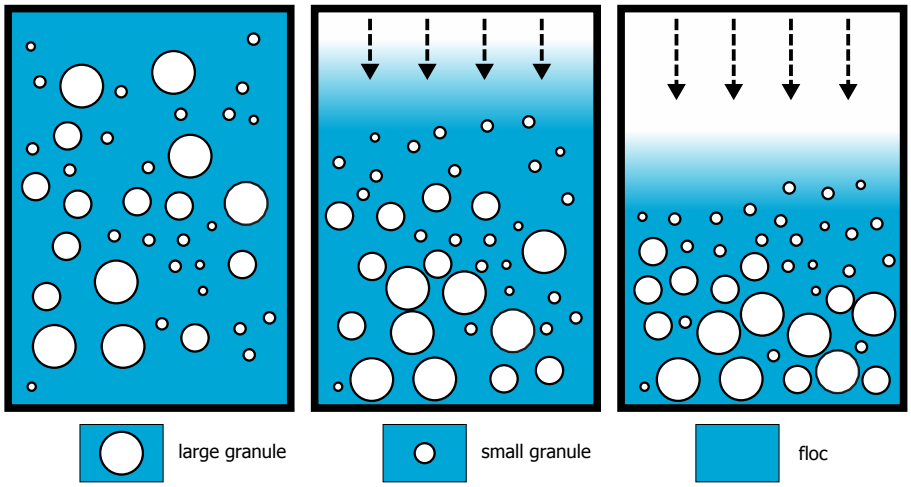

Figure 3.1: Graphical abstract.

In biological wastewater treatment, the liquid/solid separation through gravity induced settling is an important step in producing clean effluent [2]. Therefore, the settling behaviour of conventional activated sludge has been intensively studied over the years. For the design of secondary clarifiers, a good understanding of the settling behaviour of activated sludge is necessary and both design guidelines [2] and dynamic models [3, 4] are readily available. These guidelines generally use the sludge volume index or the zone settling velocity as input parameters for describing the settling behaviour of activated sludge. For dynamic modelling of the settling of activated sludge several generally accepted empirical relations are available relating the settling velocity to the solids concentration [5]. These empirical relations can be used to dynamically describe the settling of sludge in secondary clarifiers, thereby ensuring proper design and operation of the conventional activated sludge plants.

Aerobic Granular Sludge is a technology enabling removal of nutrients and liquid/solid separation in one tank due to the advantageous settling properties and unique granular structure of the aerobic granules [6–10]. The settling behaviour of aerobic granular sludge under full-scale conditions has not yet been studied. This is mostly because the full-scale aerobic granular sludge process is a novel technology. So far, the settling of aerobic granular sludge has only been studied with granules obtained from laboratory reactors [11–14]. These reactors are usually operated with synthetic influent leading to a fully granulated system without flocs. In practice there always is a non-granular sludge fraction present of 10 % to 20 % [7, 15] of the total mass which might influence the overall settling behaviour. Also, laboratory experiments mainly focused on the settling behaviour of individual granules, not the settling behaviour of the granular sludge bed as a whole. As such it is not yet possible to model settling of full-scale aerobic granular sludge.

The settling velocity of granules in a bed is much lower than that of an individual granule. Solid separation theory shows that the influence a settling particle experiences from surrounding particles depends on the degree of particle coherence [16]. Conventional activated sludge flocs will tend to flocculate, which slows down the settling velocity of the sludge [4]. Aerobic granular sludge by definition does not coagulate [17] and is thought to maintain its discrete settling properties, even in a concentrated sludge bed. For small biofilm-coated particles it was shown that the settling behaviour could be well described using fluidized bed theory [18]. Because of the similarities in size, structure and density between biofilm-coated particles and aerobic granular sludge it was theorized that the settling of aerobic granular sludge might also be described by fluidized bed theory.

Current activated sludge models, for example the widely used Takács model [3], lack the features to describe the segregation of granules based on size during the settling process. The process of hydraulic sludge selection is a key element in the operation of granular sludge reactors [19]. Larger granules have higher settling velocities than flocs and small granules [11] and as such they can be preferentially retained in the reactor under hydraulic selection pressure. In an upwards fed reactor, larger granules are more likely to receive substrate, because they settle faster to the bottom of the reactor and thus receive substrate. This differential settling of different sludge fractions is not covered in current settling models. Another feature not well described by the current models is the stacking of granules at the bottom of the reactor. Sludge flocs in a concentrated bed will slowly compress to higher concentrations, while granules will stack on top of each other, when the maximum packing grade is reached. For a better understanding of these processes a model describing the segregation of granules in the reactor based on settling properties is necessary. A potential model was proposed by [20], but not further developed. Also Dold *et al.* proposed a model, but in this model only flocs and one class of granules was used, and all granules were allowed to survive the selection pressure. While this approach might serve the purpose of describing the average conversions in an AGS reactor, no insight can be gained in the granulation process itself. Moreover, it cannot be used to predict the influence of the granular size distribution on the biological conversions. Also for the development of continuously operated granular sludge reactors [22] a good settling model will be essential.

The goal of this study was to implement a model describing the segregation of different granule sizes during settling and feeding in an aerobic granular sludge reactor. For this, the model proposed by [23] was adopted. This model is an implementation of the Richardson and Zaki model [24], allowing for multiple classes of particles. To create a granular sludge settling model, relevant parameters were identified using aerobic granular sludge from different full-scale Nereda® reactors. The settling properties of individual granules were measured as was the bulk behaviour of uniform granular sludge beds. The obtained parameters were introduced in a model containing multiple granule classes, which then was validated based on an experiment in a full-scale Nereda® reactor.

3.2. Methodology

3.2.1. Description of the plants

In this study aerobic granular sludge from three Nereda® plants was used, namely from Garmerwolde, from the full-scale in Utrecht and from the PNU. For a description of these plants see section 1.4. Sludge characteristics (mixed liquor suspended solids (MLSS), volatile suspended solids (VSS), sludge volume index after 30 minutes (SVI30), the granule fraction in sludge (AGS fraction) and the COD loading rate) of these plants during the experiments are given in Table 3.1.

Table 3.1: Characteristics of Nereda® plants during the experiments.

plant	MLSS ($kg\,m^{-3}$)	VSS ($kg\,m^{-3}$)	SVI30 ($mL\,g^{-1}$)	Gran. (%)	COD load ($kg_{COD}\,kg_{MLSS}^{-1}\,d^{-1}$)
Garmerwolde	6.5	5.0	60	64	0.10
Utrecht	6.7	5.2	42	81	0.076
PNU	8.9	7.2	39	78	0.078

3.2.2. Size distribution

The granule size distribution of the sludge in the Nereda® reactors used in these experiments varied. Aggregates larger than 200 µm are considered to be granules, although the non-granular fraction smaller than 200 µm at least partly shows the same granular morphology. These small aggregates are the proto-granules (see chapter 5). To determine the granule size distribution 1 L of sample was poured over a series of sieves with different mesh sizes (212, 425, 630, 1000, 1400 and 2000 µm). A mixed sample of 100 mL was filtered for the determination of the total dry weight. The obtained granular biomass of the different sieve fractions and the mixed sample were dried at 105 °C until no change in weight was detected anymore.

3.2.3. Density measurements

The Percoll centrifugation method was used to measure the density of the granules [25, 26]. Centrifugation was performed for 120 min at 12.000 rpm (15 777 g) in a Stratos Biofuge (Heraeus Instruments). A standard (non-swing out) rotor holding plastic tubes containing 10 mL solution was used. The speed-up setting on the Biofuge was 9, and the slow-down setting was 1. The slow reduction of speed was set to limit the change of sudden slowdown on the granule position in the Percoll. Marker beads were added ranging from $1023\,kg\,m^{-3}$ to $1084\,kg\,m^{-3}$.

3.2.4. Voidage measurements

The minimum voidage between granules was measured with the Dextran Blue method [27]. Granules were sieved with tap water and a known volume (between 300 mL to 400 mL) was added to a graduated measuring cylinder. An amount of 300 mg of Dextran Blue was weighed on an analytical balance, dissolved in a small amount of water and added to the measuring cylinder. Then the measuring cylinder

was filled to 1000 mL and stirred. After settling of the granules, a sample of the supernatant was taken and filtered with a Millipore 0.45 µm glass fiber filter to remove small particulate matter. The concentration of Dextran Blue in the sample was then measured with a spectrophotometer at 620 nm. Based on the dilution of the Dextran Blue and the known volume of the granular bed, the voidage between the granules was calculated according the following formula, where V is the volume of the cylinder, c_{db} the concentration of Dextran Blue, m_{db} the mass of the Dextran Blue and V_{bed} is the volume of the settled sludge:

$$\epsilon = 1 - \frac{V c_{db} - m_{db}}{V_{bed} c_{db}} \tag{3.1}$$

3.2.5. Measurement of terminal velocities

To determine the terminal velocity of individual granules, sludge was sieved using sieves with mesh sizes of 212, 425, 630, 1180, 1700 and 2000 µm. Sieved granules were placed in a glass measuring cylinder with a height of 43 cm and a diameter of 6 cm. The cylinder was filled with tap water at room temperature. The granules were pre-conditioned and washed with tap water. Since the difference of the total dissolved solids of tap water (254 mg L^{-1}) and effluent (439 mg L^{-1}) was small, the effect of using tap water instead of effluent on the settling velocity likely was very small. The settling of granules was recorded using a video camera in order to determine the settling time for a marked distance of 20.7 cm. The camera was placed perpendicular to the exact mid-point of the marked settling distance to minimize parallax errors. The settling velocity was subsequently calculated by dividing the marked distance by the settling time. The influence of the wall effect on the measured settling velocity was evaluated based on the method described by [28]. In the worst-case situation (granules of 2 mm) this effect was less than 2.5 %. This was deemed sufficiently low to be negligible.

3.2.6. Measurement of bed expansion

Experiments with full-scale aerobic granular sludge were performed using a setup, adapted from Baldock [29]. Using this setup (Figure 3.2) the settling characteristics of granules of different sizes were measured. The height of the column was 200 cm with an inner diameter of 153.6 mm. The lower 18 cm of the column was used as a flow equalization section, and therefore filled with glass marbles. On top of the marbles there was a mesh support, to prevent granules to cross into the equalization section. The volume above the mesh was partially filled with granules for the experiment. The granules were obtained by sieving granules directly from a full-scale aerobic granular sludge reactor, using sieves with mesh sizes of 1000 µm and 2000 µm.

Effluent of the wastewater treatment plant was fed from the bottom of the column using a peristaltic pump. The water was fed at upflow velocities between 3 m h^{-1} and 15 m h^{-1} to fluidize the granular bed. The upflow velocity was increased in steps until the granular bed reached the top of the column. Then the upflow velocity was decreased in steps until the bed was completely settled again. At

every step the upflow velocity was kept constant until no change in the bed height was detected anymore. The effluent was removed through a hole in the wall at the top of the column.

3.2.7. Full-scale settling of a mixed granular bed

Settling of a mature granular bed was measured in the full-scale Nereda® reactor in Utrecht, which is a 12 000 m^3 reactor containing 6.7 g L^{-1} of MLSS. First the reactor was intensely mixed by aerating for 20 min and a sample was taken to determine the biomass concentration. After the aeration the sludge bed was allowed to settle. Samples of the sludge bed were taken at different levels below the water surface (0, 2, 4, 6 and 7 m) after 0, 5, 10, 15 and 17 min. The samples were taken with a Kemmerer sampling bottle of 1.5 L and sieved to measure the granule size distribution.

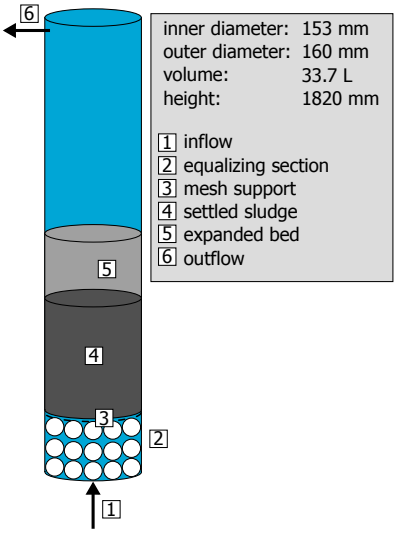

Figure 3.2: Column used for measuring bed settling characteristics of aerobic granular sludge.

3.2.8. Modelling of terminal velocity

The terminal settling velocity of a spherical particle in a fluid can be calculated based on a force balance:

$$F_W = F_B + F_D \tag{3.2}$$

Here F_W is the weight of the particle, F_B is the buoyancy and F_D is the drag force.

The weight of a particle can be calculated from the diameter d and the density ρ_B using the following equation, where g is the gravitational acceleration:

$$F_W = \frac{\pi}{6} d^3 \rho_B g \tag{3.3}$$

With a similar equation the buoyancy can be calculated, using ρ_L for the density of the surrounding liquid:

$$F_B = \frac{\pi}{6} d^3 \rho_L g \tag{3.4}$$

The drag force of the particle while falling in the fluid is calculated by:

$$F_D = \frac{1}{8} \pi C_D \rho_L d^2 v_t^2 \tag{3.5}$$

where v_t is the terminal velocity of the particle and C_D is the drag coefficient. Combining equation 3.2 to 3.5 leads to the equation for the terminal velocity of a particle:

$$v_t = \left[\frac{4g(\rho_B - \rho_L)d}{3C_D \rho_L} \right]^{\frac{1}{2}} \tag{3.6}$$

For particle Reynolds numbers (Re) below 0.1 the value of C_D can be calculated using Stokes law. Since settling of aerobic granular mostly takes place in the intermediate flow regime ($0.1 < Re < 1000$) another relationship needs to be adopted. Also, equations 3.3 to 3.6 assume smooth, rigid, spherical particles. Although aerobic granules have a nearly spherical shape, they are not always smooth or rigid. Therefore, a specific empirical relation for the drag coefficient has to be established for aerobic granular sludge. Several empirical relationships exist to relate the drag coefficient C_D to the particle Reynolds number [18]. A common approach is the use of the equation:

$$C_D = aRe^b \tag{3.7}$$

where a and b are empirical constants to be fitted to the type of particles. The parameters a and b are only valid in a specific range of the particle Reynolds number. The latter is calculated by:

$$Re = \frac{\rho_L d v_t}{\mu} \tag{3.8}$$

Here μ is the dynamic viscosity of the liquid.

In this study the values of a and b where measured using the column set-up described earlier.

3.2.9. Modelling of bed behaviour

The Richardson and Zaki equation [24] is widely used to model the bed expansion of rigid spherical particles:

$$v = v_f \epsilon^n \tag{3.9}$$

Here v is the fluidizing velocity, ϵ is the voidage fraction, v_f is the extrapolated fluidizing velocity at a voidage fraction of unity and n is the expansion index. In

the original work of Richardson and Zaki, v_f was found to be equal to the terminal velocity v_t for installations where the reactor diameter was much larger than the particle diameter, according to equation:

$$v_f = v_t 10^{-d/d_R} \tag{3.10}$$

Later it was shown that if the density of the particles approaches the density of the fluid, this relation is incorrect and v_f is at least 20 % smaller than v_t [18, 30].

The expansion index n is also a function of the flow regime. Richardson and Zaki proposed a relation with the particle Reynolds number. Others studies [31] found a relation to the Archimedes number more suitable for describing the relation between flow regime and expansion index. In this study we use the relation given by Mulcahy and Shieh which is based on the Reynolds number (equation 3.11), but in chapter 5 we use a relation based on the Archimedes number (equation 5.13) as we found that better suits a integral model, also describing settling of flocs.

$$n = 10.35 Re_p^{-0.18} \tag{3.11}$$

The Richardson and Zaki equation is only valid for mono-disperse solids. Since an aerobic granular sludge bed generally consists of granules with sizes in the range of 200 µm to 5000 µm (see Table 3.2), a multi-disperse approach is needed to model the fluidization and settling of aerobic granular sludge beds. Multiple solutions describing multi-disperse solids exist [33] and here the approach described by Patwardhan and Tien was used. The granules are divided in N classes with subscript j, and the local settling velocity is calculated based on an apparent voidage ϵ_j. This leads to the following equation:

$$v_j = k_j v_{f,j} \epsilon_j^{n_j - 2} \frac{\rho_{B,j} - \rho_{bed}}{\rho_{B,j} - \rho_L} \tag{3.12}$$

Here k_j is a correction factor for wall effects. This factor can be set to unity for large full-scale reactors where the diameter of the reactor d_R is much larger than the granule diameter and consequently has less impact. For smaller reactors (for example lab reactors), the value of k can be calculated according to:

$$k_j = 1 - 1.15 \left(\frac{d_j}{d_R} \right)^{0.6} \tag{3.13}$$

The density of the sludge bed ρ_{bed} is based on the density and the volumetric concentration θ of each class:

$$\rho_{bed} = \sum_{j=1}^{N} \rho_{B,j} \theta_j + \rho \left[1 - \sum_{j=1}^{N} \theta_j \right] \tag{3.14}$$

The apparent voidage factor ϵ_j is calculated for every fraction based on the bulk voidage ϵ_L using equation 3.15:

$$\epsilon_j = 1 - \left[1 + \left(\frac{\overline{d}}{d_j}\right)\left[(1-\epsilon_L)^{-\frac{1}{3}} - 1\right]\right]^{-3} \tag{3.15}$$

The average granule size is calculated based on the volumetric concentration, the granule diameter and the voidage:

$$\overline{d} = \frac{\sum_{i=1}^{N} \theta_j d_j}{1-\epsilon_L} \tag{3.16}$$

When the sludge bed reaches the minimum voidage, no settling of granules will occur anymore. In the model this is simulated by simply setting the settling velocity to zero below the minimum voidage. This also implies a minimum fluidization velocity, corresponding with the settling velocity at minimum voidage. Although this was not specifically measured in the experiments, this behaviour was observed during the experiments that were performed.

3.3. Results

3.3.1. Terminal velocity

The terminal velocities of granules obtained from the Nereda® reactor in Garmerwolde were measured by dropping individual granules in a measuring cylinder. The obtained terminal velocities with granule sizes between 200 µm and 2000 µm are presented in Figure 3.3. Since the granules were sieved, this yielded a range of granule sizes per class, for example between 212 µm and 425 µm and thus a range of settling velocities. Per class a minimum, average and maximum settling velocity was calculated, and these values were attributed to the minimum, average and maximum granule size of the class. The terminal velocity varied between 10.6 m h^{-1} and 86.5 m h^{-1} as shown in Figure 3.3.

Using the Percoll method a density for granules of 1035 ± 14 kg m^{-3} was found for full-scale granules. With this density the drag coefficient can be calculated using equation 3.6. Also the particle Reynolds number can be calculated using equation 3.8. Then a plot can be made of the drag coefficient versus the particle Reynolds number (Figure 3.4). These data were used to estimate the coefficients a and b of equation 3.7. At values $a = 22.57$ and $b = -0.690$ we found the best fit with the data.

The experiments resulting in Figure 3.3 were all obtained with relatively spherical and smooth granules. Sometimes granules are not smooth and spherical and for example finger-type outgrowths exist at the surface of the granules. This can have a negative effect on the settling velocity. Figure 3.5 shows the difference between smooth spherical granules and granules with finger-type outgrowth on the granule surface for granules of 1.7 mm and 2.0 mm. The difference in terminal velocity is up to 27 %. and seems to be larger for smaller granules. A comparison of smooth granules and granules with outgrowth is shown in Figure 3.6.

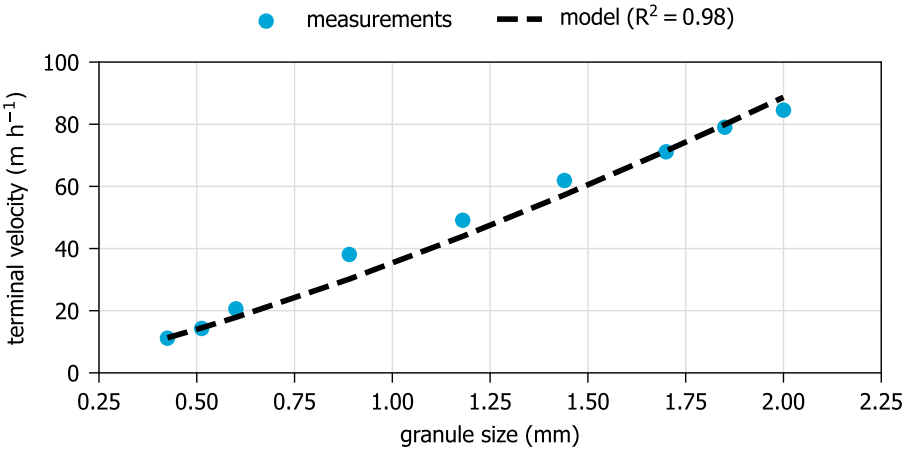

Figure 3.3: Terminal velocity of individual granules from the full-scale Nereda® plant in Garmerwolde; the data points were used to fit the drag coefficient C_D according to equation 3.6.

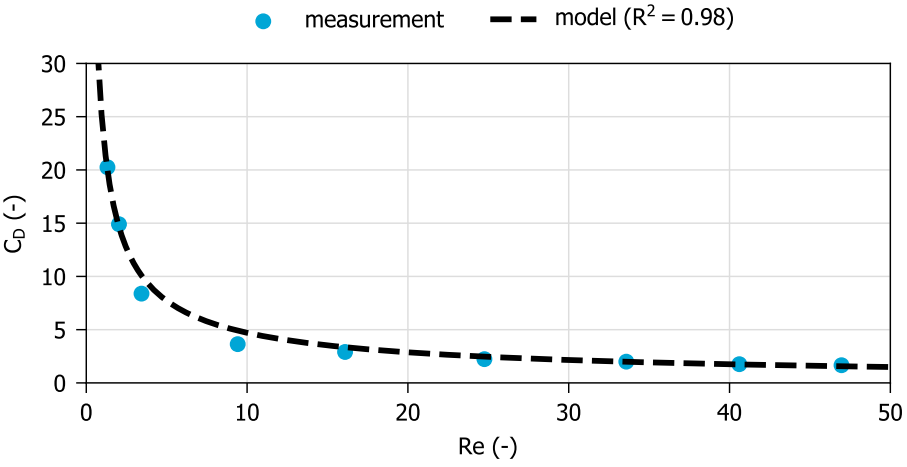

Figure 3.4: Drag coefficient of individual granules from the full-scale Nereda® plant in Garmerwolde; the data points were used to fit the a and b parameters of equation 3.7.

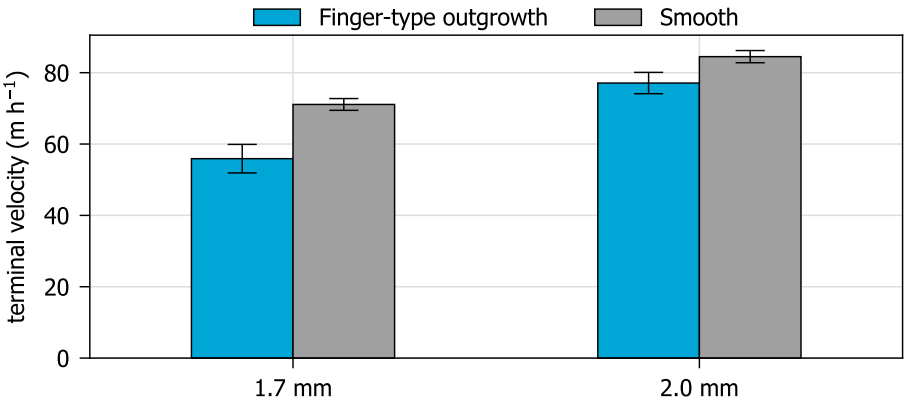

Figure 3.5: Comparison of settling velocity of smooth granules and granules with finger-type outgrowth. Granules from the Nereda® plant in Garmerwolde.

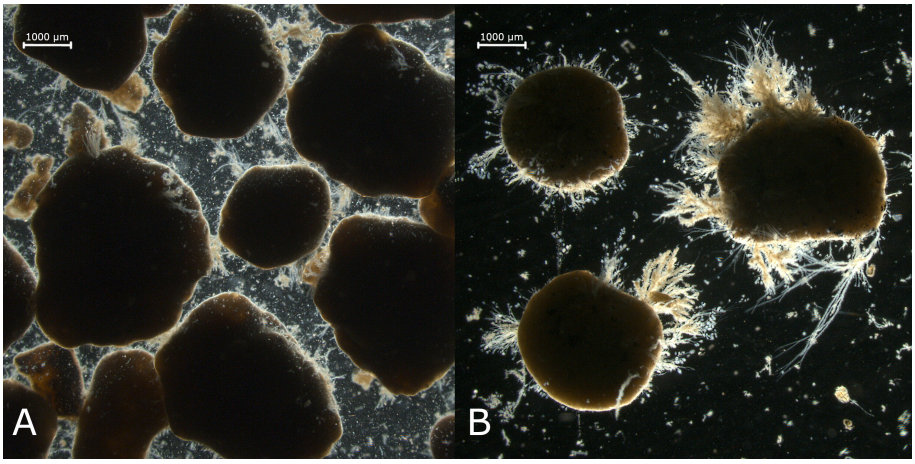

Figure 3.6: Comparison of smooth granules (A) and granules with finger-type outgrowth (B). Granules from the Nereda® plant in Garmerwolde.

3.3.2. Bed expansion

The results of the bed expansion experiment for granules from the PNU of sizes between 1 mm and 2 mm are shown in Figure 3.7. The experiment was started with a sludge bed of 47 cm of sieved granules. The voidage fraction of de sludge bed was 51.9 %. The up-flow velocity was increased in steps from 6.0 m h^{-1} to 14.1 m h^{-1}. At an up-flow velocity of 14.1 m h^{-1} some of the granules started to wash out, because the top of the sludge blanket reached the outlet of the column. Subsequently the up-flow velocity was reduced in steps from 14.1 m h^{-1} to 3.3 m h^{-1}. After the experiment some segregation in the sludge bed could be noticed, showing larger granules at the bottom of the column and smaller granules at the top of the sludge blanket.

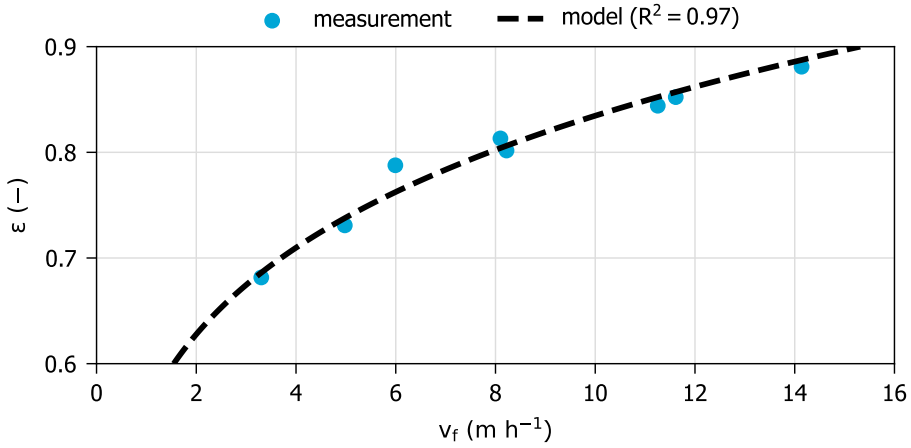

Figure 3.7: Bed expansion experiment with sieved granules (1 to 2 mm) from the Prototype Nereda® Utrecht; data points were used to fit the extrapolated fluidizing velocity and the expansion index according to equation 3.9.

The data from the bed expansion experiment were used to estimate the parameters of the Richardson and Zaki model. At an average granule size of 1.5 mm we found a value of v_f of 29.9 m h^{-1} and an expansion index n of 5.65. The extrapolated fluidizing velocity v_f of 29.9 m h^{-1} is 50 % lower than the terminal velocity for granules of 1.5 mm calculated with equation 3.6 to 3.8 and the parameters for a and b calculated in the previous paragraph, which yield a v_t of 60.4 m h^{-1}.

3.3.3. Full-scale bed settling

In the full-scale Nereda® reactor in Utrecht a settling experiment was performed to measure the settling of a mature granular bed. The results were used to validate the multi-disperse settling model. The parameters that were identified using the sludge from Garmerwolde and from the Prototype Nereda® in Utrecht were used in this multi-disperse settling model for the full-scale Nereda® in Utrecht. Since

all three plants are treating domestic wastewater, we expect that the observed parameters are valid for granular sludge reactors operated with similar type of domestic wastewater.

The granule size distribution of the sludge bed is shown in Table 3.2. The table also shows the class average diameter, which is used in the model.

class (μm)	class mean diameter (μm)	concentration ($kg\,m^{-3}$)
0-212	106	1.28
212-425	318	0.82
425-630	527	0.28
630-1000	815	0.63
1000-1400	1200	1.03
1400-2000	1700	1.39
>2000	3000	1.22

Table 3.2: Granule size distribution in the full-scale Nereda® of Utrecht.

In Figure 3.8 an example of the results is shown. The figure shows the measurements and simulation results for the different granule fractions at the start of the experiment (0 min) and after 15 min of settling. The concentration of the granule fraction is shown on the x-axis and the depth below the water surface is shown on the y-axis. At the start of the simulation the reactor is assumed to be completely mixed. In the experiment this was done by intense aerating for 20 min. After the aeration was stopped the sludge started to settle.

After 15 min the model shows that the largest fraction (>2000 mm) is almost settled, and granules are stacking on top of each other at the bottom of the reactor. The model calculates that at the bottom the minimum voidage fraction is already reached after 5 min. On the other hand, the smallest fraction (212 to 425 μm) only just started to settle. Only in first meter from the top of the reactor a decrease of this fraction can be seen in the model results. At the sampling point 2 m below the water surface even no change compared to the start was detected, which is also observed in the model results. Only at the bottom first meter of the reactor an increase of this fraction can be seen. The measured sludge concentrations are well resembled by the model for all fractions.

For the middle fractions and especially for the fraction of 1400 to 2000 μm a peak in the solids concentration can be seen at a depth just below 6 m. This is caused by the lower concentration of the largest fraction at this water depth, because this fraction is already almost completely settled below 6 m. The smaller fractions settle on top of the larger fraction, allowing for the smaller fractions to reach higher concentrations.

Figure 3.9 shows the measurements and simulation results for the granule fraction between 1000 and 1400 μm. For every time frame the concentration of the granule fraction is shown on the x-axis and the depth below the water surface is shown on the y-axis. After 5 min no change was measured at the sampling points, which is resembled by the model. After 10 min the concentrations at the upper sampling point goes down and the concentration at the lower sampling point goes up. This behaviour is also resembled by the model, although at the lower sampling point the concentrations seems to increase a bit faster than in the model.

After 15 min and 17 min the model and the sampling show similar behaviour.

The results for the other fractions also showed a good agreement between model and the measurements performed at the full-scale installation. These results can be found in appendix A.

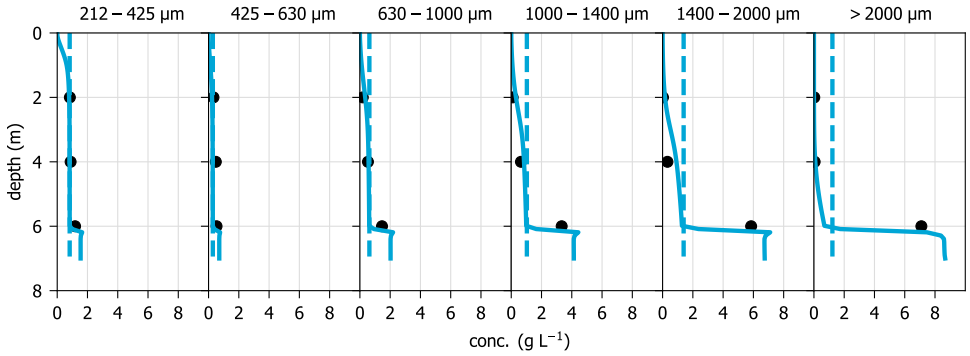

Figure 3.8: Settling of 6 classes of granules in a full-scale Nereda® reactor in Utrecht after 0 minutes and after 15 minutes; model results (dashed line: 0 minutes, solid line: 15 minutes) and measurements (dots).

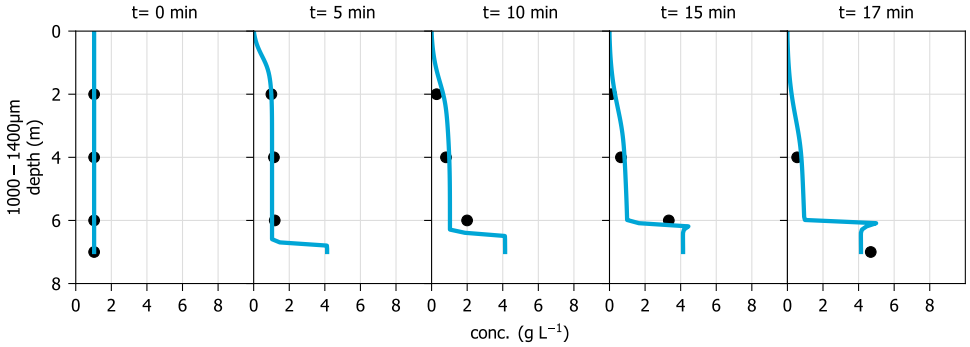

Figure 3.9: Settling of granules of sizes between 1000 and 1400 µm in a full-scale Nereda® reactor in Utrecht; model results (line) and measurements (dots) at settling times between 0 min and 17 min.

3.4. Discussion

3.4.1. Terminal settling velocity

This study showed that the terminal settling velocity of aerobic granular sludge can be well described by a model based on Newtonian drag. The proposed formula to calculate the drag coefficient (equation 3.17) was tested for particle Reynolds numbers between 1 and 50. The coefficients of the formula are different from the values reported in literature [18] for biofilm coated particles. This is not remarkable since the average density of the aerobic sludge granules used in this study was

considerably lower than the density of the biofilm coated particles.

$$C_D = 22.57Re^{-0.690} \qquad 1 < Re < 50 \tag{3.17}$$

3.4.2. Bed expansion characteristics

The bed expansion experiment showed good correlation with the Richardson and Zaki model (equation 3.9). In the experiment sieved granules were used in the range of 1 mm to 2 mm. The experiment yielded an expansion index n of 5.65 for an average granule size of 1.5 mm, which is close to the value of 5.79 given by equation 3.11. The ratio between the terminal velocity v_t and the extrapolated fluidizing velocity v_i was close to 0.5. For biofilm-coated particles a value of 0.8 was found by [18]. According to [18] it is not uncommon for large low-density solids that this ratio is lower than unity, but no explanation was given.

3.4.3. Full-scale validation

As shown in the full-scale experiment in the Nereda® reactor in Utrecht, a mature aerobic granular sludge bed can consist of a wide range of granule sizes. The difference in setting velocity can be an order of magnitude, leading to segregation in the sludge bed: the largest granules will settle much faster than the smallest granules. This leads to a high concentration of large granules at the bottom of the reactor after only a few minutes of settling, while the smallest granules are still distributed throughout the reactor. To describe this behaviour a single fraction Richardson and Zaki model does not suffice and a multi-disperse version of the Richardson and Zaki model was adopted, using the Patwardhan and Tien extension. With this extended model it was possible to describe the settling experiments performed at the full-scale Nereda® reactor in Utrecht well, without any further calibration of the model.

3.4.4. Selection pressure

In AGS reactors a hydraulic selection pressure to selectively retain granules over flocs is applied. This is especially relevant during the start-up phase when granules are still relatively small. The differential settling rate of granules and flocs is essential for this selection process. Excess sludge is typically removed from the top of the sludge blanket after a settling period, removing the slower settling sludge (flocculent matter, small granules or eroded material from larger granules) from the reactor and thereby selecting for the better settling granules in the reactor. Using the hydraulic selection pressure as a sludge wasting mechanism is a good method for making the cut-off between granules and flocs and it is often used as the only sludge wasting mechanism. The downside of using the selection pressure as the only wasting mechanism is that it does not directly influence the granule size distribution. This is important, because the granule size distribution will influence overall nutrient removal. The differences in diffusion limitation into the granules and differences in overall MLSS concentrations will lead to different nutrient removal rates [34–36].

Using the model, it can be shown that different stable granule size distributions

can exist at the same selection pressure. A uniform sludge bed with granules of 700 µm can be as stable regarding selection pressure as a disperse bed with granules in the range of 200 to 5000 µm. This is shown in Figure 3.10. After 30 minutes of settling the bed height of the uniform bed and the disperse bed are equal. However, when granules grow too large, they become difficult to suspend by aeration and they will get diffusion-limited during the anaerobic feeding phase. Therefore, it is necessary to remove both selection sludge and excess granular sludge in aerobic granular sludge reactors with a well-developed sludge bed. This implies that a dynamic selection pressure is needed to control the granule size distribution in the reactor. In full-scale reactors this can be done by increasing the selection pressure to remove specific granule sizes. The here developed model combined with a bioconversion model [35] could be used to predict the optimal selection pressure and granule size for every cycle of an AGS reactor.

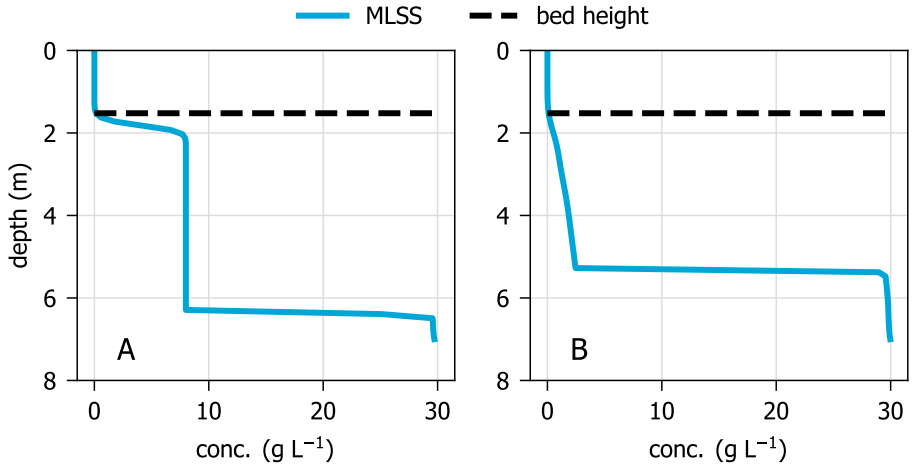

Figure 3.10: Comparison of the settling of a uniformly sized (A) and a disperse (B) granular sludge bed both after 30 minutes of settling. Left: uniform bed with 8 g L^{-1} granules of 700 µm, right: disperse bed with 8 g L^{-1} (sizes: 318, 527, 815, 1200, 1700 and 3000 µm; concentration: 1, 1, 1, 1, 2 and 2 g L^{-1}).

3.4.5. Differences between settling of flocs and granules

Figure 3.11 schematically shows the effect of the degree of particle coherence on the settling behaviour of sludge particles. Conventional activated sludge flocs typically reside on the right part of this schematic: small flocs coagulate into larger flocs adapting a zone settling regime and at higher concentrations, under influence of the surrounding sludge flocs, a compression regime. In contrast, aerobic granules typically reside on the left side of the schematic: per definition they do not coagulate [17] and will remain in the particle settling regime even at high concentrations. As shown in the full-scale experiment in the Nereda® reactor in Utrecht, after reaching the minimum voidage fraction the granules are stacked on top of each other, and they do not undergo an extensive compression regime.

This will especially be the case for laboratory AGS reactors. In a full-scale AGS reactor a mature granular bed will typically have a fraction of 1 to 2 kg m^{-3} smaller than 200 µm because of wash-in of suspended solids in the influent, sheared off parts of large granules and because of less optimal sludge selection compared to a laboratory reactor. The fraction smaller than 200 µm will also for a part consist of proto-granules. The question arises if the multi-disperse Richardson and Zaki also applies for the non-granular fraction smaller than 200 µm. In the full-scale test this fraction was not measured, so no data is available. Although the floc fraction was not taken into account in the full-scale experiment in Utrecht there was a good resemblance between measurements and model, also for the smallest granule fractions. If the non-granular fraction would have a large impact on the settling behaviour of the granules, it would likely be influencing the smallest fractions. This was not observed in the experiment. It therefore appears that the effect of flocs on the settling behaviour was limited in the experiment. In chapter 5 a slightly modified version of the model is used, which better describes the settling of the proto-granules and flocs.

3.4.6. Sludge morphology

Figure 3.5 shows the difference in terminal velocity of smooth spherical granules and granules with outgrowth on the sphere surface. A difference of 27 % was measured for granules of 1.7 mm. No measurements were done on the interaction between granules with outgrowth in a sludge bed, but it is expected that in a reactor with many granules with outgrowth on the surface the settling velocity will be even more reduced. When an AGS reactor is operated at a certain selection pressure, a sudden increase of granules with outgrowth can lead to a drop in the sludge concentration in the reactor, because many granules with outgrowth will be removed via sludge selection (which typically is set to maintain a constant sludge bed height after the set settling time). Small changes in granule morphology therefore can have a major impact on the stability of the granular bed and ultimately effluent quality can be affected.

3.4.7. Potential applications of the settling model

To show the effect of the granule size distribution on nutrient removal in full-scale aerobic granular sludge reactors, a settling model is required, since nitrogen and phosphorus removal will depend on both sludge concentration and granule size [37]. Large granules will be more diffusion-limited for processes requiring oxygen in comparison to small granules [38]. Small granules will therefore have a lower anoxic volume and their contribution to simultaneous denitrification will consequently be less. Moreover, larger granules will reside more at the bottom of the reactor because of superior settling behaviour. Since the currently used batch fed reactor types are fed from the bottom [34], large granules will receive more COD during anaerobic uptake. The combination of larger granules storing more COD during anaerobic feeding and larger granules being more diffusion-limited for oxygen during aeration gives them a large role in simultaneous nitrification/denitrification [39]. Our proposed settling model could be combined with already existing

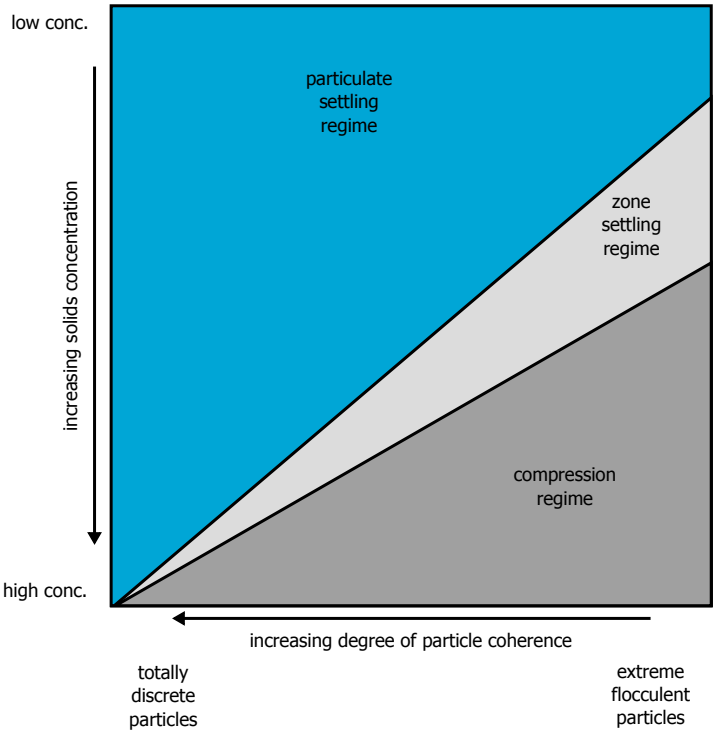

Figure 3.11: Effect of particle coherence on settling behaviour, adapted from Perry [16].

conversion models to gain more insight in the influence of settling and segregation of granules on overall conversion rates. The model could also be used for optimizing other operational parameters, such as the MLSS concentration, mixing energy and aeration strategy.

Another potential application of the multi-disperse settling model is in the understanding of continuously fed AGS reactors. These reactors are currently under development [40, 41]. Conventional activated sludge systems operated with clarifiers for sludge/water separation will require different design and operation, when the sludge partially consists of granules. Larger granules will settle faster than small granules and flocs, resulting in a different distribution of granules and flocs over the clarifier depth. This differential sedimentation can even be used to perform a form of sludge selection [41]. The flow patterns in a final clarifier are more complex than in batch wise operated granular sludge reactors with feeding from the bottom and need to be better investigated. The here proposed multi-disperse settling model in combination with a CFD model can be used to investigate and optimize the clarification process in traditional settlers of continuous AGS reactors.

3.5. Conclusion

A multi-dispersed settling model was made describing the settling and fluidization of aerobic granular sludge. Validation of this model with measurements in a full-scale AGS reactor showed a good resemblance between model and measurements.

- The model is based on the Richardson and Zaki model for multi-disperse particles.
- A relation between granule size and drag coefficient was established describing the terminal velocity of individual granules based on granule size.
- The parameters of the Richardson and Zaki model were measured with mono-disperse granules. The extrapolation at a voidage of unity of the fluidizing velocity is approximately 50 % of the terminal settling velocity.
- The model can be used for optimizing the selection pressure in AGS reactors and for improving nutrient removal. The presented results can be used to better understand the granulation process and can be valuable for future research of continuously fed AGS reactors.

Bibliography

[1] E. J. H. van Dijk, M. Pronk, and M. C. M. van Loosdrecht, *A settling model for full-scale aerobic granular sludge,* Water Res. **186**, 116135 (2020).

[2] M. Henze, M. C. M. van Loosdrecht, G. Ekama, and D. Brdjanovic, *Biol. Wastewater Treat. Princ. Model. Des.* (IWA Pub., London, 2008) pp. 307–334.

[3] I. Takács, G. G. Patry, and D. Nolasco, *A dynamic model of the clarification-thickening process,* Water Res. **25**, 1263 (1991).

[4] P. A. Vesilind, *Design of prototype thickeners from batch settling tests,* Water Sew. Work. **115**, 302 (1968).

[5] E. Torfs, S. Balemans, F. Locatelli, S. Diehl, R. Bürger, J. Laurent, P. François, and I. Nopens, *On constitutive functions for hindered settling velocity in 1-D settler models: Selection of appropriate model structure,* Water Res. **110**, 38 (2017).

[6] J. J. Heijnen and M. C. M. van Loosdrecht, *Method for acquiring grain-shaped growth of a microorganism in a reactor,* (1998).

[7] M. Pronk, M. K. de Kreuk, L. M. M. de Bruin, P. Kamminga, R. Kleerebezem, and M. C. M. van Loosdrecht, *Full scale performance of the aerobic granular sludge process for sewage treatment,* Water Res. **84**, 207 (2015).

[8] H. F. van der Roest, L. M. M. de Bruin, G. Gademan, and F. Coelho, *Towards sustainable waste water treatment with Dutch Nereda® technology,* Water Pract. Technol. **6**, 1 (2011).

[9] S. Adav, D. J. Lee, K. Y. Show, and J. H. Tay, *Aerobic granular sludge: Recent advances,* Biotechnol. Adv. **26**, 411 (2008).

[10] D. Gao, L. Liu, H. Liang, and W. M. Wu, *Aerobic granular sludge: Characterization, mechanism of granulation and application to wastewater treatment,* Crit. Rev. Biotechnol. **31**, 137 (2011).

[11] M. K. H. Winkler, J. P. Bassin, R. Kleerebezem, R. G. J. M. van der Lans, and M. C. M. van Loosdrecht, *Temperature and salt effects on settling velocity in granular sludge technology,* Water Res. **46**, 3897 (2012).

[12] A. Nor Anuar, Z. Ujang, M. C. M. van Loosdrecht, and M. K. de Kreuk, *Settling behaviour of aerobic granular sludge,* Water Sci. Technol. **56**, 55 (2007).

[13] B. J. Ni, W. M. Xie, S. G. Liu, H. Q. Yu, Y. Z. Wang, G. Wang, and X. L. Dai, *Granulation of activated sludge in a pilot-scale sequencing batch reactor for the treatment of low-strength municipal wastewater,* Water Res. **43**, 751 (2009).

[14] Y. Liu, W. W. Wang, Y. Q. Liu, L. Qin, and J. H. Tay, *A generalized model for settling velocity of aerobic granular sludge,* Biotechnol. Prog. **21**, 621 (2005).

[15] E. J. H. van Dijk, M. Pronk, and M. C. M. van Loosdrecht, *Controlling effluent suspended solids in the aerobic granular sludge process,* Water Res. **147**, 50 (2018).

[16] R. H. Perry, D. W. Green, and J. O. Maloney, *Perry's Chemical Engineers' Handbook*, 7th ed. (McGraw-Hill, New York, 1997) pp. 18–60.

[17] M. K. de Kreuk, N. Kishida, and M. C. M. van Loosdrecht, *Aerobic granular sludge - State of the art,* Water Sci. Technol. **55**, 75 (2007).

[18] C. Nicolella, M. C. M. van Loosdrecht, R. Di Felice, and M. Rovatti, *Terminal settling velocity and bed-expansion characteristics of biofilm coated particles,* Biotechnol. Bioeng. **62**, 62 (1999).

[19] L. Qin, J. H. Tay, and Y. Liu, *Selection pressure is a driving force of aerobic granulation in sequencing batch reactors,* Process Biochem. **39**, 579 (2004).

[20] Y. Cui, J. Ravnik, P. Steinmann, and M. Hriberšek, *Settling characteristics of nonspherical porous sludge flocs with nonhomogeneous mass distribution,* Water Res. **158**, 159 (2019).

[21] P. Dold, B. Alexander, G. Burger, M. Fairlamb, D. Conidi, C. Bye, and W. Du, *Modeling full-scale granular sludge sequencing tank performance,* 91st Annu. Water Environ. Fed. Tech. Exhib. Conf. WEFTEC 2018 , 3813 (2019).

[22] T. R. Kent, C. B. Bott, and Z. W. Wang, *State of the art of aerobic granulation in continuous flow bioreactors,* Biotechnol. Adv. **36**, 1139 (2018).

[23] V. S. Patwardhan and C. Tien, *Sedimentation and liquid fluidization of solid particles of different sizes and densities,* Chem. Eng. Sci. **40**, 1051 (1985).

[24] J. F. Richardson and W. N. Zaki, *Sedimentation and fluidisation: Part I,* Chem. Eng. Res. Des. **75**, S82 (1954).

[25] T. Etterer and P. A. Wilderer, *Generation and properties of aerobic granular sludge,* Water Sci. Technol. **43**, 19 (2001).

[26] M. K. H. Winkler, R. Kleerebezem, M. Strous, K. Chandran, and M. C. M. van Loosdrecht, *Factors influencing the density of aerobic granular sludge,* Appl. Microbiol. Biotechnol. **97**, 7459 (2013).

[27] J. J. Beun, M. C. M. van Loosdrecht, and J. J. Heijnen, *Aerobic granulation in a sequencing batch airlift reactor,* Water Res. **36**, 702 (2002).

[28] R. Di Felice, *A relationship for the wall effect on the settling velocity of a sphere at any flow regime,* Int. J. Multiph. Flow **22**, 527 (1996).

[29] T. E. Baldock, M. R. Tomkins, P. Nielsen, and M. G. Hughes, *Settling velocity of sediments at high concentrations,* Coast. Eng. **51**, 91 (2004).

[30] R. Di Felice, *Hydrodynamics of liquid fluidisation,* Chem. Eng. Sci. **50**, 1213 (1995).

[31] M. Andalib, J. Zhu, and G. Nakhla, *A new definition of bed expansion index and voidage for fluidized biofilm-coated particles,* Chem. Eng. J. **189-190**, 244 (2012).

[32] L. T. Mulcahy and W. K. Shieh, *Fluidization and reactor biomass characteristics of the denitrification fluidized bed biofilm reactor,* Water Res. **21**, 451 (1987).

[33] W. C. Yang, *Handb. Fluid. Fluid-Particle Syst.* (CRC Press, 2003) pp. 706–733.

[34] M. K. de Kreuk, J. J. Heijnen, and M. C. M. van Loosdrecht, *Simultaneous COD, nitrogen, and phosphate removal by aerobic granular sludge,* Biotechnol. Bioeng. **90**, 761 (2005).

[35] B. J. Ni and H. Q. Yu, *Mathematical modeling of aerobic granular sludge: A review,* Biotechnol. Adv. **28**, 895 (2010).

[36] F. Y. Chen, Y. Q. Liu, J. H. Tay, and P. Ning, *Operational strategies for nitrogen removal in granular sequencing batch reactor,* J. Hazard. Mater. **189**, 342 (2011).

[37] M. K. de Kreuk, C. Picioreanu, M. Hosseini, J. B. Xavier, and M. C. M. van Loosdrecht, *Kinetic model of a granular sludge SBR: Influences on nutrient removal,* Biotechnol. Bioeng. **97**, 801 (2007).

[38] J. Pérez, C. Picioreanu, and M. C. M. van Loosdrecht, *Modeling biofilm and floc diffusion processes based on analytical solution of reaction-diffusion equations,* Water Res. **39**, 1311 (2005).

[39] J. B. Xavier, M. K. de Kreuk, C. Picioreanu, and M. C. M. van Loosdrecht, *Multi-scale individual-based model of microbial and byconversion dynamics in aerobic granular sludge,* Environ. Sci. Technol. **41**, 6410 (2007).

[40] T. R. Devlin and J. A. Oleszkiewicz, *Cultivation of aerobic granular sludge in continuous flow under various selective pressure,* Bioresour. Technol. **253**, 281 (2018).

[41] J. Zou, Y. Tao, J. Li, S. Wu, and Y. Ni, *Cultivating aerobic granular sludge in a developed continuous-flow reactor with two-zone sedimentation tank treating real and low-strength wastewater,* Bioresour. Technol. **247**, 776 (2018).

4

Nitrous oxide emission

The nitrous oxides emission was measured over 7 months in the full-scale aerobic granular sludge plant in Dinxperlo. Nitrous oxide concentrations were measured in the bulk liquid and the off-gas of the Nereda® reactor. Combined with the batch wise operation of the reactor, this gave a high information density and a better insight into nitrous oxide emission in general. The average emission factor was 0.33 % based on the total nitrogen concentration in the influent. The yearly average emission factor was estimated to be between 0.25 % and 0.30 % of the nitrogen load. The average emission factor is comparable to continuous activated sludge plants, and it is low compared to other sequencing batch systems. The variability in the emission factor increased when the reactor temperature was below 14 °C, showing higher emission factors during the winter period. A change in the process control in the winter period reduced the variability, reducing the emission factors to a level comparable to the summer period. Different process control might be necessary at high and low temperatures to obtain a consistently low nitrous oxide emission. Rainy weather conditions lowered the emission factor, both in the rainy weather batches and the subsequent dry weather flow batches. This was attributed to the first flush from the sewer at the start of rainy weather conditions, resulting in a temporarily increased sludge loading.

Parts of this chapter have been published in Water Research **198**, 117159 (2021) [1].

4.1. Introduction

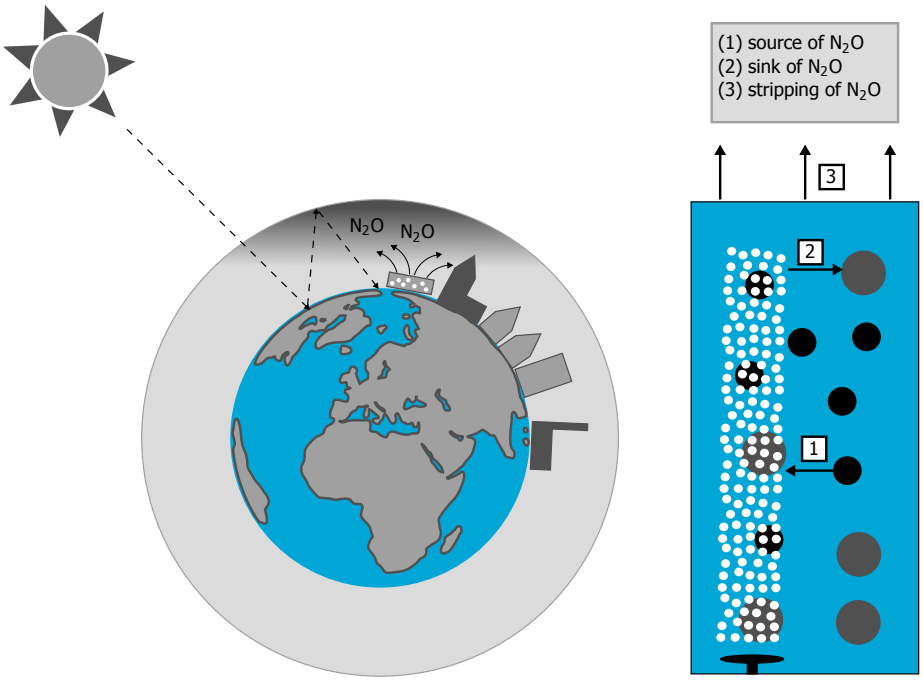

Figure 4.1: Graphical abstract.

Nitrous oxide is a greenhouse gas contributing to global warming. Nitrous oxide has a 298 times greater effect on global warming than carbon dioxide [2]. Nitrous oxide can be produced as a by-product of nitrification and denitrification processes [3]. Although in general only a small fraction of the influent ammonium is emitted as nitrous oxide, the large greenhouse warming potential can make nitrous oxide emission the dominant factor in the carbon footprint of a wastewater treatment plant [4, 5]. Emission of nitrous oxide has been studied for many wastewater treatment process configurations under many process conditions, showing a wide range of Emission Factors (EFs). These emission factors, defined as the amount of nitrous oxide emitted relative to the nitrogen load to the plant, generally fall between 0 % and 5 %, but higher values are also reported [6].

Several pathways are shown to be of importance for nitrous oxide production in the wastewater treatment process [7, 8]. In the nitrification process, the intermediate product hydroxylamine can be oxidized to nitrous oxide (both biologically and chemically). Under oxygen-limited conditions, nitrifiers can denitrify nitrite to nitrous oxide, the so-called nitrifier-denitrification pathway. Under anoxic conditions nitrous oxide can be produced by heterotrophic denitrifiers by imbalanced enzyme activity, nitrite accumulation or lack of biodegradable COD [8]. At the same time denitrification can be a sink for nitrous oxide, when the reducing capacity of

nitrous oxide exceeds the production capacity during denitrification [9]. Fluctuating influent concentrations and seasonal variations in full scale plants combined with the variety of pathways leading to nitrous oxide formation make it very complex to find the underlying processes that lead to elevated nitrous oxide emissions [4, 6].

Research on nitrous oxide emissions has mainly focused on wastewater treatment processes with flocculent sludge and few laboratory studies have been performed with aerobic granular sludge [10]. This is mainly because the AGS process is a relatively new wastewater treatment process. For the Nereda® process, only short-term (2 weeks) measurements were reported in a pilot reactor and the full-scale reactor in Epe. Both showed an average nitrous oxide emission factor of about 0.7 % of the total nitrogen in the influent [11], which is comparable to conventional activated sludge plants. However, other studies have shown that to get reliable data on nitrous oxide emissions long-term measurement campaigns are required [4, 6, 12].

There are several laboratory studies reporting on nitrous oxide formation in AGS reactors. These studies reported a wide range of emission factors from 1 % [13] to 22 % [14]. Due to the strong deviation from conditions in full-scale reactors in these experiments, it is uncertain how relevant the reported values are regarding full-scale installations. Laboratory systems are very good at isolating a specific parameter, but translation towards full-scale wastewater treatment plants is challenging because of differences in influent composition, process control and reactor design and operation.

Because of the potentially significant contribution to the carbon footprint of full-scale AGS processes, it is important to quantify the nitrous oxide emission factors. Hereto the nitrous oxide emission from a full scale Nereda® plant treating domestic wastewater was monitored for 7 consecutive months. Two different methods were used to measure the nitrous oxide emissions, namely by measuring the nitrous oxide concentrations continuously in the water phase and by measuring it in the off-gas during aeration. The former has the advantage of showing nitrous oxide kinetics under anoxic conditions, when the aeration is turned off. The latter has the benefit of measuring the direct nitrous oxide emission without the need for a conversion algorithm. Combined with the dynamic behaviour of the repeated batch-wise operated system, a high information density could be obtained on the nitrous oxide behaviour from the plant. The goal was to get better insight in the nitrous oxide emissions of the full-scale AGS process, as well as to understand the major factors preventing and leading to elevated nitrous oxide emissions in full scale AGS systems.

4.2. Methodology

4.2.1. Plant description

All the measurements took place at the Dinxperlo wastewater treatment plant (see also section 1.4). The influent consists mainly of domestic wastewater (see Table 4.1), treating on average 3100 $m^3\,d^{-1}$, with a peak flow of 570 $m^3\,h^{-1}$. Current effluent requirements are: COD of 125 $mg\,L^{-1}$, total nitrogen of 15 $mg\,L^{-1}$, total

phosphorus of 2 mg L^{-1}, and total suspended solids of 30 mg L^{-1}, all yearly averaged values. On top of this, the effluent requirement for phosphorus is 1 mg L^{-1} in the summer and 3 mg L^{-1} in the winter. The influent is collected in an influent buffer and then treated in one of the three Nereda® reactors. The effluent is polished by means of a sand filter with the possibility of iron dosing to remove remaining phosphorus.

Figure 4.2: Photograph of the wastewater treatment plant in Dinxperlo. The Nereda® reactors are located on the right, attached to the building with the sloped roof. The sludge buffer and the sand filter are located to the right of the Nereda® reactors. The inlet works, including the influent buffer are located at the bottom. The old pre-existing aeration tank and clarifier on the left are now part of a public water garden (on the top).

4.2.2. Nitrous oxide measurements

The nitrous oxide emission from the reactor was measured by determining the nitrous oxide concentration in the off-gas of the reactor during aeration (Figure 4.3). A polyethylene floating hood with a cross-sectional area of 0.55 m^2 was used to capture the air escaping the surface area of the reactor during aeration. The inside of the hood was partially filled with polyurethane foam to reduce the headspace and limit the gas retention time to the analysers. Part of the off-gas that passed through the hood was transported via a transparent hose and cooled to 4 °C to remove the moisture. The gas concentrations were measured in two online gas analysers (Rosemount NGA 2000 MLT for oxygen and carbon dioxide; Servomex 4900 for methane and nitrous oxide). Calibration of the analysers was performed using gas cylinders containing known concentrations of the studied gases. For accurate calculations, the temperature, pressure and relative humidity of the outside

air were also measured, using a micro sensor (Bosch BME280). The nitrous oxide concentrations were converted into mass fluxes using the method described by Baeten [15].

Additional to the nitrous oxide concentration in the off-gas, the nitrous oxide concentration in the bulk liquid was measured using a nitrous oxide sensor from Unisense Environment. This sensor was placed a meter below the water surface of the reactor.

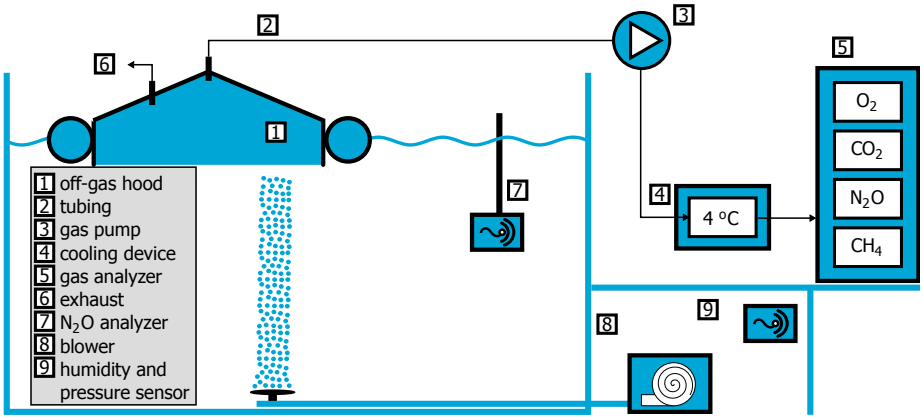

Figure 4.3: Schematic representation of the off-gas measurement set-up. Both reactor off-gas and outside air were cooled to 4 °C to remove the moisture before it passed through the analysers.

4.2.3. Size distribution

The granule size distribution of the aerobic granular sludge in the reactors was measured by pouring a sample of the sludge over a series of sieves with different mesh sizes 212, 425, 630, 1000, 1400 and 2000 µm. A mixed sample of 100 mL was filtered for the determination of the total dry weight. The obtained granular biomass of the different sieve fractions and the mixed sample were dried at 105 °C until no change in weight was detected anymore.

4.2.4. Online measurements

The reactor was equipped with probes for dissolved oxygen and temperature (Hach; LDO), redox potential (Hach; Redox), water level (Endress+Hauser, radar), suspended solids (Hach, SOLITAX TS), and nitrate (Hach; NITRATAX). Ammonium and phosphate were continuously measured using a filter unit and auto sampling device (Hach; FILTRAX, AMTAX and PHOSPHAX). The filter unit was situated 0.5 m below the water surface. Sampling was done at an interval of 5 min.

4.2.5. Offline sampling

Samples for analyses of influent and effluent were collected using refrigerated auto samplers, collecting 24-hours flow-proportional samples for both influent and

effluent. The chemical analyses of COD, total nitrogen, ammonium, phosphate, nitrite and nitrate in the reactor were performed by using the appropriate Hach Lange cuvette kits.

4.2.6. Emission factors

Offline samples were taken every 14 days. To calculate the emission factor, a total nitrogen concentration in the influent ($c_{TN,in}$) per batch was needed. Therefore, the total nitrogen concentration in the influent was calculated for every batch using the peak ammonium concentration during aeration measured by the analyser ($c_{NH4,max}$), the remaining effluent ammonium concentration of the previous batch measured by the analyser ($c_{NH4,e}$), and the exchange ratio (VER).

$$c_{TN,in} = \frac{c_{NH4,max} - c_{NH4,e}(1 - VER)}{VER} f_{ads} f_{org} \tag{4.1}$$

Here the f_{ads} is the factor compensating for adsorption of ammonium to the granules [16] and f_{org} is the ratio between total nitrogen and ammonium in the influent. The combined effect of these two factors was found by correlating the estimated c_{TN} with the actual values found by the 14 days offline sampling. An average value of $f_{ads}f_{org}$ of 1.79 was found with an r-squared of 0.75.

The emission factor was calculated by dividing the total outgoing load of nitrous oxide with the total incoming load of total nitrogen, according to the following equation:

$$EF = \frac{m_{N2O}}{c_{TN,in} V_{batch}} \tag{4.2}$$

Here m_{N2O} is the total mass of the nitrous oxide in the off-gas of the batch, expressed in mg-N and V_{batch} is the batch size.

4.2.7. Simultaneous nitrification/denitrification

During the aerated phase part of the nitrified nitrogen is directly converted to nitrogen gas because of the anoxic conditions in the granule. The average efficiency of simultaneous nitrification/denitrification (SND) during aeration is expressed as:

$$SND = 1 - \frac{c_{NO_3,e} - c_{NO_3,\min}}{f_{ads} f_{org} c_{NH_4,\max} - c_{NH_4,e} - c_{Norg,e}} \tag{4.3}$$

Here $c_{NO3,min}$ is the minimum nitrate concentration at the start of the aeration phase, $c_{NO3,e}$ is the nitrate concentration at the end of the aeration phase and $c_{Norg,e}$ is the estimated value of the organic nitrogen in the effluent. For the latter a value of 1.5 mg L^{-1} is assumed.

4.2.8. Process control

The aeration was controlled using a novel process control developed for aerobic granular sludge [17]. This control strategy targets a nitrate production rate to maximize simultaneous nitrification/denitrification. As a result, dissolved oxygen levels in the reactor are minimized as is the energy consumption.

During dry weather conditions the reactors have a fixed cycle time of 6 hours. When the flow increases due to rainy weather, the cycle will adapt to treat the increased amount of water. The feeding time will increase from 60 min minutes to 75 min and the feed flow from the buffer increases from about 180 $m^3\,h^{-1}$ to a maximum of 600 $m^3\,h^{-1}$. As a result, the cycle time will decrease to a minimum of 4 h (see Figure 4.4).

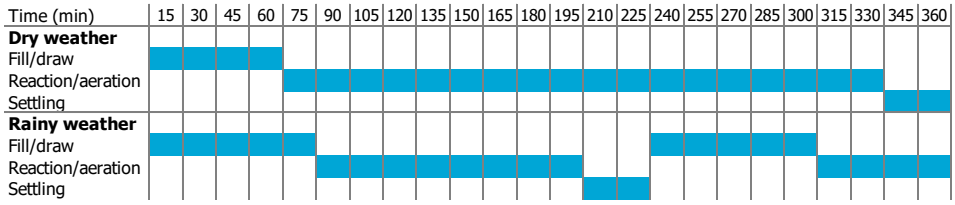

Figure 4.4: Batch scheduling for the Nereda® reactor in Dinxperlo.

4.3. Results

4.3.1. Plant performance and operation

When the trial started the plant was already in operation for four years and the reactors contained an aerobic granular sludge bed with a biomass concentration of 8.0 $g\,L^{-1}$. The three reactors showed normal operation during the whole trial period. The measurements were done in Reactor #1. In Table 4.1 the average influent and effluent quality during the measurement campaign is shown.

Table 4.1: Average influent and effluent composition during the nitrous oxide measurement campaign at the wastewater treatment plant of Dinxperlo (period August 2017 - March 2018).

Parameter	Unit	Influent	Effluent
COD	$mg\,L^{-1}$	531	28
BOD	$mg\,L^{-1}$	202	2.0
N_{tot}-N	$mg\,L^{-1}$	54	6.0
NO_2-N	$mg\,L^{-1}$		0.05
NO_3-N	$mg\,L^{-1}$		3.3
P_{tot}-P	$mg\,L^{-1}$	6.4	1.1
PO_4-P	$mg\,L^{-1}$		0.9
Susp. Sol.	$mg\,L^{-1}$	198	5.0

In Figure 4.5 a typical batch from Dinxperlo is shown. The figure shows online measurements of the concentration of ammonium, nitrate, phosphate and dissolved oxygen during three cycles. Since these sensors were positioned at the top of the reactor, and the reactor was plug flow fed from the bottom, the measurements during feeding represent the effluent concentrations. The cycle started with a feed phase, where influent was added to the bottom of reactor and effluent was decanted from the top simultaneously. After feeding, the reaction phase started, where the reactor was aerated. The reactor was mixed by the aeration. At the start of the aeration phase the concentrations of ammonium and phosphate appear to increase, which was caused by the mixing of the bottom layer with influent water and top

layer with the effluent water. After the reaction phase the biomass was allowed to settle and the cycle restarted for the next batch.

4.3.2. Monthly average nitrous oxide emission

The nitrous oxide emission through off-gas from Reactor #1 was measured from the 9th August 2017 to 18th March 2018 (the water phase sensor was available from the 4th of October 2017). In this period the average nitrous oxide emission factor was 0.33 %.

Figure 4.6 shows the monthly nitrous oxide emissions over the whole measuring period. There was a distinct difference between the summer and autumn period, compared to the winter period. In December the nitrous oxide emission factor started to rise from an average of 0.22 % in the first 4 months to a maximum of 0.64 % in February. In March, the emissions dropped again to the pre-December levels. The average water temperature declined steadily over the same period, from 20.6 °C in August down to 9.7 °C in March 2018.

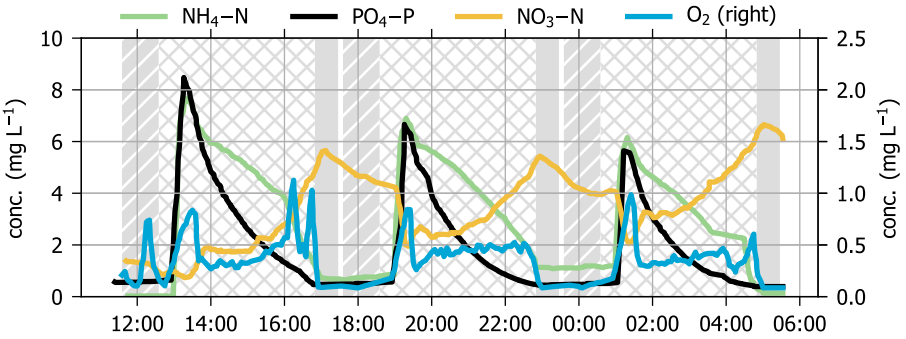

Figure 4.5: Concentration profiles of ammonium (green), nitrate (orange), phosphate (black) and oxygen (blue) for three typical consecutive batches. The grey diagonal striped area indicates the feeding phase, the grey diamond grid shows the reaction phase and the grey solid area shows the settling phase.

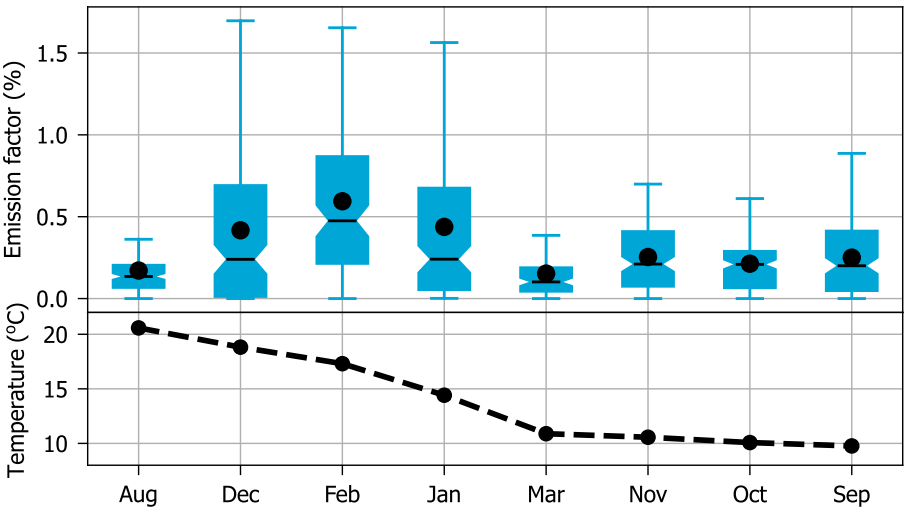

Figure 4.6: Top: boxplot of the monthly averaged nitrous oxide emission factor (the box extends from 25 % to 75 % values, the black line shows the median value, the black dot shows the average value and the wiskers extend the range of the data); bottom: monthly average temperature profile.

4.3.3. Batch average nitrous oxide emission

Figure 4.7 shows the emission factors as well as the water temperature per batch. The graphs show that in the period between August 2017 and mid December 2017 the emission factor for most batches was between 0 % and 0.5 %, with a limited number of batches rising above 0.5 %. In this period the emission factor averaged to 0.22 %. Starting from December 2017 the variability of the emission factors increased. There were still many batches present with an emission factor of almost zero, but the maximum values increased up to 2 %. In the period between December 2017 and the end of February 2018 the emission factor averaged to 0.42 %. Starting from the last week of February 2018 this variability was again comparable to the period before December 2017.

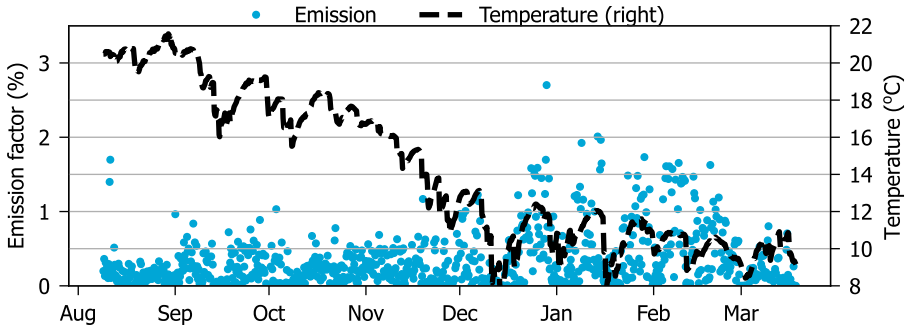

Figure 4.7: Emission factor (blue dots) and average temperature (black dashed line) per batch.

4.3.4. Effect of organic loading rate/N-load

The variability of the nitrous oxide emission factor (and with that the total emission factor) seems to be influenced by the maximum ammonium concentration in the batch (Figure 4.8). The maximum emission factor (up to 2 %) was reached at ammonium concentrations between 5 and 10 mg L^{-1}, but in this range many values close to zero were also measured. At ammonium concentrations below 5 mg L^{-1} and above 10 mg L^{-1}, only few emission factors above 1 % were measured with most values between 0 % and 0.5 %.

4.3.5. Effect of rain events

Figure 4.9 shows the effect of the flow to the plant on the nitrous oxide emission factor. During dry weather flow conditions (DWF) the influent flow ranged between 0 and 150 $m^3 h^{-1}$. Rain weather flow (RWF) conditions are characterized with an influent flow up to 600 $m^3 h^{-1}$ (RWF/DWF ratio of 6). During dry weather flow the emission factor (0.40 %) was higher than during rainy weather flow (0.13 %). Although the total load of nitrogen transported to the plant will not differ much between DWF and RWF conditions, the cycle time was shortened during RWF to handle the increased influent flow. The cycle time for DWF batches was typically 6 hours, while the cycle time for RWF batches was shortened to a minimum of 4

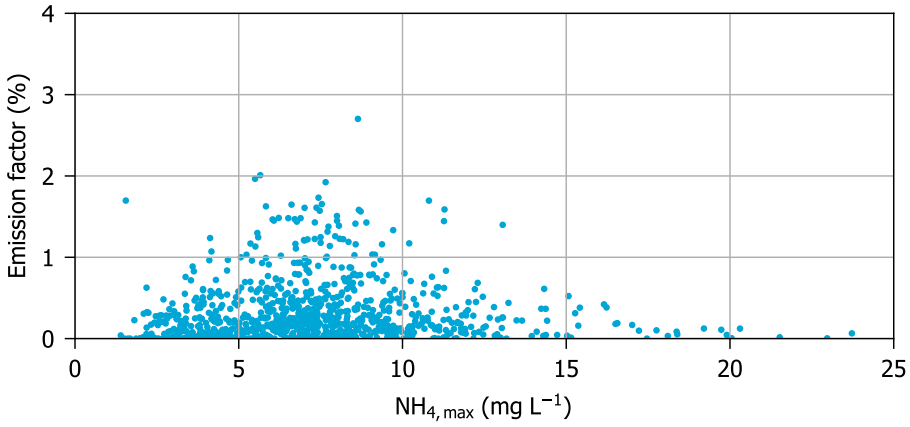

Figure 4.8: The nitrous oxide emission factor related to the ammonium peak calculated per batch.

hours.

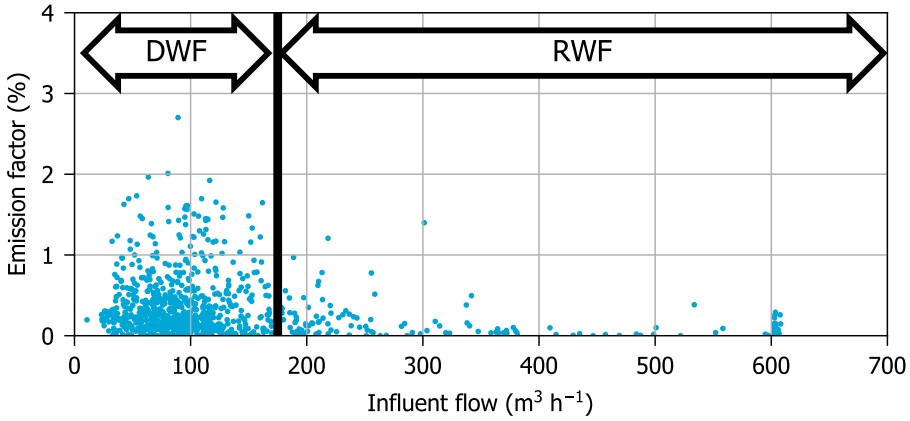

Figure 4.9: Difference in emission factor of nitrous oxide between dry and rainy weather flow conditions.

4.3.6. Effect of temperature

Temperature had some effect on the variability of the emission factor as shown in Figure 4.10. Temperatures above 14 °C resulted for most batches in an emission factor between 0 and 0.50 % while at temperatures below 14 °C the emission factor varied between 0 and 2 %. It is uncertain whether this was solely related to temperature, because in March the temperature was low (average at 10 °C) while the emission factor did not show this increased variability.

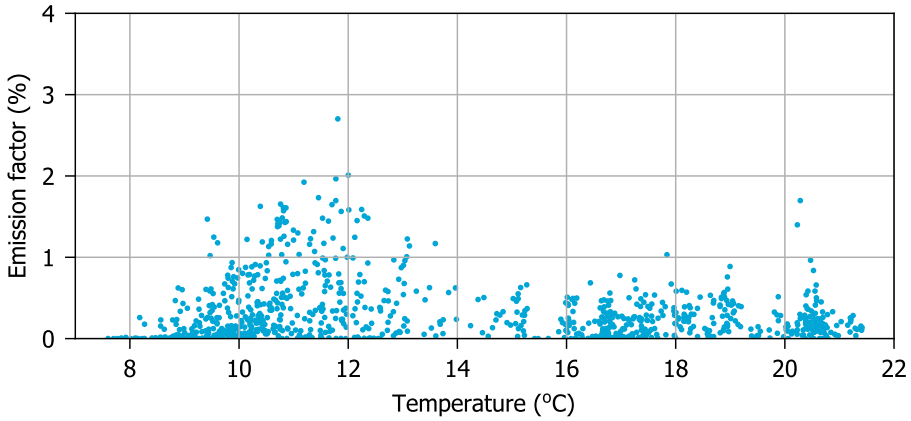

Figure 4.10: Effect of temperature on the nitrous oxide emission factor.

4.3.7. Diurnal pattern

The emission factor did not show a clear diurnal pattern. In Figure 4.11 the average emission factor per batch is shown as a function of the time of the day. The same variability was present as in the previous graphs, leading to a relatively high standard deviation. The values of the batches starting between 3:00h and 16:00h showed a lower emission than the batches between 17:00h and 02:00h. A problem in this analysis was the batch-wise operation of the reactor. The analysis was done based on the starting time of the batch, which was several hours before the actual emission of nitrous oxide was measured. Due to the 6 hours cycle time during DWF out of 1043 batches analysed in this study, only 19 started between 3 AM and 4 AM, while 71 batches started 6 PM and 7 PM.

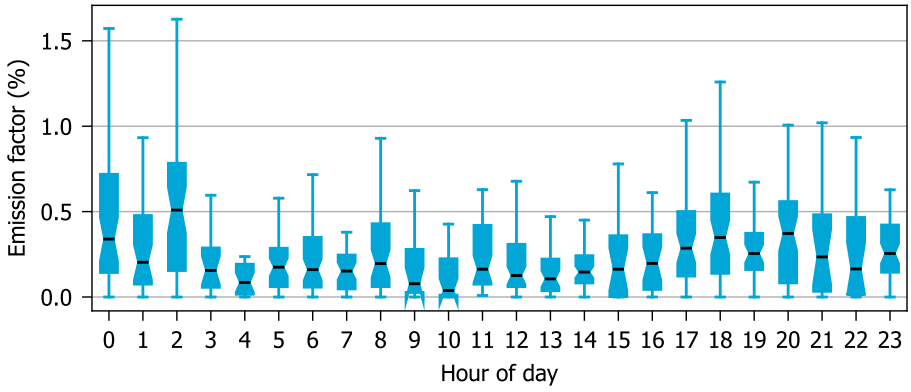

Figure 4.11: Boxplot of the diurnal pattern of nitrous oxide emission. Median value (black) based on start time of the batch (the box extends from 25 % to 75 % values, the black line shows the median value, the whiskers extend the range of the data).

4.3.8. Dynamic nitrous oxide behaviour

The complexity and dynamics of nitrous oxide emissions is illustrated in Figure 4.12. Net production of nitrous oxide as well as net consumption of nitrous oxide was visible in the online measurements. The first batch started [marker 1] without any nitrous oxide in the bulk liquid and therefore also no emission through the off-gas at the start of the aeration phase. At the start of the aeration, the dissolved oxygen concentration increased, and a first peak of nitrous oxide emission could be observed [marker 2]. Also, a simultaneous decrease of the nitrate concentration was observed, caused by mixing of the nitrate remaining from the previous batch with newly fed influent, low in nitrate. When the dissolved oxygen concentration increased further, the nitrous oxide concentration in the bulk liquid and off-gas decreased again (marker [2] to [3]). In this period, the nitrous oxide production rate was lower than the combined effect of stripping through the off-gas and denitrification of nitrous oxide. Further on in the aeration phase, the nitrous oxide concentration in both the bulk liquid and the off-gas increased [marker 3]. Towards the end of the aeration phase the dissolved oxygen concentration was lowered [marker 4] and a sudden increase of the nitrous oxide concentration in the bulk liquid was seen. Hereafter the aeration, and thus mixing, was stopped allowing the biomass to settle [marker 5]. The reactor was ready to receive the next influent batch [marker 5]. During the feeding (marker [5] to [6]) the nitrous oxide concentration in the bulk liquid stayed constant because the sensor was situated at the top of the reactor and the sludge bed had settled to the bottom of the reactor. There was no sludge present in the top layer and no biological processes occurred in the top part of the reactor. After this feeding phase, the aeration phase started again, and the nitrous oxide concentration dropped due to mixing before the production started again [marker 7]. Halfway through the reaction phase, the oxygen concentration in the bulk liquid was lowered [marker 8]. This led to a period where the production of nitrate was limited, but ammonium was still being converted, thus optimizing for simultaneous nitrification and denitrification. After lowering of the oxygen concentration, a similar, although lower, initial increase of the nitrous oxide could be seen [marker 9] as was visible in the previous batch [marker 2]. At the end of this second batch the nitrous oxide was almost completely removed [marker 10].

The process control used here automatically balances nitrification and denitrification to optimize simultaneous nitrification and denitrification to get a maximum total nitrogen removal. This was done by dynamically altering the dissolved oxygen set-point and sometimes this resulted in a drop of the oxygen concentration in the reaction phase as previously described. In Figure 4.14 an example of this behaviour is shown. This seems to trigger a nitrous oxide production response. When the oxygen concentration dropped [marker 1] the nitrous oxide production in the bulk liquid and the off-gas increased [marker 2].

On the 24th of February the process control was changed to a fixed oxygen set-point (2.5 $mg\,L^{-1}$) during the reaction phase, with the reaction phase being split-up in an aeration phase and an unaerated post-denitrification phase. This had an immediate effect on the nitrous oxide production. An example of a batch

under this new process control is shown in Figure 4.14. During the reaction phase, almost no nitrous oxide was produced. Only when the aeration was stopped in the post-denitrification phase, some nitrous oxide was produced, but this did not lead to any emission, because the aeration was switched off and the nitrous oxide was denitrified before the end of the cycle. This change led to a decrease of the emission factor to 0.15 % during the three weeks this process control was used.

The nitrogen removal also changed slightly by the change in the process control. The average ammonium effluent concentration was 10 % higher (3.2 mg L^{-1} after the change, compared to 2.9 mg L^{-1} before the change). The average nitrate effluent concentration was similar under both process controls (5.3 mg L^{-1}). The SND efficiency over the whole period was 69 $\pm$ 15 %. It was 58 $\pm$ 12 % after the change compared to 70 $\pm$ 15 %.

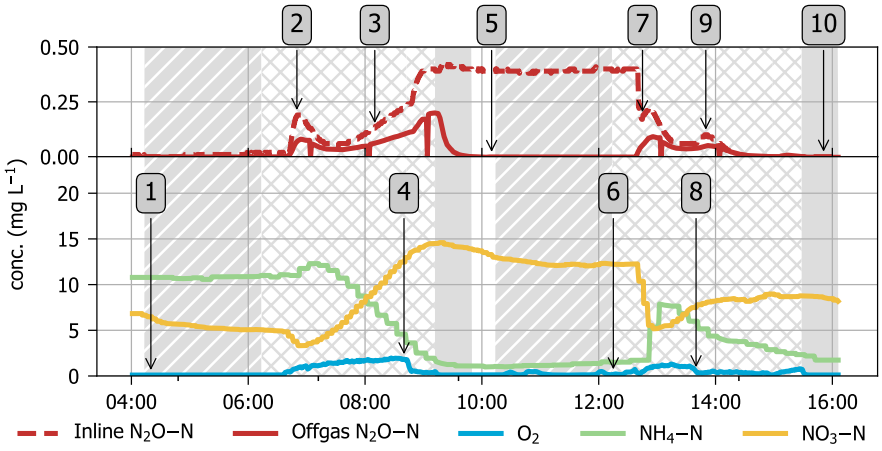

Figure 4.12: Batch with high concentrations of nitrous oxide (start at marker [marker 1]): initial peak due to denitrification of residual NO3- [marker 2]; after a decline of nitrous oxide in the bulk liquid production of nitrous oxide [marker 3]; after a drop in the O2 concentration an increase of the nitrous oxide concentration in the bulk liquid [marker 4]; no denitrification of nitrous oxide at the end of the cycle at the top of the reactor because sludge has settled [marker 5]; second reaction phase starts [marker 6]; drop of nitrous oxide in the bulk liquid by pre-denitrification and mixing [marker 7]; drop in the oxygen concentration [marker 8] led to increase in nitrous oxide production [marker 9]; and no nitrous oxide left at the end of the next cycle [marker 10]. The grey diagonal striped area indicates the feeding phase, the grey diamond grid shows the reaction phase and the grey solid area shows the settling phase.

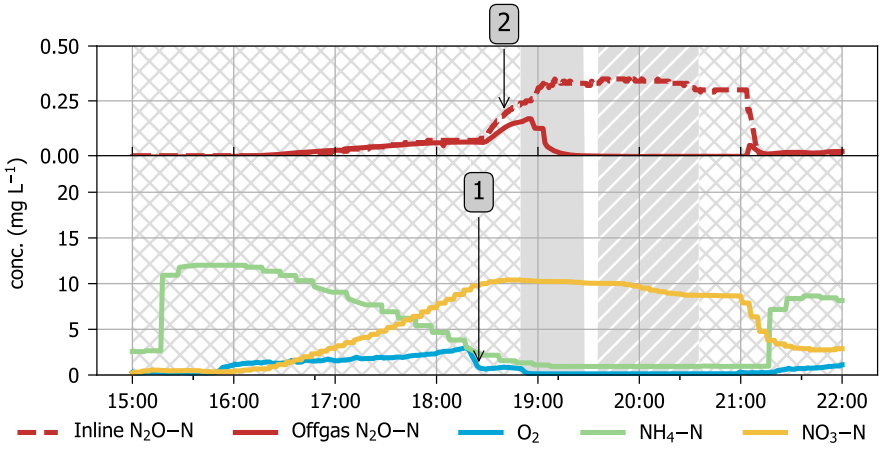

Figure 4.13: Increase of the nitrous oxide production [marker 2] when the oxygen concentration dropped to a value below 1 mg L^{-1} [marker 1]. The grey diagonal striped area indicates the feeding phase, the grey diamond grid shows the reaction phase and the grey solid area shows the settling phase.

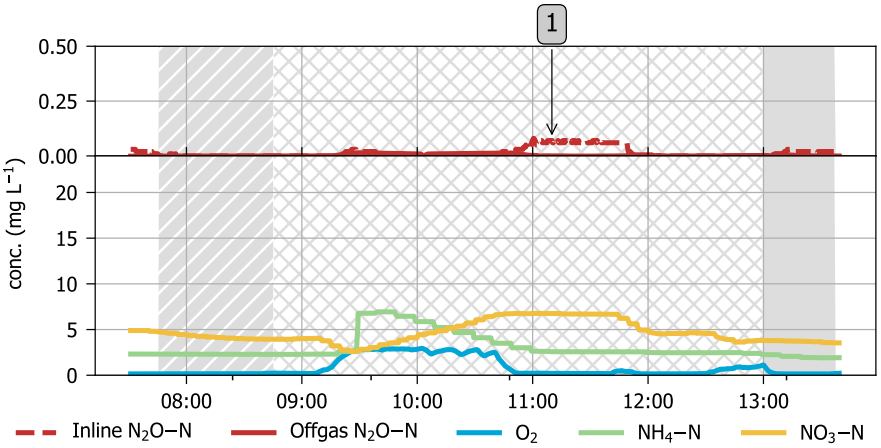

Figure 4.14: Dynamics within a Nereda® cycle; different process control. The nitrous oxide appeared only in the water phase when the aeration was turned off [marker 1], leading to a very low emission factor. The grey diagonal striped area indicates the feeding phase, the grey diamond grid shows the reaction phase and the grey solid area shows the settling phase.

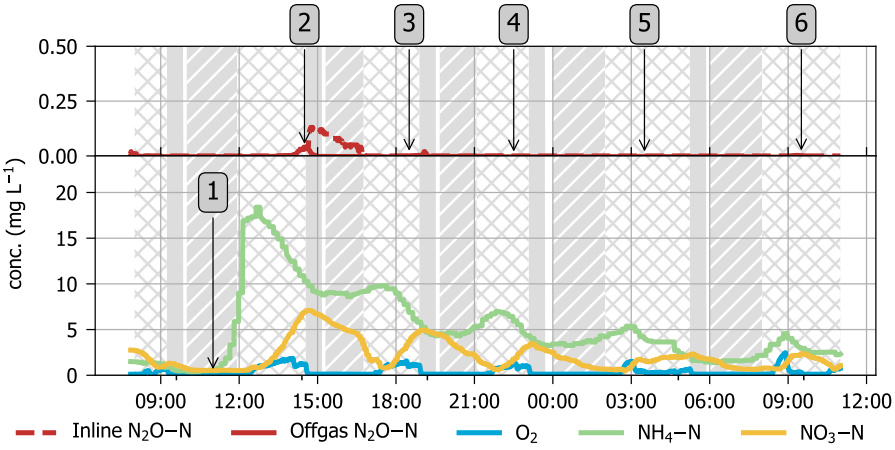

Figure 4.15: Typical RWF event showing a first flush [marker 1], showing little emission in the first batch [marker 2] and almost zero emission in the consecutive rainy weather batches [marker 2 to 3]; after the RWF event the emission factor stayed almost zero for a few batches [marker 4 to 6]. The grey diagonal striped area indicates the feeding phase, the grey diamond grid shows the reaction phase and the grey solid area shows the settling phase.

A typical RWF event is shown in Figure 4.15. When the flow towards the plant increased because of rainy weather, a first flush arrived at the plant, increasing the ammonium load in the reactor. The load in this batch was too high for the aeration capacity and the reduced aeration duration, leaving some elevated levels of ammonium in the effluent. The process control focussed mainly on nitrification, aerating the system at maximum capacity. Little nitrous oxide is formed in this batch. In the two batches hereafter, the load returned to normal levels, but still the focus was mainly on nitrification. In these batches, little nitrous oxide was formed. When the RWF event was finished and the flow to the plant returned to normal, the cycle times lengthened again, but still the emission of nitrous oxides remained close to zero.

4.4. Discussion

4.4.1. Long term nitrous oxide emissions

This study is the first long-term campaign measuring nitrous oxide emissions of a full-scale AGS reactor treating sewage. A Nereda® reactor at the wastewater treatment plant of Dinxperlo was monitored for 7 consecutive months. In this period an average emission factor of 0.33 % was measured. This means that 0.33 % of the incoming nitrogen load was emitted as nitrous oxide with the off-gas. The daily averaged emission factor ranged from 0.02 % to 1.58 %. These values are comparable to the values found in previous (short term) Nereda® research [11]. The average value found in the short-term research 0.7 % are higher than the average value found in the current research, but the value of 0.7 % is well within the variability of this long-term study, stressing the importance of long-term research. Since the emission was measured for only 7 months, the higher winter values contribute proportionately strong in the average value presented. A 12 month yearly averaged emission factor is estimated to be in the range of 0.25 % to 0.3 %.

Compared to conventional activated sludge (CAS) systems, the values obtained fall well within the reported ranges in literature. For example, in a study investigating seven CAS plants in Australia, the emission factor ranged between 0.6 % and 25.3 %, based on the amount of nitrogen denitrified [18]. Another study performing short term measurements in 12 plants in the United States showed an emission factor ranging from 0.01 % to 1.5 % [19]. More recently a long-term measurement campaign in Switzerland showed an emission factor for the CAS system of 1.6 % to 2.0 % while a flocculent sludge SBR system showed an emission factor of 2.4 % [12]. An overview of the emission factors for different wastewater treatment systems, adapted from Vasilaki *et al.* is shown Figure 4.16. This underlines that the values found in this study are comparable to most other wastewater treatment systems but are considerably lower than the values generally reported for sequencing batch reactors (SBR) systems. This is remarkable, since the AGS system used in this study is operated as an SBR. This shows high emission factors are not intrinsic to SBR systems and that the correct process conditions can also lead to low emission factors.

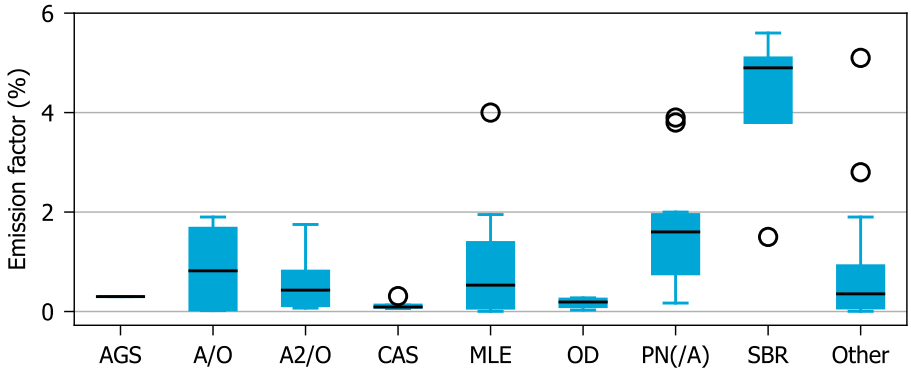

Figure 4.16: Emission factor of nitrous oxide for different wastewater treatment systems, adapted from [6]. Process groups: AGS: Aerobic Granular Sludge, A/O: Anoxic/oxic reactor, A2/O: anaerobic-anoxic-oxic reactor, CAS: conventional activated sludge, MLE: Modified Ludzack-Ettinger reactor, OD: oxidation ditch, SBR: sequencing batch reactor, PN and PN/A: partial-nitritation and partial-nitritation-anammox process.

4.4.2. Seasonal and diurnal variations

For CAS systems a strong seasonal effect has been reported for the emission factor [4, 12], showing higher emissions at lower temperatures or increasing temperatures in early spring. In this study, a seasonal effect is also visible, as can be seen in Figure 4.6 and Figure 4.10. The variability of the nitrous oxide emission increases when the water temperature drops below 14 °C in December. At temperatures above 14 °C the emission factor per batch varies between 0 % and 0.5 %, while below 14 °C the emission factor ranges between 0 % and 2.5 %. Contradictorily, March shows the lowest monthly emission factor (0.15 %), at the lowest average temperature of 9.7 °C. This difference may be caused by a change in process control in March. Daelman *et al.* suggested this seasonal effect was primarily caused by an increase of nitrite concentrations in early spring [4]. In the current study effluent nitrite concentrations were consistently low, with an average value of 0.05 mg L^{-1} (Table 4.1). Although nitrite concentrations were not measured during the cycle, elevated levels of nitrite during the cycle would also, at least partially, have ended up in the effluent. Since this was not the case here, no major effect of nitrite on the nitrous oxide emissions is expected.

The drop in the temperature in December was related to the inflow of melting snow, and in 4 days the water temperature in the reactor dropped from 13 °C to 8 °C. At these low temperatures of 8 °C the nitrification rates dropped considerably, but the ammonium effluent concentration was still below the consent value. At the same time, the nitrous oxide concentrations in both off-gas and bulk liquid were almost zero or below the detection limit for several days, until the temperature increased again above 9 °C. In the week before this event the variability of the emission factor was already increasing, but after this event the variability of the emission factor of nitrous oxide further increased after the water temperature was recovered to temperatures above 10 °C.

A diurnal pattern is observed in the data (Figure 4.11). The batches starting between 4h and 14h show a lower average emission factor than the batches starting between 15h and 3h. The relation is not as clear as for CAS systems [4], which is mainly caused by the fact that the AGS reactor is a batch system, running about 4 batches per day, which does not give a high resolution over the day as in CAS systems. The lowest average emission is found between 3h and 15h. It is uncertain what causes this, but variations in batch loading may play a role. Since the reactors are operated with a fixed cycle time of 6 hours during DWF conditions, the volumetric exchange ratio is lower if the total flow to the wastewater treatment plant is lower.

4.4.3. Nitrous oxide in the cycle

Nitrous oxide can be produced by both nitrification and by denitrification [7, 8]. Ammonia-oxidizing bacteria can produce nitrous oxide from oxidation of hydroxylamine and from denitrification of nitrite under oxygen deprived circumstances. Denitrification can be both a source and a sink for nitrous oxide [9]. Nitrous oxide is also an intermediate in the heterotrophic denitrification of nitrate. At the same time, nitrous oxide can be removed by denitrification [9]. In aerobic granular sludge nitrification and denitrification happen simultaneously during the aeration phase, which make it difficult to distinguish nitrous oxide production from nitrification and denitrification during the aeration phase [20]. Nevertheless, there seems to be clear evidence that both processes contribute to the production of nitrous oxides. In most batches there is no dissolved nitrous oxide present at the start of the cycle. In these cycles nitrous oxide production coincides with the conversion of ammonium and the production of nitrate (Figure 4.12 at [marker 3]). Often, a peak of nitrous oxide at the start of the aeration phase is observed (Figure 4.12 at [marker 2]). This peak seems to be caused by denitrification of nitrate left over from the previous cycle, because nitrification has not started yet. It is not clear if nitrous oxide is produced by partial denitrification caused by lack of COD at the end of the previous cycle or by rapid denitrification on readily biodegradable COD from the fresh influent. In both cases the increase of the nitrous oxide concentration is primarily caused by mixing of the reactor (aeration) and the decrease seems to be primarily caused by denitrification of nitrous oxides on readily biodegradable COD, although in the latter case stripping of nitrous oxide also plays a role.

It is likely that denitrification acts more as a sink for nitrous oxide at the start of the cycle after feeding and that denitrification acts more as a source for nitrous oxide at the end of the cycle, when most COD from the feeding phase (both storage polymers in the sludge and COD in the bulk liquid) is consumed. That would implicate the nitrous oxide production observed when nitrification starts as a net production rate resulting from production by ammonia oxidizing bacteria and denitrification by heterotrophic organisms. Understanding the mechanisms and when nitrous oxide production exceeds consumption could be important for the development of nitrous oxide emission control strategies.

The dissolved oxygen concentration is considered an important parameter to control nitrous oxide emissions, and concentrations below $1\,mg\,L^{-1}$ during

nitrification would stimulate nitrifier denitrification due to oxygen limitation [3]. Oxygen limitation in biofilms is a well-known factor even under higher oxygen concentrations [21]. It is therefore not surprising that lower oxygen concentrations seem to result in higher nitrous oxide emissions. In Figure 4.12 and Figure 4.13 an increase of the nitrous oxide emission can be seen if the dissolved oxygen concentration drops below 1 mg L^{-1}. A decreasing dissolved oxygen concentration will also shift the process to denitrification because the size of the anoxic zone within the aerobic granules will increase [20]. Since this decreasing dissolved oxygen concentration mostly happens towards the end of the reaction phase, denitrification might act more as a source than a sink of nitrous oxide as carbon availability is low. This would result in a double effect on the nitrous oxide emission: both the nitrifier pathway and the denitrifier pathway could increase nitrous oxide production in this situation.

A clear effect of rain events is shown in Figure 4.15. Rain events cause the batch size to increase, because more water arrives at the plant. In total 173 batches (18 %) were classified as RWF batches. These batches had an average emission factor of 0.09 %, which is less than one-third of the 0.33 % found for all batches. The reason for these lower emissions during RWF conditions is uncertain, but there are several processes influencing the emission factor during RWF. Under RWF conditions the flow to the plant increases from 0 to 175 $m^3 h^{-1}$ during DWF conditions to up to 600 $m^3 h^{-1}$ under RWF conditions. Since the reactor is operated as a sequencing batch reactor, the scheduling needs to be adapted to handle the increased inflow of wastewater [22]. This is done by decreasing the total cycle time and running more batches per day. This leads to shorter, more intense aeration phases, with higher oxygen concentrations. On average, the aeration phase during RWF is 35 minutes shorter than during DWF. Secondly RWF batches can be split in two groups. At the start of a rain event a first flush arrives at the plant, due to the presence of pressure pipelines in the sewer. The load exceeds the aeration capacity, leading to incomplete nitrification and thus less potential for nitrous oxide production. After this initial peak load, the load returns to a more average value, but the aeration remains relatively short and intense, focussing on nitrification. The lack of cycle time during RWF results in an increased nitrate effluent concentration (1.7 mg L^{-1} under DWF conditions and 4.4 mg L^{-1} under RWF conditions). The total SND efficiency on average was 69 ± 15 %, but was slightly lower during RWF (65 ± 13 %) compared to DWF (70 ± 15 %), but during DWF batches, SND happens at lower dissolved oxygen concentrations. It also appears that the RWF event influences the DWF batches following the RWF event (Figure 4.15, [5] and [6]). In these DWF batches nitrous oxide emissions are close to zero. This might be the result of the first flush at the start of the rain event, which results in a high sludge loading. A high sludge load will result in higher storage polymer concentration in the granular biomass in this specific batch, which might stretch out to the following batches. This leads to more denitrification capability of the plant. It appears that the denitrification process in these batches acts mainly as a sink for nitrous oxide, denitrifying nitrous oxide at a higher rate than it is produced. Eventually, the positive effect of the higher sludge loading will dissipate, and normal nitrous oxide emissions

will return.

The nitrous oxide concentrations in the bulk liquid are seldom higher than 0.3 mg L^{-1} and in most cases the concentration at the end of the cycle is close to zero. This means that in most cycles the denitrification capacity of nitrous oxide is also present towards the end of the cycle. This study observed nitrous oxide conversion rates up to 1 mg L^{-1} h^{-1}. This rate is a net rate, because it happens simultaneously with denitrification of nitrate, which also can produce nitrous oxide as an intermediate product. In most cases in less than 30 minutes of anoxic conditions all nitrous oxide in the bulk liquid is denitrified. This suggests a high nitrous oxide conversion potential is present, if the right conditions are met.

4.4.4. Effect of process control

The nitrous oxide emission factors varied between 0.02 % and 1.58 % per day, most of the batches being below 0.5 %. The emission of nitrous oxide might be lowered by changing the process control. The decrease of the emission factor from 0.57 % in February to 0.15 % in March by changing the process control to a fixed aeration strategy is an example of this. A more stable dissolve oxygen concentration during the aeration phase led to a remarkable decrease in the emission of nitrous oxide. On the other hand, the process control focusing on simultaneous nitrification and denitrification did not lead to elevated nitrous oxide emission in the summer period.

Different process control strategies may be necessary during summer and winter conditions to limit nitrous oxide emission under all conditions.

It also seems that the production of nitrous oxide during the cycle is increasing, when the DO drops below 1 mg L^{-1}. This could be easily prevented by adjusting the process control as to not allow for the oxygen to dip below the required set point. Another potential improvement relates to the initial peak at the start of the aeration (Figure 4.12). This initial peak could be prevented by adding a pre-denitrification phase to the cycle, aiming to remove this residual nitrate, simultaneously removing the nitrous oxide formed during settling and feeding. Another option is to focus on post-denitrification to prevent high amounts of residual nitrate to be present in the next cycle, thereby limiting the nitrous oxide emission peak.

Compared with a continuously fed activated sludge system, an SBR system gives a much higher information density on the changes in nitrous oxide production and consumption. This gives the possibility to develop effective process control strategies to minimize the nitrous oxide emissions. A maximum nitrous oxide concentration of 0.3 mg L^{-1} and a net denitrification rate up to 1 mg L^{-1} h^{-1} was measured. This would mean that a denitrification phase of 20 minutes should be enough to remove nitrous oxide from the water phase in most cases. Splitting the main aeration phase and adding one or more intermediate denitrification steps could be an effective measure to minimize nitrous oxide emission.

4.4.5. Difference with conventional SBR systems

The AGS reactor was operated as a sequencing batch reactor. A comparison with flocculent SBR systems is therefore of interest. As shown in Figure 4.16, regular SBR systems have shown to have higher emission factors than continuously fed activated

sludge systems. High nitrous oxide emissions in SBRs are attributed to sudden changes in the concentrations of ammonium, nitrate and nitrite within the cycle or to accumulated dissolved nitrous oxide during anoxic settling and decanting in the subsequent aerobic phase [6]. These conventional SBR systems show emission factors up to 5.6 % which is much higher than the value of 0.33 % found in this study. This might be caused by differences in process conditions. The feeding in the AGS process is strictly anaerobic, which is achieved by plug flow feeding from the bottom of the reactor. By this plug flow, the nitrate remaining in the reactor from the previous cycle is pushed upwards while the reactor is filled with fresh influent from the bottom. This limits the contact between sludge, COD and nitrate, preventing production of high levels of nitrous oxide during the feeding phase. While anaerobic plug flow feeding is a requirement in AGS systems, it is uncommon in SBR systems. For example, in a study by [23] the SBR reactors were alternatingly fed anoxically and aerobically resulting in an emission factor of 6.4 %.

4.4.6. Comparison water phase and gas phase measurement

The nitrous oxide concentration was measured by two different methods: firstly, by measuring the nitrous oxide concentration in the bulk liquid by means of an online sensor and secondly by measuring the nitrous oxide concentrations in the off-gas via a gas analyser. The latter has the benefit of measuring the emission during aeration directly without the need for converting water phase concentration into emissions to the air. The downside of the off-gas method is the lack of information about what happens during the anaerobic and the anoxic phase, when the aeration is turned off. The water phase sensor gives direct insight into the production of nitrous oxide in the anoxic phase and the denitrification of nitrous oxide in the anoxic phase. The water phase sensor thus provides information that otherwise would be lost or obscured by other nitrous oxide forming processes during aeration. For the use in process control both methods can be used, but the water phase sensor is likely more effective, as it also gives information about the non-aerated phases.

4.5. Conclusions

A 7-month measurement campaign of the emission of nitrous oxide was performed in the Nereda® reactor of Dinxperlo. Key findings include:

- An average nitrous oxide emission factor of 0.33 % was found over a 7-month measuring campaign spanning summer and winter.
- The yearly average emission factor was estimated between 0.25 % and 0.30 %.
- The emission factor was comparable with continuously fed activated sludge plants with low emissions and lower than values found for conventional SBR systems.
- Both nitrification and denitrification appeared to contribute to the nitrous oxide production, denitrification acting both as a source and a sink for nitrous oxide.

- Post-denitrification significantly reduced the nitrous oxide concentration in the reactor.
- An increased variability of the emission factor was observed at low temperatures.
- Different process control between summer and winter could limit the emission factor.
- In the winter period, aeration on a fixed oxygen setpoint reduced the emission factor compared to aeration using variable oxygen setpoint.
- A temporary increase of the sludge loading decreased the emission factor for several batches.

Bibliography

[1] E. J. H. van Dijk, M. C. M. van Loosdrecht, and M. Pronk, *Nitrous oxide emission from full-scale municipal aerobic granular sludge,* Water Res. **198**, 117159 (2021).

[2] S. Solomon, M. Manning, M. Marquis, and D. Qin, *Climate Change 2007 - The Physical Science Basis: Working Group I Contribution to the Fourth Assessment Report of the IPCC*, Vol. 4 (Cambridge university press, 2007).

[3] M. J. Kampschreur, H. Temmink, R. Kleerebezem, M. S. M. Jetten, and M. C. M. van Loosdrecht, *Nitrous oxide emission during wastewater treatment,* Water Res. **43**, 4093 (2009).

[4] M. R. J. Daelman, E. M. van Voorthuizen, U. G. J. M. van Dongen, E. I. P. Volcke, and M. C. M. van Loosdrecht, *Seasonal and diurnal variability of N2O emissions from a full-scale municipal wastewater treatment plant,* Sci. Total Environ. **536**, 1 (2015).

[5] J. Desloover, S. E. Vlaeminck, P. Clauwaert, W. Verstraete, and N. Boon, *Strategies to mitigate N2O emissions from biological nitrogen removal systems,* Curr. Opin. Biotechnol. **23**, 474 (2012).

[6] V. Vasilaki, T. M. Massara, P. Stanchev, F. Fatone, and E. Katsou, *A decade of nitrous oxide (N2O) monitoring in full-scale wastewater treatment processes: A critical review,* Water Res. **161**, 392 (2019).

[7] M. J. Kampschreur, W. R. van der Star, H. A. Wielders, J. W. Mulder, M. S. Jetten, and M. C. van Loosdrecht, *Dynamics of nitric oxide and nitrous oxide emission during full-scale reject water treatment,* Water Res. **42**, 812 (2008).

[8] P. Wunderlin, J. Mohn, A. Joss, L. Emmenegger, and H. Siegrist, *Mechanisms of N2O production in biological wastewater treatment under nitrifying and denitrifying conditions,* Water Res. **46**, 1027 (2012).

[9] M. Conthe, P. Lycus, M. Arntzen, A. Ramos da Silva, A. Frostegård, L. R. Bakken, R. Kleerebezem, and M. C. M. van Loosdrecht, *Denitrification as an N2O sink,* Water Res. **151**, 381 (2019).

[10] L. Jahn, K. Svardal, and J. Krampe, *Nitrous oxide emissions from aerobic granular sludge,* Water Sci. Technol. **80**, 1304 (2019).

[11] H. F. van der Roest, L. M. M. de Bruin, R. van Dalen, and C. Uijterlinde, *Maakt Nereda-installatie Epe hooggespannen verwachtingen waar?* Vakbl. H2O , 30 (2012).

[12] W. Gruber, K. Villez, M. Kipf, P. Wunderlin, H. Siegrist, L. Vogt, and A. Joss, *N2O emission in full-scale wastewater treatment: Proposing a refined monitoring strategy,* Sci. Total Environ. **699**, 134157 (2020).

[13] S. Lochmatter, J. Maillard, and C. Holliger, *Nitrogen removal over nitrite by aeration control in aerobic granular sludge sequencing batch reactors.* Int. J. Environ. Res. Public Health **11**, 6955 (2014).

[14] F. Zhang, P. Li, M. Chen, J. Wu, N. Zhu, P. Wu, P. Chiang, and Z. Hu, *Effect of operational modes on nitrogen removal and nitrous oxide emission in the process of simultaneous nitrification and denitrification,* Chem. Eng. J. **280**, 549 (2015).

[15] J. E. Baeten, E. J. H. van Dijk, M. Pronk, M. C. M. van Loosdrecht, and E. I. P. Volcke, *Potential of off-gas analyses for sequentially operated reactors demonstrated on full-scale aerobic granular sludge technology,* Sci. Total Environ. **787**, 147651 (2021).

[16] J. P. Bassin, M. Pronk, R. Kraan, R. Kleerebezem, and M. C. M. van Loosdrecht, *Ammonium adsorption in aerobic granular sludge, activated sludge and anammox granules,* Water Res. **45**, 5257 (2011).

[17] E. J. H. van Dijk, K. M. van Schagen, and A. T. Oosterhoff, *Controlled Simultaneous Nitrification and Denitrification in Wastewater Treatment,* (2020).

[18] J. Foley, D. de Haas, Z. Yuan, and P. Lant, *Nitrous oxide generation in full-scale biological nutrient removal wastewater treatment plants,* Water Res. **44**, 831 (2010).

[19] J. H. Ahn, S. Kim, H. Park, B. Rahm, K. Pagilla, and K. Chandran, *N2O emissions from activated sludge processes, 2008-2009: Results of a national monitoring survey in the united states,* Environ. Sci. Technol. **44**, 4505 (2010).

[20] M. K. de Kreuk, J. J. Heijnen, and M. C. M. van Loosdrecht, *Simultaneous COD, nitrogen, and phosphate removal by aerobic granular sludge,* Biotechnol. Bioeng. **90**, 761 (2005).

[21] H. Odegaard, B. Rusten, and T. Westrum, *A new moving bed biofilm reactor - applications and results,* Water Sci. Technol. **29**, 157 (1994).

[22] G. H. Chen, M. C. M. van Loosdrecht, G. A. Ekama, and D. Brdjanovic, *Biol. Wastewater Treat. Princ. Model. Des.* (2020).

[23] A. Rodriguez-Caballero, I. Aymerich, R. Marques, M. Poch, and M. Pijuan, *Minimizing N2O emissions and carbon footprint on a full-scale activated sludge sequencing batch reactor,* Water Res. **71**, 1 (2015).

5

On the mechanisms

Edward van Dijk, Viktor Haaksman

In this chapter a mathematical framework was developed to describe aerobic granulation based on 6 main mechanisms: microbial selection, selective wasting, maximizing transport of substrate into the biofilm, selective feeding, substrate type and breakage. A numerical model was developed using four main components; a 1D convection/dispersion model to describe the flow dynamics in a reactor, a reaction/diffusion model describing the essential conversions for granule growth, a setting model to track granules during settling and feeding, and a population model containing up to 100.000 clusters of granules to model the stochastic behaviour of the granulation process. With this approach the model can explain the dynamics of the granulation process observed in practice. This includes the presence of a lag phase and a granulation phase. Selective feeding was identified as an important mechanism that was not yet reported in literature. When aerobic granules are grown from activated sludge flocs, a lag phase occurs, in which few granules are formed, followed by a granulation phase in which granules rapidly appear. The ratio of granule forming to non-granule forming substrate together with the feast/famine ratio determine if the transition from the lag phase to the granulation phase is successful. The efficiency of selective wasting and selective feeding both determine the rate of this transition. Breakup of large granules into smaller well settling particles was shown to be an important source of new granules. The granulation process was found to be the combined result of all 6 mechanisms and if conditions for one are not optimal, other mechanisms can, to some extent, compensate.

Parts of this chapter have been published in Water Research **216**, 118365 (2022) [1].

This model provides a theoretical framework to analyse the different relevant mechanisms for aerobic granular sludge formation and can form the basis for a comprehensive model that includes detailed nutrient removal aspects.

5.1. Introduction

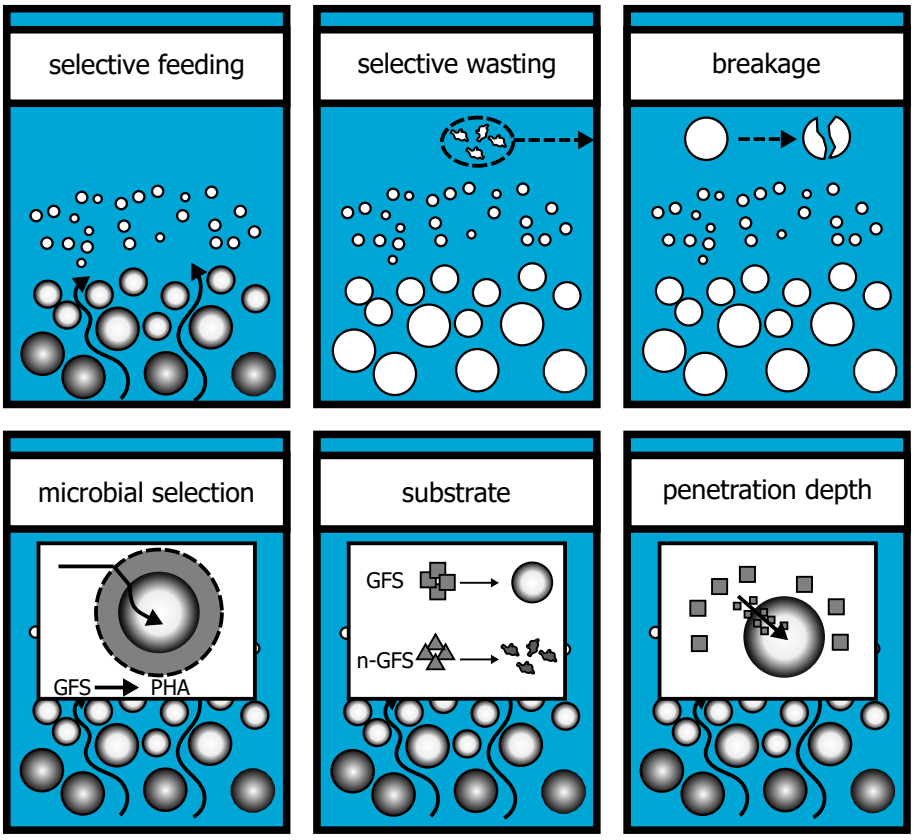

Figure 5.1: Graphical abstract.

The process of aerobic granulation is influenced by many factors [2]. Factors often described are hydrodynamic shear [3–5], physical selection on settling velocity [6, 7], the flow regime during contact of the sludge with influent [8–10], dissolved oxygen concentration [11], feast/famine ratio [12–14], influent substrate composition [15, 16], organic loading rate [17], quorum sensing [18] and aggregation through EPS [19]. It is unclear which factors matter most and how their interplay is affected by the process conditions applied. A framework for biofilm morphology has been proposed [20], but this framework only explains granule stability on the micro-scale, but it cannot explain granulation dynamics on a reactor scale. For anaerobic granular sludge, such a framework has been developed [21], but this framework is not as such applicable for aerobic granular sludge.

When a AGS reactor is seeded with activated sludge, under the right circumstances, granular sludge will develop from flocculent sludge. In practice this granulation process shows dynamics that are not easily explained. The granulation process commonly has a lag phase, in which not much change in the granulation

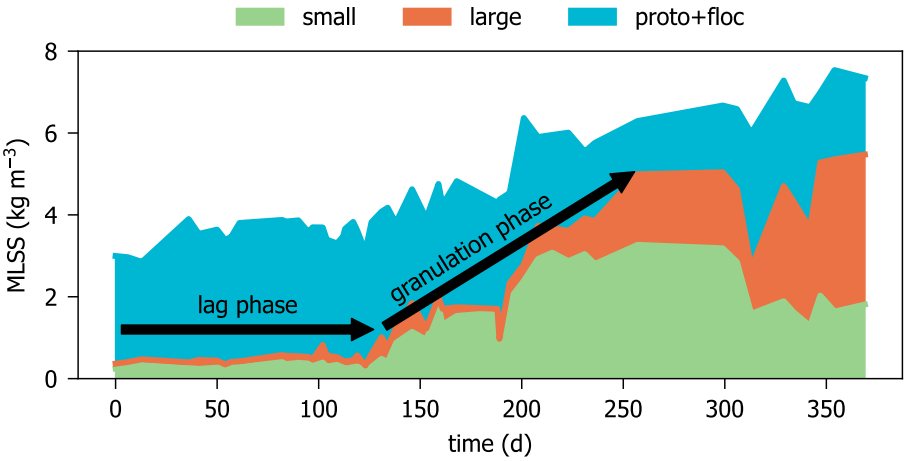

Figure 5.2: Typical startup of an aerobic granular sludge reactor from flocs, showing an initial lag phase with slow improvement of the sludge morphology, followed by the granulation phase, where granules appear in the reactor. The colours indicate the size of the biomass aggregates, showing proto-granules and flocs (<200 µm), small granules (>200 µm) and large granules (>1000 µm). Data derived from the Nereda® reactor in Utrecht, the Netherlands.

grade (biomass fraction of the granules) seems to happen. Secondly, there is the granulation phase, in which granules start to appear in the reactor and the granulation grade increases (figure 5.2). The reason behind the lag phase and the trigger for the sudden start of granulation is unclear. We hypothesize that there are six main mechanisms that are of most importance for successful granulation (figure 5.3).

Microbial selection is important for the formation of granules. It has been shown that a stable dense biofilm can be best achieved, when the uptake rate of substrates is lower than the transport rate of the substrates into the granules [22]. Therefore, the process is optimized towards organisms that anaerobically sequester readily biodegradable substrate by converting it into storage polymers and subsequently utilizing these polymers for aerobic growth [13, 23, 24]. This effectively separates the substrate uptake and the growth into two processes (called feast and famine). Phosphate accumulating organisms (PAO) and glycogen accumulating organisms (GAO) are examples of species that can make this split and these organisms are commonly observed in full-scale aerobic granular sludge processes [25]. Not all substrates can be sequestered anaerobically into storage polymers for aerobic growth of bacteria in the granules. We call these substrates, non-Granule Forming Substrate (n-GFS). Substrates that can lead to growth of aerobic granules (e.g. volatile fatty acids, but also readily biodegradable substrates that can be converted anaerobically) we call Granule Forming Substrate (GFS).

Physical selection is also an important driver for growing aerobic granular sludge [12, 13, 26, 27]. AGS has advantageous settling properties compared to activated sludge flocs [26, 28]. In AGS reactors flocs will always be present to some extent

[29] as not all carbon sources present in sewage can be converted to storage polymers during anaerobic feeding [30]. Therefore, it is needed to preferentially remove the flocculent sludge fraction with the excess sludge to give granules a competitive advantage. This is achieved by using the differential settling velocity between flocculent and granular sludge [7, 31]. This is called the physical selection pressure.

Another well-known driver is *maximizing transport of substrate* into the biofilm. Higher substrate concentrations in the bulk liquid result in a deeper penetration of the substrate in the biofilm [32]. This helps to grow and support a thicker biofilm. In AGS reactors a higher substrate concentration is achieved by either pulse feeding at the start [12] or more practical relevant by plug flow feeding from the bottom of the reactor [13, 29]. This gives a competitive advantage for larger granules. Larger granules settle faster than smaller granules and flocs, and therefore accumulate at the bottom of the settled sludge bed [7]. Feeding from the bottom therefore results in a longer contact time with the influent and contact with higher substrate concentrations for the larger granules. As a result, they will have more opportunity for growth than smaller fraction. Hence the term *selective feeding*.

Aerobic granules go through a typical life cycle that has a strong influence on the granulation process and reactor performance. When an AGS reactor is seeded with activated sludge flocs, these flocs will first form proto-granules. Flocs and proto-granules share similar bulk settling properties. An important difference is that the proto-granules already have the granular morphology but are smaller than 200 µm, which is considered to be the minimum size for an aggregate to be called an aerobic granule [33]. Proto-granules already have been observed in conventional activated sludge processes, especially in systems with high anaerobic food to mass ratios, unmixed in-line fermentation, and a high influent soluble COD fraction [34]. Proto-granules are embedded in the floc matrix and settle together with the flocculent material.

Biological conversions in proto-granules are comparable to conversions in flocs, because the small radius of the proto-granules allows for full penetration with oxygen. Simultaneous nitrification and denitrification (SND) thus will be limited to very low DO conditions. When proto-granules grow out into small granules (>200 µm), these small granules will settle significant faster and independent of the flocculent mass. The result is that small granules can experience the benefits regarding sludge selection, remain longer in the reactor with selective wasting and receive more influent with bottom feeding. When the granules continue to grow, the biofilm kinetics become more pronounced and full penetration of oxygen is less likely and SND will increase. Large granules (>1000 µm) are more susceptible to breakage [35]. When a granule breaks into smaller pieces some will be spilled and others will become a seed for new granules, restarting the granule life cycle. Thus we hypothesized that *breakage of granules* is an integral part of the granulation process, similar as proposed for anaerobic sludge [21].

The aforementioned factors for aerobic granulation are not absolute. For example, only part of the substrate of domestic wastewater can be taken up anaerobically by the AGS directly or after fermentation. Still, it is possible to grow

AGS on the complex composition of domestic wastewater [16, 29]. The selection pressure applied in full-scale reactors will be less effective than in lab-reactors, because of less favourable H/D ratios and other scaling factors. Apparently, the favourable mechanisms can be allowed to be non-optimally implemented to a certain extent without harming the granulation process. It is however unclear, how the different mechanisms influence one another positively or negatively if the process conditions become less favourable.

Analysis of the quantitative interplay between the aforementioned mechanisms in combination with varying process conditions requires a mathematical modelling approach. A mature granular bed in practice exists of a collection of granules with sizes up to 5 mm [7]. For the purpose of this study, a framework was required in which the lifecycle of granules could be tracked. Simulated granules should be allowed to have different time-variable spatial positions in the reactor and should be exposed to different bulk-liquid conditions, within a cycle and from one cycle to the next. This approach is required to capture the stochastic properties of an AGS system. Several models are available describing the AGS process with different emphases [36]. Models that describe granulation as the development of a characteristic mean granule size [37, 38] or assume a single granule size to study, for example, microbial speciation in granules and nutrient removal [39, 40] are not suitable for the purpose of this study. The same holds for models that assume successful granulation using a fixed granule size distribution to investigate reactor performance [30, 41]. Models with a dynamic granule size distribution [21, 42] often use a Population Balance Model (PBM) to describe the number of granules in a certain size class and the processes that influence these amounts (i.e. growth and detachment) via transitions from or to another size class. However, the available PBMs are only suited for completely mixed reactors, not for typical AGS reactors with combined spatial and temporal differences between the conditions experienced by aggregates. We hypothesized that the process for aerobic granulation can be described by six mechanisms (figure 5.3) with a minimal required description of the biological conversions, tracking the development of individual granule clusters in the reactor over time.

In this study, we aimed to understand the underlying principles for aerobic granulation. A mathematical model was constructed that describes the full life cycle of aerobic granules. We performed a sensitivity analysis on the six mechanisms proposed and we evaluated their individual contribution to the granulation process.

5.2. Methodology

A model was developed integrating several sub-models describing all the proposed mechanisms responsible for the granulation process. The main process steps in current full-scale AGS reactors according to the Nereda® concept are the feeding phase, in which fresh influent is fed to the reactor from the bottom, the reaction phase, where the wastewater is cleaned by different aeration strategies and finally the settling and decanting phase, in which the selective wasting takes place. In full-scale applications feeding and effluent decanting happens simultaneously [29, 43].

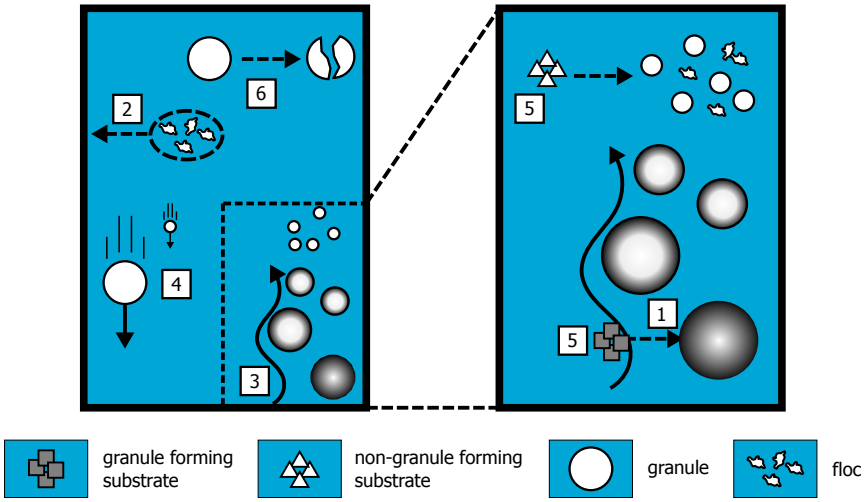

Figure 5.3: A graphical representation of the six mechanisms for granulation: (1) microbial selection, (2) selective wasting, (3) maximizing transport of substrate into the biofilm, (4) selective feeding, (5) (non-) granule forming substrate, (6) breakage of granules.

5.2.1. Theoretical background

Biomass morphology

The morphology of biofilms is dependent on a combination of convection, diffusion, reaction, growth and detachment [44]. All biomass clusters are assumed to have constant smooth and spherical morphology with a constant density. This specific biofilm morphology occurs when substrate uptake is limited by the maximum biomass specific uptake rate and not by transport [45]. Since substrate uptake (anaerobic) is uncoupled from growth (aerobic) in full-scale AGS, a smooth, spherical biofilm morphology was assumed for all simulations. Wherever the distinction is made between flocs and granules, this is solely based on the sludge particle diameter. The smallest particles of 100 µm are referred to as flocs, while all larger particles are considered (proto-) granules.

Microbial ecology

The microbial population differs over the radius of the biofilm due to concentration gradients of substrates [20]. Different organisms present in the biofilm are responsible for processes like nitrification, denitrification and phosphate removal [46, 47]. However, since the aim of this study was to investigate the impact of the different mechanisms on the growth of aerobic granules, the biomass clusters are assumed to have constant ecology. Furthermore, biomass formation in wastewater treatment plants is mostly related to COD conversions. No nitrogen and phosphorus conversions are considered in the model as they contribute marginally to biomass formation. All modelled biomass can store COD anaerobically as storage polymers. Therefore, only the conversions of COD into storage polymers, and

storage polymers into biomass, were simulated to describe granular growth.

Biological fate of COD-types in wastewater

The chemical oxygen demand (COD) present in domestic wastewater can be divided into multiple fractions [48]. These fractions can be divided based on the availability for biological conversions [16]. The soluble and suspended inert COD and inorganic solids are not available for any biological conversion and are thus disregarded in this model. Both the soluble readily biodegradable COD and the colloid fast hydrolysable COD are available for anaerobic conversion into storage polymers and are thus categorized as GFS. The suspended slowly hydrolysable COD is available for biological conversions, but not for anaerobic storage and are categorized as n-GFS. A schematic representation is shown in figure 5.4.

5.2.2. Model description

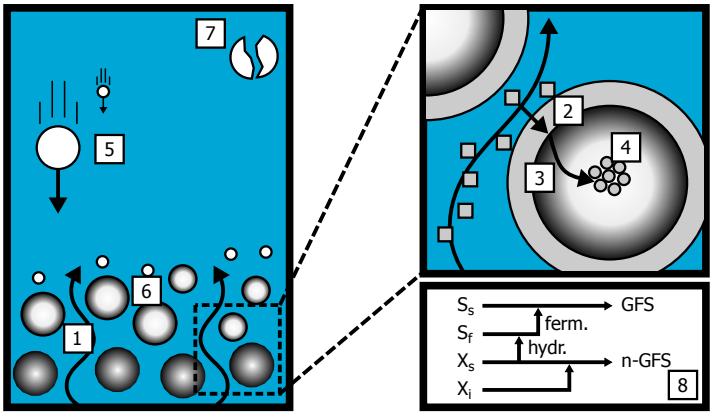

Figure 5.4: Model overview, with (1) convection and dispersion in the bulk liquid, (2) mass transfer through the boundary layer, (3) 1D radial diffusion, (4) conversion of GFS to PHA, (5) settling of granules in the reactor, (6) individual based population model, (7) breakage. Schematic representation of the translation from organic substrates in ASM2d [49] into the granulation model (8).

Four mathematical models were combined to perform a sensitivity analysis on the hypothesized main mechanisms for aerobic granulation (see also figure 5.4). The four model components are described below.

1. *Cluster-based biomass population model*: An AGS reactor typically contains a dynamic distribution of granule sizes, all of different age, shape and ecology. To capture the probability of granules of similar size to be at the different locations in the reactor at the same time, a cluster-based approach was used. The sludge population was discretized into clusters of aggregates with the same diameter, where each simulated cluster represented the same amount of physical biomass in the reactor. The amount of biomass represented by a cluster scaled linearly with the surface area of the simulated reactor, since

the spatial gradients in an AGS reactor are mainly 1D (i.e. over the height). A convergence analysis showed that a discretization of 1.75×10^{-2} simulated mass per real mass per reactor area (kg/kg/m^2) yielded a discretization-independent solution. This resulted in ~10 000 clusters at start-up in the reference case with only flocs of 100 µm, and the population increased to ~100 000 upon successful granulation. New clusters were formed from n-GFS as clusters with a diameter of 100 µm. The clusters could be subjected to the following mechanisms:

- Growth: in the reaction phase, the diameter of each cluster of particles grew according to the amount of PHA formed during the anaerobic feeding phase. This resulted in a different increase in volume for each cluster of granules. The increase was based on an apparent yield coefficient (including decay) and a constant biomass concentration in the granule, resulting in a constant VSS/TSS ratio. All PHA was assumed to be consumed and converted to new biomass, without any time dependence in the reaction phase.
- Breakage: the larger aerobic granules become, the more likely they will break up into smaller pieces [35]. In the model, granule clusters larger than 3 mm have an increasing chance of breaking (increasing to 99 % for granules larger than 5 mm). Breakage leads to two clusters with random diameter between 100 µm and the original diameter, with a combined biomass equal to the original cluster.
- Redistribution: if a cluster of granules exceeded the maximum amount of represented real biomass, it was split into two clusters of granules with same diameter. Each cluster would represent half of the original biomass.
- Wasting: Biomass discharge from the reactor was performed by the removal of number of complete clusters. Clusters were selected, depending on the wasting method used (a mixed sample for MLSS control or based on settling velocity for selective wasting).

2. *Bulk-liquid solute mass balance*: the anaerobic feeding in an AGS reactor is mainly a 1D process, since reactors are fed from the bottom and the process is designed to get an optimal plug flow. Some axial mixing does occur [50]. Therefore, the concentration profile of GFS during feeding was described by an 1D convection-dispersion model [50, 51]. It was solved with one-way coupling to the settling model, since during the feeding phase granules will still be settling and partially fluidize. The calculated effective voidage is thus dynamic and will influence the local fluid velocity.

3. *Biofilm solute mass balance*: The flux of GFS into a granule depends on the local concentration in the bulk-liquid surrounding the granule and the rate of mass transfer, which varies over the height of the reactor. It is in turn affected by the rate of diffusion in the granules and rate of reaction of GFS to PHA. Furthermore, anaerobic storage capacity of PHA is limited by a maximum PHA

content, used as a simplification for depletion of glycogen [39]. The dynamic mass balances of GFS and PHA were modelled using a 1D radial reaction-diffusion model for each cluster of particles, solved fully coupled to the bulk-liquid mass balance. The combined processes in the bulk-liquid phase, biofilm phase and the settling model determined the total amount of storage polymer per cluster of granules after the feeding phase.

4. *Settling model*: the settling velocity of a granule depends on the physical properties of the granule (size and density) and the biomass concentration in the near vicinity of the granule. As a result, every granule will have a unique settling velocity, eventually determining the position in the reactor during feeding. To describe this settling behaviour, we used the Van Dijk settling model [7] and adapted it to describe the settling and fluidization of clusters of granules. The model was also adapted to better describe the settling of flocs and proto-granules. The latter involved a change in the calculation of the expansion index, which is now calculated based on the Archimedes number.

5.2.3. Mathematical model

The model consists of several components to simulate the change in time and in space of the dependent variables listed in table 5.1.

Table 5.1: Dependent variables and interdependence in submodels. An 'X' denotes that the variable is used in a submodel. A shaded 'O' indicates that the variable is dynamically computed in that submodel. Arrows indicate the extent of coupling between submodels (either one-way coupled (← or →) or fully coupled (←→)). Subscript j denotes the index of the cluster of sludge particles.

	Bulk-liquid solute mass balance	Biofilm solute mass balance	Settling model	Granule population model
$c_{GFS,L}(x,t)$	O→	←X		X
$c_{GFS,B,j}(r,t)$	X→	←O→		X
$c_{PHA,B,j}(r,t)$		O→		X
$x_j(t)$	X	X	←O	
$d_j(t)$	X	X	X	←O

Bulk-liquid solute mass balance

The mass balance of GFS during anaerobic feeding was formulated as follows, describing axial dispersion, convective transport and mass transfer between the bulk and the biofilm (from/to all granules in the set of clusters N_i at a certain height):

$$\frac{\partial c_{GFS,L}}{\partial t} = -D_{ax}\frac{\partial^2 c_{GFS,L}}{\partial x^2} + \frac{v_{in}}{\epsilon_L(x)}\frac{\partial c_{GFS,L}}{\partial x} + \sum_{j=1}^{N_i} k_{LB,GFS}\frac{a_j}{\epsilon_L(x)}(c_{GFS,B,j}|_{r=d_j/2} - c_{GFS,L}) \tag{5.1}$$

For the bottom inlet boundary we used a Danckwerts condition:

$$\left(\frac{v_{in}}{\epsilon_L(x)}c_{GFS,L} - D_{ax}\frac{\partial c_{GFS,L}}{\partial x}\right)\Bigg|_{x=0} = v_{in}c_{GFS,in}, t > 0 \tag{5.2}$$

The top outlet boundary was based on a zero zero-dispersion condition:

$$-D_{ax}\frac{\partial c_{GFS,L}}{\partial x}\bigg|_{x=H} = 0, t > 0 \tag{5.3}$$

Biofilm phase solute mass balance

The mass balance of GFS and storage polymers (PHA) over the biofilm phase was modelled according to the following equation:

$$\frac{\partial c_{GFS,B,j}}{\partial t} = -D_{GFS,B}\left(\frac{\partial^2 c_{GFS,B,j}}{\partial r^2} + \frac{2}{r}\frac{\partial c_{GFS,B,j}}{\partial r}\right) + R_{GFS}\left(c_{GFS,B,j}(r), c_{PHA,B,j}(r)\right) \tag{5.4}$$

and

$$\frac{\partial c_{PHA,B,j}}{\partial t} = R_{PHA}\left(c_{GFS,B,j}(r), c_{PHA,B,j}(r)\right) \tag{5.5}$$

Here the volumetric reaction rate *R* is based on Monod kinetics [39]. Both Monod constants are two orders of magnitude smaller than the actual concentrations, therefore practically serve as switching terms:

$$\begin{aligned} R_{GFS} &= q_{AN,\max} X \frac{c_{GFS,B,j}}{K_{GFS}+c_{GFS,B,j}} \frac{c_{PHA,\max}-c_{PHA,B,j}}{K_{PHA}+c_{PHA,\max}-c_{PHA,B,j}} \\ R_{PHA} &= -R_{GFS} \end{aligned} \tag{5.6}$$

On the biofilm surface the boundary was defined through flux-continuity with transfer in both directions between bulk-liquid and biofilm:

$$-D_{GFS,B}\frac{\partial c_{GFS,B,j}}{\partial r}\bigg|_{r=d_j/2} = k_{LB,GFS}(c_{GFS,B,j}|_{r=d_j/2} - c_{GFS,L}|_{x=x_j}), t > 0 \tag{5.7}$$

The boundary in the centre of the biofilm was defined through symmetry:

$$-D_{GFS,B}\frac{\partial c_{GFS,B,j}}{\partial r}\bigg|_{r=0} = 0, t > 0 \tag{5.8}$$

Mass transfer between bulk-liquid and biofilm

The mass transfer coefficient was calculated based on Sherwood relations for forced convection around a free sphere [52] (top relation) or semi-fluidized beds [53] (bottom relation). The choice depended on the local voidage of the sludge bed during feeding since no relation covered the complete voidage range (from settled granular bed (0.5) to nearly void of biomass):

$$k_{LB,GFS}\left(\epsilon_L, d_j\right) = \max\left(\begin{array}{c} \left(2.0 + 0.6\left(\frac{d_j v_{in}}{\nu \epsilon_L}\right)^{\frac{1}{2}}\left(\frac{\nu}{D_{GFS,L}}\right)^{\frac{1}{3}}\right)\frac{D_{GFS,L}}{d_j} \\ \left(2.0 + 1.51\left((1-\epsilon_L)\frac{d_j v_{in}}{\nu}\right)^{\frac{1}{2}}\left(\frac{\nu}{D_{GFS,L}}\right)^{\frac{1}{3}}\right)\frac{D_{GFS,L}}{d_j} \end{array}\right) \tag{5.9}$$

Settling model

The settling model from chapter 3 was used to describe the settling of the individual groups of granules. Since this model only describes the settling behaviour of classes of granules, it was adapted to describe the settling behaviour of individual clusters of granules of the same size (j):

$$v_j = k v_{f,j} \epsilon_j^{n_j - 2} \frac{\rho_{B,j} - \rho_{bed,i}}{\rho_{B,j} - \rho_L}. \tag{5.10}$$

Furthermore, every cluster of granules (instead of classes) experienced an apparent voidage fraction of the surrounding liquid ϵ_L. The calculation of this apparent voidage fraction for individual granules is identical to the calculation for granule classes, only in this case is the diameter represents the individual granule instead of the granule class.

$$\epsilon_j = 1 - \left[1 + \left(\frac{\overline{d_i}}{d_j}\right)\left[(1-\epsilon_L)^{-\frac{1}{3}} - 1\right]\right]^{-3} \tag{5.11}$$

Similarly, the average granule diameter can be calculated based on groups of similarly sized granules at the same height in the reactor:

$$\overline{d_i} = \frac{\sum_{j=1}^{N_i} \theta_j d_j}{1 - \epsilon_L} \tag{5.12}$$

Although this approach works well for classes of granules, the model outcome is unrealistic when a large granule is surrounded by lots of small granules or flocs. Here $\overline{d_i}$ will approach the size of the flocs in this case, leading to a very low value of ϵ_j for the large granule. The resulting low value of $\frac{\overline{d_i}}{d_j}$ makes the large granules stop settling all together. To cope with these rare cases, the value of ϵ_j is set to ϵ_L when $\epsilon_j - \epsilon_L < 0.1$.

In chapter 3 the ratio between the fluidizing velocity and the terminal velocity was found to be 0.5, after calibration with a single fraction between 1.0 and 2.0 mm. In this study we found that a value of 0.8 would give a better estimate for the smallest size fraction 100 and 200 µm, and still agree with the original data. A similar correction was made for the calculation of the expansion index. In this case it was calculated based on the Archimedes number [54]:

$$n_j = \frac{1}{9.143 \times 10^{-6} Ar^{0.7728} + 0.2} \tag{5.13}$$

The position of a cluster of granules during feeding or settling (i.e. $v_{in} = 0$) was modelled as follows:

$$\frac{dx_j}{dt} = v_j + v_{in} \tag{5.14}$$

Growth of granules within a cluster

During each reaction phase, the volume (and thus the diameter) of a granule cluster was increased according to the amount of GFS accumulated as storage polymers during the anaerobic feeding phase, and a constant density and apparent yield throughout the granule. The new diameter of a granule cluster (j) was calculated using the following equation, assuming a spherical geometry:

$$d_j = 2\left(\frac{V_{j,old} + \frac{Y_{X,PHA}}{c_X}\int_0^{d_{j,old}/2} c_{PHA,j} A dr}{\frac{4}{3}\pi}\right)^{\frac{1}{3}} \tag{5.15}$$

Breakage of biofilm clusters

The probability of breakage is calculated with a logistic function:

$$P_j = \frac{1}{e^{-5000*(d_j-0.004)}+1} \tag{5.16}$$

Aerobic reaction phase

Processes taking place during the reaction phase were not modelled with time dependence, nor with a spatial dependence, but as a sequence of events. First, the residual GFS that was not stored anaerobically was distributed over all existing clusters based on specific biofilm surface area. Next, the diameter of all clusters was increased due to growth, based on an apparent yield (i.e. including loss from decay). All n-GFS fed during the anaerobic phase was subsequently converted into new flocs. The final step was breakage of particles. This is different from the time dependent approach often used in single biofilm modelling [55], but the simplification was justified due to the requirement of a discrete, cluster-based approach. Mixed wasting of sludge was applied for MLSS control at the end of the aeration phase.

Cycle build-up

A typical Nereda® cycle was simulated in the model. This typical cycle has a duration of 6 hours, and consists of 60 min of anaerobic feeding and decanting, 270 min of reaction time, and 30 min for settling and wasting of biomass. These typical values could vary in the scenarios. Figure 5.5 shows the different processes being modelled in the different phases of the cycle.

5.2.4. Lorenz-curve and Gini-coefficient

For analyses of the model result, we used a method for calculating inequality called the Gini coefficient [57]. This Gini coefficient quantifies the inequality using the Lorenz-curve, which plots the cumulative fraction of the total income (y-axis) earned by a population fraction sorted (x-axis) [58]. The Gini coefficient is determined by the ratio of the area between the equality line and the Lorenz curve, and the area below the Lorenz curve. To utilize the Gini coefficient for the quantitative analysis of the distribution of GFS in the feeding phase, the amount of GFS accumulated

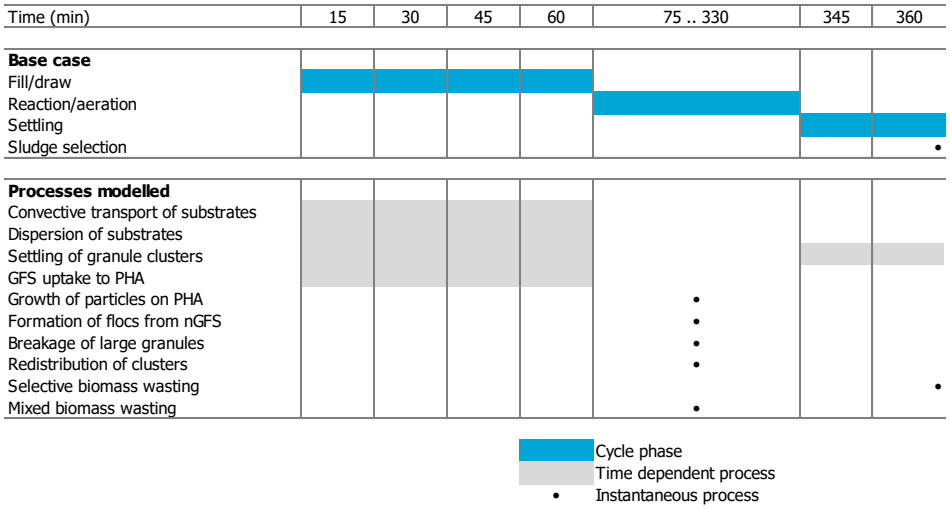

Figure 5.5: Typical batch scheduling for the AGS process and the various active processes in the model.

as storage polymers by each cluster was calculated weighted by the number of granules (G) represented by a simulated cluster (j). Before calculation, the clusters were sorted based on the amount of accumulated GFS from low to high. The y-axis of the Lorenz curve was defined as:

$$y_j = \frac{\sum_{m=1}^{j} G_m \int_0^{d_m/2} c_{PHA,m} A \, dr}{\sum_{m=1}^{N} G_m \int_0^{d_m/2} c_{PHA,m} A \, dr} \tag{5.17}$$

The x-axis was calculated via:

$$x_j = \frac{\sum_{m=1}^{j} G_m}{\sum_{m=1}^{N} G_m} \tag{5.18}$$

5.2.5. Size distribution

The granule size distribution of the sludge in the Nereda® reactor used as reference in figure 5.2 was measured over time. To determine the granule size distribution 1 L of sample was poured over a series of sieves with different mesh sizes (212, 425, 630, 1000, 1400 and 2000 µm). A mixed sample of 100 mL was filtered for the determination of the total dry weight. The obtained granular biomass of the different sieve fractions and the mixed sample were dried at 105 °C until no change in weight was detected anymore. Then the sieve fractions are grouped together:

Table 5.2: Biological and physical constants used for the sensitivity analyses.

Constant	Symbol	Value	Unit	Reference
Péclet number	Pe	2.5×10^{2}	-	[50]
Reactor height	H	6	m	this study
Feeding velocity	v_{in}	4	$m\,h^{-1}$	this study
Bulk-liquid density	ρ_L	1×10^{3}	$kg\,m^{-3}$	[7]
Granule density	ρ_B	1.035×10^{3}	$kg\,m^{-3}$	[7]
Temperature	T	293	K	this study
Biomass concentration granule	c_X	5×10^{1}	$kg\,m^{-3}$	[7]
Diffusion coefficient GFS in bulk (298 K)	$D_{GFS,L}$	1.21×10^{-9}	$m^2\,s^{-1}$	[52]
Diffusion coefficient GFS in biofilm (298 K)	$D_{GFS,B}$	2.4×10^{-10}	$m^2\,s^{-1}$	[56]
Monod constant for GFS	K_{GFS}	1×10^{-3}	$kg\,m^{-3}$	this study
Monod constant for PHA	K_{PHA}	1×10^{-3}	$kg\,m^{-3}$	this study
Maximum biomass specific substrate uptake rate	$q_{AN,max}$	2.78×10^{-5}	$kg\,kg^{-1}\,s^{-1}$	this study
Maximum storage capacity of GFS	$c_{PHA,max}$	7.5	$kg\,m^{-3}$	this study
Yield of biomass on storage polymers	$Y_{X,PHA}$	0.32	$kg\,kg^{-1}$	this study
Yield of biomass on n-GFS	$Y_{X,n\text{-}GFS}$	0.32	$kg\,kg^{-1}$	this study

small granules are the sum of 212, 425 and 630 µm, large granules are the sum of 1000, 1400 and 2000 µm and the concentration of proto-granules and flocs is obtained by subtracting the sum of all granule fractions from the concentration of the mixed sample.

5.3. Results and discussion

A sensitivity analysis was done to compare the influence of the major mechanisms on the granulation process. The main results for all scenarios are summarized in table 5.3 and figure 5.6.

5.3.1. Reference case

A reference case was defined and the different scenarios in the sensitivity analysis were compared to this reference case. The reference case was a full-scale reactor with a water depth of 6 m, that was seeded with $2\,g\,L^{-1}$ of flocs of 100 µm. The selection pressure at the start was $3\,m\,h^{-1}$ and it was slowly increased whenever the sludge concentration reached $3.0\,g\,L^{-1}$. The reactor was fed from the bottom of the reactor, with a Péclet number of 250. The exchange ratio was 25 % and there were no rainy weather conditions, or other variation to the influent flow or composition. The reactor was fed four batches per day, containing $500\,mg\,L^{-1}$ of COD, which was composed of $200\,mg\,L^{-1}$ granule forming substrate and $300\,mg\,L^{-1}$ non-granule forming substrate. The feeding time was 60 min. Feeding and decanting was done simultaneously, as is normal for full-scale AGS installations.

For analyses the particles in the reactor are classified in three main types: the *proto granules*, which are particles in the range of 100 to 200 µm. These particles have the granular morphology, but settling behaviour is floc-like, so they are not able to separate from the sludge matrix. *Flocs* are mathematically treated similar to the proto-granules, because they both have the same floc-like behaviour. In the model a floc is represented by particles of 100 µm and smaller. *Small granules* are particles in the range of 200 to 1000 µm. These particles (larger than 200 µm) are aerobic granules according to the definition of AGS [33]. These granules settle

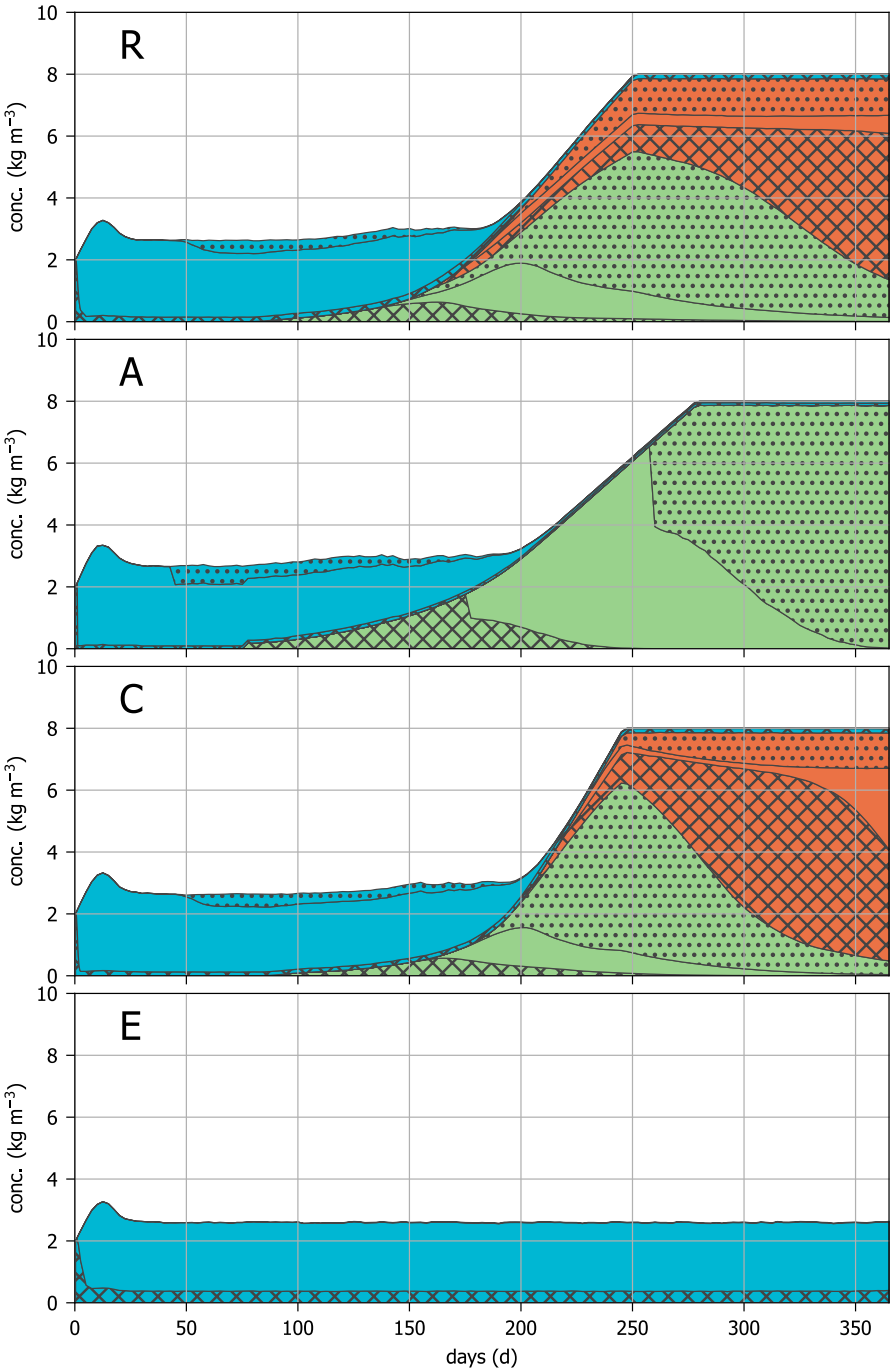
R
A
C
E
conc. (kg m^{-3})
0
2
4
6
8
10
0
50
100
150
200
250
300
350
days (d)

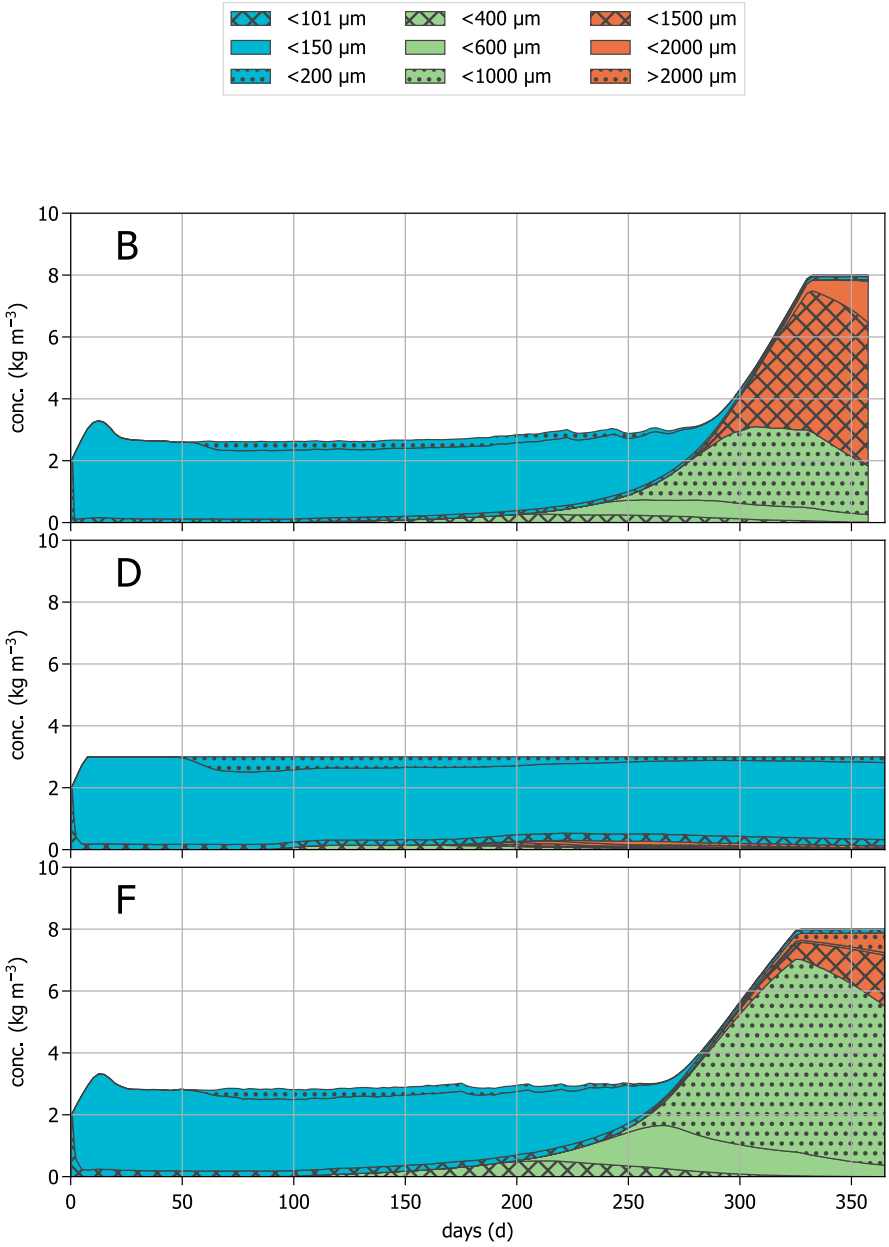

Figure 5.6: Concentration and evolution of granule fractions in the scenarios: blue area shows flocs and proto-granules, green area shows small granules, orange area shows large granules. R: reference case, A: mixed feeding, B: 15 min feeding, C: 30 min feeding, D: no selective wasting, E: 100 mg L^{-1} GFS, F: no selective feeding.

better than the proto-granule fraction and are small enough to be fully penetrated with substrate (acetate and oxygen). Particles larger than 1000 µm are called *large granules*. These granules settle very quickly and accumulate near the bottom of the reactor during the feeding phase. Large granules are large enough to only be partially penetrated with substrates.

The granulation process in the reference case is shown in figure 5.6. Since the reactor is seeded with particles of 100 µm, it takes time before the first small granules appear in the reactor. All proto-granules have the same bulk-like settling behaviour, so selective wasting has no effect yet. This means every particle has the same chance of being spilled. Until this point the growth of the granules is based on chance. The proto-granules will not not receive substrate every cycle. The substrate load depends on the position in the sludge bed, the volumetric exchange ratio and the amount of sequestered substrate by the particles beneath it. Over the course of multiple cycles, the combination of these factors will determine whether a proto-granule will receive enough substrate to grow into a small granule before it is spilled.

After 90 d the first small granules appear, and these granules settle faster than the proto-granules. This gives these granules a competitive advantage: the granules will be fed more frequently, because they settle towards the bottom of the reactor. This can be seen as a race towards the substrate. The fastest settling granule will always win the race and can take up a maximum amount of substrate. On top of this, the fastest settling granule will also be spilled less likely in the selective wasting from the top of the settled sludge bed. Larger granules therefore have a double benefit: they receive more substrate and they are less likely to be spilled. This process is also visible in figure 5.6: small granules dominate the population in the reactor a few weeks after the first small granules appeared.

In the simulation the first large granules appear after 165 d. These granules have better settling properties then the small granules, the largest ones having settling velocities well over 100 $m\,h^{-1}$. This means the large granules will reach the bottom of the reactor in several minutes and they will be fed every cycle. The chance of being spilled through selective wasting is close to zero, because the settling velocity of large granules is much larger than the maximum applied selection pressure of 6 $m\,h^{-1}$. This is a matter of the winner takes it all. The large granules will accumulate most of the granule forming substrate (figure 5.7), essentially leading to the extinction of the proto-granules.

The end of the lag phase is defined as the moment the biomass concentration increases more than 10 % above the target concentration of 3 $g\,L^{-1}$. This means the maximum selection pressure of 6 $m\,h^{-1}$ is reached and due to the increasing amount of granules, the biomass concentrations keeps increasing. The reference case has a lag phase of 193 d. The end of the lag phase marks the start of the granulation phase, which ends when the target biomass concentration of 8 $g\,L^{-1}$ is reached. Hereafter the biomass concentration is kept on 8 $g\,L^{-1}$ through mixed wasting in the aeration phase. The duration of the granulation phase was 58 d (see Table 5.3).

The granulation process in the reference case is very similar to what is observed

in practice (figure 5.2). It shows a similar apparent steady state in the lag phase after which large granules appear in the granulation phase. Granulation in practice shows a bit more variation due to processes that are not taken into account in the model, such as rain weather events, load variations and temperature variations, but the overall process compares well.

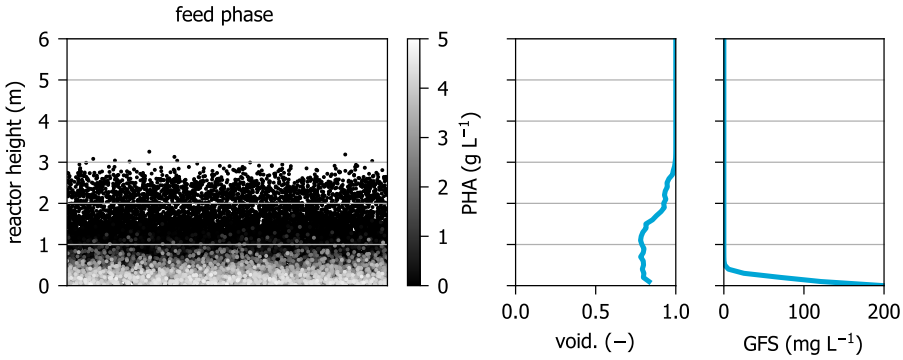

Figure 5.7: Granules in the reference after the feeding phase at day 75. All graphs show the depth of the reactor on the y-axis. Left: individual groups of granules, color based on PHA concentration (g L^{-1}) in the granule, x location is randomly chosen for visualization. Middle: the voidage fraction in the bed. Right: granule forming substrate in the bulk liquid.

Table 5.3: Results of sensitivity analysis.

	first granule		phases		granule size	
	small (d)	large (d)	lag (d)	granulation (d)	average (µm)	maximum (µm)
reference case	90	165	193	58	1371	3742
no plug flow	78	-	205	73	695	742
15 minutes feeding	125	278	290	42	1206	2399
30 minutes feeding	95	203	205	42	1575	3716
no selective wasting	98	193	-	-	189	3518
100 mg L^{-1} GFS	-	-	-	-	110	736
no selective feeding	115	278	275	52	1126	3886

5.3.2. Microbial selection

The effect of changing feast/famine conditions was shown by shortening the anaerobic feeding time, thus limiting the anaerobic uptake of granule forming substrate. Since the batch size (and thus the loading rate) was kept constant, shortening the feeding time resulted in a higher feed flow velocity. In the reference case the anaerobic feeding time was 60 min, which was reduced to 30 min and 15 min. The shorter feeding time has a clear effect on the duration of the lag phase, which was 193 d in the reference case and was increased to 290 d in the case with a 15 minute feeding phase (table 5.3). The granulation phase was a bit faster, when the feeding phase was shortened, reducing from 58 to 42 d. The final granule size distribution after 365 d was quite similar.

The difference in the lag phase is a consequence of the higher up-flow velocity and the shorter contact time in the scenarios. A consequence of the higher up-flow velocity is a larger sludge bed expansion, leading to less proto-granules in contact with the influent. The shorter contact time also leads to less uptake of substrate by the particles. As a result, less proto-granules grow into small granules due to the more even distribution of the residual granule forming substrate left over after the feeding phase.

In the granulation phase the bed expansion is no issue anymore, because small granules can settle faster than flocs and proto-granules. So, the substrate-rich influent is more effectively in contact with the largest granule size fraction. The higher up-flow velocity causes a distribution of the GFS to be more skewed towards the small granules. As a result, small granules are converted into larger granules more quickly, slightly reducing length of the granulation phase.

Overall, the duration of the feast period is especially important in the lag phase, which is shortened by a longer feast period at equal daily volumetric loading rates. In the granulation period, the duration of the feast period is of less importance and might even provide a means to control the granule size distribution.

5.3.3. Selective wasting

The contribution of selective wasting to the aerobic granulation process was shown by switching from selective wasting to mixed wasting. In selective wasting the slowest settling biomass is removed from the top of the sludge bed, while faster settling particles remain in the reactor. In mixed wasting, the biomass concentration is kept constant by wasting both fast and slow settling biomass, all particles having the same chance to be spilled. The mixed wasting is representative for the situation in a conventional activated sludge process. The biomass was spilled to maintain a concentration of $3\,g\,L^{-1}$. This mixed wasting did not lead to a significant granular fraction, although after 98 d the first small granules appeared in the reactor. Some large granules were present at the end of the simulation, although their contribution was small ($0.3\,g\,L^{-1}$) and with insufficient effect on the settleablility to allow for an increase in MLSS.

This scenario clearly shows the importance of selective wasting, because without it, significant granulation does not happen. It also shows the drive towards granulation from the other mechanisms in the reactor. Although the granules are not preferentially maintained in the reactor as they are randomly spilled, new granules are constantly formed, due to spread in anaerobic distribution of GFS. This might explain, why (small) granules are observed in many conventional activated sludge systems [34]. Even without selective wasting, some growth of granules can happen, when the other drivers for granulation are sufficiently present in the reactor. However, selective wasting is essential to drive the sludge towards full granulation.

5.3.4. Concentration gradients

To show the positive effect of upwards plug flow feeding on the granule formation, in the simulation the plug flow feeding was removed. The reactor was changed

into an ideally mixed reactor during the feeding period. In full-scale AGS reactor feeding and decanting is done simultaneously, which is possible because of the plug flow [50]. When the reactor would be ideally mixed during feeding, biomass would wash-out, resulting in poor effluent quality. For a good comparison between the scenarios, in the simulation biomass was not allowed to leave the reactor with the effluent. The results show a strong shift towards smaller granules. Compared to the reference case the duration of the lag phase was only slightly longer (205 d compared to 193 d). Also, the duration of granulation phase was very similar. The real difference is visible in the granule size distribution at the end of the simulation. Without the plug flow feeding, no large granules appeared in the reactor and the average granule size was 703 µm (compared to 1371 µm in the reference case).

This shift towards smaller granules is caused by several different processes. Lower substrate concentrations in the bulk liquid limit the diffusion depth of substrate into the granules. This results in slower granule growth. Also, all substrate is distributed evenly over all particles, where in the reference case the best settling fraction receives most of the substrate. Pilot-scale work with anaerobic pulse-feeding of municipal wastewater showed a smaller mean granule size compared to the plug flow of full-scale bottom-fed reactors [59]. Because the other mechanisms for granulation are still present (microbial selection, selective wasting and granule forming substrate), the system can still achieve a high granulation grade, but only with small granules.

5.3.5. Selective feeding

The effect of the selective feeding was shown by removing the differences in settling velocity between the different particle sizes during the feeding phase. As a result, all particles have the same chance to be exposed to substrate, regardless of their settling properties, while the concentration gradient resulting from the plug flow was kept intact. The effect is most noticeable in the duration of the lag phase, which takes 275 d compared to 193 d in the reference case. The duration of granulation phase is comparable with the reference case, but the granulation phase starts without any large granules present. In the end the average granule size is slightly smaller than in the reference case. This outcome indicates that whether a system transitions from the lag phase to the granulation phase is not only determined by the formation of some small granules that settle faster than proto-granules and flocs. The ability to exploit the faster settling properties of small granules for the uptake of GFS is key in accelerating the transition from the lag-phase to the granulation-phase and of the granulation phase itself.

The selective feeding can thus be seen as a race to the substrate: the best settling granules will have the longest exposure to the substrate and will see the highest concentration gradients. Because the settling properties of granules get better as they get larger, selective feeding allows for an increase substrate utilization with an increasing granule size. Removing selective feeding from the simulation shows, as expected, a shift towards smaller granules. Although in the end large granules still appear in the reactor, selective feeding is an important driver for granulation, which has not been recognized before in literature.

5.3.6. Granule forming substrate

In the model non-granule forming substrate will always lead to the formation of flocs and granule forming substrate can lead to the formation of granules, if it is converted into storage polymers. Especially in the lag phase the ratio between GFS and n-GFS will influence the chance of proto-granules to grow into small granules. When too many flocs are formed compared to the growth of the proto-granules, the proto-granules will get spilled before they grow into small granules and can preferentially be retained in the reactor. This is clearly shown in the scenario where the GFS was reduced from 200 mg L^{-1} to 100 mg L^{-1} (i.e. decreased from 40 % to 20 % of the influent COD). Under these conditions the lag phase does not finish in the 365 d of simulation. Although some small granules appear in the reactor (the maximum granule size is 736 µm), the average granule size is only 110 µm and the simulation clearly shows a shift towards flocs in the lag phase.

In the model transport and conversion characteristics of GFS were modelled as acetate, which is the most abundant granule forming substrate in municipal wastewater treatment. GFS is derived from the fatty acids in the influent supplemented with the fatty acids formed by fermentation and hydrolysis of more complex influent COD [16, 60]. The amount of GFS is in this context partly depending on the process conditions. Fermentation and hydrolysis were not included in the presented modelling framework, since for this sensitivity analysis the origin of the GFS is not important. The amount of GFS will determine if the wastewater is suitable for AGS. For future modelling and better design of AGS processes these fermentation and hydrolysis processes will need better characterization in order to include them in a reliable manner in aerobic granular sludge simulation platforms.

5.3.7. Breakage

Granules will eventually break into smaller pieces. In the model the chance of breaking is coupled to the granule size: larger granules have higher chance of breaking. The resulting pieces can become a seed for new granules. In the simulations the origin of granules (floc or breakage) was monitored. At the start, all granules originate from flocs. When large granules appear in the reactor, an increasing fraction of the biomass originates from broken-up granules. At the end of the simulation (after 365 d) almost 20 % originates from broken-up large granules. This process can be seen as a bypass of the lag phase. Some pieces will be larger than proto-granules and can develop into new granules, without going through the stochastic growth process of the proto-granules. In this work, the probability of breakage was increased with increasing granule size, based on a decreasing granule strength, as was reported by [35]. The granule size beyond which a granule would have a definite probability to break-up was based on the maximum granule size observed in full scale Nereda® [7]. Granules can break-up in two parts of random volume, adding up to the volume of the original granule. In practice, breakage into multiple parts as well as attrition will occur [21]. Reality is clearly more complicated than the implementation used for the sensitivity analysis in this study. However, all implementations would have the same qualitative effect as was observed in this

study, determining the maximum granule size and generate nuclei of varying size for granulation to continue. For a part the breakage of large granules will be a driver for the acceleration of the granulation process in the granulation phase. Breakage of granules has a similar effect as adding an external seed of granules to a reactor [61]. Both act as a source of new granules, bypassing the slow stochastic process of growing small granules out of flocs and proto-granules. So during start-up of AGS systems in practice a granular seed could speed up start-up times significantly.

5.3.8. Model validity

Various mathematical models have been developed to describe biofilm growth [55] and biochemical conversions in (partially) aerobic reactors for wastewater treatment [49]. For the sensitivity analysis presented here, we opted to implement only conversions required to capture the basic dynamics a mechanism has on distribution of biomass over the size classes of granules. The model was intended for systems with an anaerobic feast phase and an aerobic famine phase. Only heterotrophic growth was assumed, with a constant VSS/TSS ratio, using two substrates (n-GFS and GFS) and an apparent yield for growth (modelling decay and growth combined). Consequently, the active biomass density was constant, homogeneous over the radius of a granule and independent of the historical substrate loading rate of a cluster. This history could also not impact the storage capacity of PHA. Regardless of these simplifications, the model was able to describe the principal behaviour of the granulation process, consisting of a lag phase and a granulation phase, without focus on mimicking actual reactor performance. In the future the model could be extended to incorporate biological nutrient removal to investigate the effects of the mechanisms on reactor performance.

5.3.9. Further analysis

The sensitivity analysis performed in this study shows how delicate the start-up of a AGS reactor from flocs is. The lag phase that is seen in practice can be explained by the slow stochastic process of turning flocs into proto-granules and proto-granules into small granules. Selective wasting is an important mechanism for granulation, but in the lag phase, because of the entrapment of proto-granules in the sludge flocs, it has a limited effect. Granules are only selectively retained in the reactor, when they settle faster than the flocculent sludge fraction. So the selective wasting only starts to be effective when small granules appear in the reactor. The lag phase seems to be mainly driven by the presence of granule forming substrate and the ratio between proto-granule growth and production of new flocs. The latter is important for the retention time distribution of the proto-granules. Flocs and proto-granules will have a different age. The distribution of age needs to allow for small granules to be formed, so the maximum retention time distribution determines, if and how fast small granules are formed.

In the granulation phase the other mechanisms become more important for the granulation process. Large granules will not be spilled through the selective wasting and will only disappear from the reactor through breakage. The largest granules receive the largest amount of substrate, because of the selective feeding. Their

substrate uptake capacity combined with their abundance is large enough to take up all the substrate. As a consequence, only a limited amount of granule forming substrate is available for the flocs and proto-granules in a mature granular bed. The large granules will filter out all substrate from the influent at the bottom of the reactor. It is a matter of "the winner takes it all", as can be seen in figure 5.8, where we used a Lorenz curve to visualize this process. In economics the Lorenz curve [58] is used to visualize the inequality of the wealth distribution. We used it to visualize the inequality in the substrate sequestered by the granules. The accompanying Gini coefficients [57] are also shown. In the plot the cumulative amount of substrate taken up by the granules was plotted versus the cumulative amount of granules. The diagonal line would represent a completely even distribution of the substrate over all granules. The Lorenz curve at 3 different days is plotted. At the start of the simulation there is some inequality, but this is caused by the batch size that is smaller than the bed height. At the end of the lag phase there is already a large inequality with a Gini coefficient increasing from 0.354 to 0.952, indicating a large change in substrate distribution. So at the end of the lag phase, already a large part of the substrate is sequestered by a small part of the granules. At the end of the granulation phase the inequality is even larger, with a Gini coefficient of 0.998, indicating that only a small fraction of granules sequester almost all the substrate, clearly showing the effect of the selective feeding.

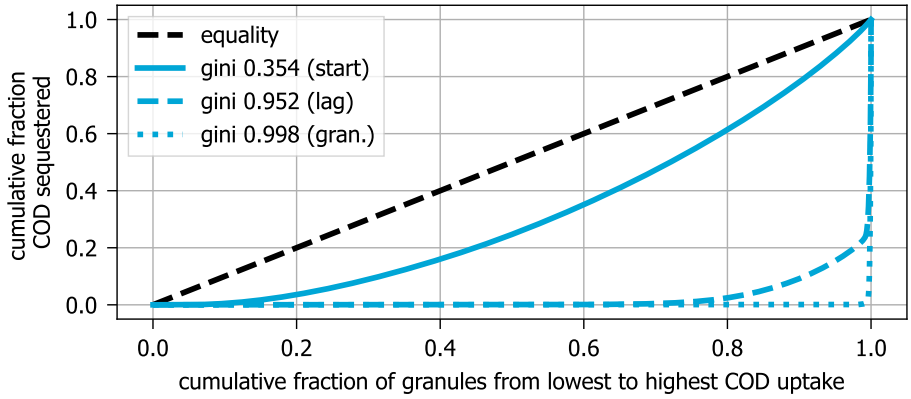

Figure 5.8: Lorenz curve showing the inequality in substrate distribution over the granules in the reference case. The curves are given at the start of the simulation, at the end of the lag phase and the end of the granulation phase, indicating an increasing inequality in substrate distribution. The numbers in the legend indicate the Gini coefficient (0 for equal distribution, 1 of complete unequal distribution).

5.3.10. Practical implications

Growing granules from activated sludge flocs in a full-scale reactor can be a lengthy process, as shown in figure 5.2. The model shows that a lag phase is a natural part of the granulation process. In practice reactors are often seeded with AGS from other plants to shorten the lag phase. Seeding is a method to break out of the stochastic processes that dominate the length of the lag-phase. Besides providing

insights on the granulation process, the model can help to optimize the start-up process and find an optimum between cost for seeding and length of the start-up process. The model can also be used to optimize the start-up strategy regarding selective wasting, applied batch size and cycle times. When in the future the model is extended with a more elaborate biological model, it can also be used to investigate the effect of granule size distribution on conversion rates and effluent quality.

5.4. Conclusion

A model was developed to provide a theoretical framework to analyse the different relevant mechanisms for aerobic granular sludge formation, which can form the basis for a comprehensive model that includes detailed nutrient removal aspects. The insights from this study can be used to further improve the granule formation in AGS reactors.

- The model describes the dynamics of a lag and a granulation phase, found in practice.
- Selective feeding and breakage of large granules were identified as important mechanisms, not reported in literature.
- Granulation is a combined result from 6 mechanisms, allowing a sub-optimal mechanism to be compensated by the other mechanisms.
- The GFS/n-GFS ratio and feast/famine ratio are the most important mechanisms in determining whether a system *can* transition from the lag phase to the granulation phase.
- Selective wasting and selective feeding mainly determine whether the transition from lag to the granulation phase *will* occur and at which rate.
- Breaking of granules can have a positive effect on granulation, similar to seeding of reactors with granules.

Bibliography

[1] E. J. H. van Dijk, V. A. Haaksman, M. C. M. van Loosdrecht, and M. Pronk, *On the mechanisms for aerobic granulation - model based evaluation,* Water Res. **216**, 118365 (2022).

[2] M. K. H. Winkler, C. Meunier, O. Henriet, J. Mahillon, M. E. Suárez-Ojeda, G. Del Moro, M. De Sanctis, C. Di Iaconi, and D. G. Weissbrodt, *An integrative review of granular sludge for the biological removal of nutrients and recalcitrant organic matter from wastewater,* Chem. Eng. J. **336**, 489 (2018).

[3] Y. Liu and J. H. Tay, *The essential role of hydrodynamic shear force in the formation of biofilm and granular sludge,* Water Res. **36**, 1653 (2002).

[4] J. H. Tay, Q. S. Liu, and Y. Liu, *The effects of shear force on the formation, structure and metabolism of aerobic granules,* Appl. Microbiol. Biotechnol. 2001 571 **57**, 227 (2001).

[5] J. Wu, F. L. de los Reyes, and J. J. Ducoste, *Modeling cell aggregate morphology during aerobic granulation in activated sludge processes reveals the combined effect of substrate and shear,* Water Res. **170**, 115384 (2020).

[6] B. S. McSwain, R. L. Irvine, and P. A. Wilderer, *The influence of settling time on the formation of aerobic granules,* Water Sci. Technol. **50**, 195 (2004).

[7] E. J. H. van Dijk, M. Pronk, and M. C. M. van Loosdrecht, *A settling model for full-scale aerobic granular sludge,* Water Res. **186**, 116135 (2020).

[8] T. Rocktäschel, C. Klarmann, B. Helmreich, J. Ochoa, P. Boisson, K. H. Sørensen, and H. Horn, *Comparison of two different anaerobic feeding strategies to establish a stable aerobic granulated sludge bed,* Water Res. **47**, 6423 (2013).

[9] S. Lochmatter and C. Holliger, *Optimization of operation conditions for the startup of aerobic granular sludge reactors biologically removing carbon, nitrogen, and phosphorous,* Water Res. **59**, 58 (2014).

[10] V. A. Haaksman, M. C. M. van Loosdrecht, and M. Pronk, *Influence of anaerobic contact regime on substrate distribution,* unpublished (2022).

[11] A. Mosquera-Corral, M. K. de Kreuk, J. J. Heijnen, and M. C. M. van Loosdrecht, *Effects of oxygen concentration on N-removal in an aerobic granular sludge reactor,* Water Res. **39**, 2676 (2005).

[12] J. J. Beun, M. C. M. van Loosdrecht, and J. J. Heijnen, *Aerobic granulation in a sequencing batch airlift reactor,* Water Res. **36**, 702 (2002).

[13] M. K. de Kreuk and M. C. M. van Loosdrecht, *Selection of slow growing organisms as a means for improving aerobic granular sludge stability,* Water Sci. Technol. **49**, 9 (2004).

[14] C. Cofré, J. L. Campos, D. Valenzuela-Heredia, J. P. Pavissich, N. Camus, M. Belmonte, A. Pedrouso, P. Carrera, A. Mosquera-Corral, and A. Val del Río, *Novel system configuration with activated sludge like-geometry to develop aerobic granular biomass under continuous flow,* Bioresour. Technol. **267**, 778 (2018).

[15] M. Pronk, B. Abbas, S. H. K. Al-zuhairy, R. Kraan, R. Kleerebezem, and M. C. M. van Loosdrecht, *Effect and behaviour of different substrates in relation to the formation of aerobic granular sludge,* Appl. Microbiol. Biotechnol. **99**, 5257 (2015).

[16] M. Layer, A. Adler, E. Reynaert, A. Hernandez, M. Pagni, E. Morgenroth, C. Holliger, and N. Derlon, *Organic substrate diffusibility governs microbial community composition, nutrient removal performance and kinetics of granulation of aerobic granular sludge,* Water Res. X **4**, 100033 (2019).

[17] O. T. Iorhemen and Y. Liu, *Effect of feeding strategy and organic loading rate on the formation and stability of aerobic granular sludge,* J. Water Process Eng. **39**, 101709 (2021).

[18] S. Wang, W. Shi, T. Tang, Y. Wang, L. Zhi, J. Lv, and J. Li, *Function of quorum sensing and cell signaling in the formation of aerobic granular sludge,* Rev. Environ. Sci. Biotechnol. **16**, 1 (2017).

[19] X. M. Liu, G. P. Sheng, H. W. Luo, F. Zhang, S. J. Yuan, J. Xu, R. J. Zeng, J. G. Wu, and H. Q. Yu, *Contribution of extracellular polymeric substances (EPS) to the sludge aggregation,* Environ. Sci. Technol. **44**, 4355 (2010).

[20] C. Picioreanu, M. C. M. van Loosdrecht, and J. J. Heijnen, *Mathematical modeling of biofilm structure with a hybrid differential- discrete cellular automaton approach,* Biotechnol. Bioeng. **58**, 101 (1998).

[21] H. H. Beeftink and J. C. van den Heuvel, *Bacterial aggregates of various and varying size and density: a structured model for biomass retention,* Chem. Eng. J. **44**, B1 (1990).

[22] M. C. M. van Loosdrecht, J. J. Heijnen, H. Eberl, J. Kreft, and C. Picioreanu, *Mathematical modelling of biofilm structures,* Antonie van Leeuwenhoek, Int. J. Gen. Mol. Microbiol. **81**, 245 (2002).

[23] H. A. Nicholls and D. W. Osborn, *Bacterial stress: Prerequisite for biological removal of phosphorus,* J. Water Pollut. Control Fed. **51**, 557 (1979).

[24] G. J. F. Smolders, J. van der Meij, M. C. M. van Loosdrecht, and J. J. Heijnen, *Model of the anaerobic metabolism of the biological phosphorus removal process: Stoichiometry and pH influence,* Biotechnol. Bioeng. **43**, 461 (1994).

[25] M. Ali, Z. Wang, K. W. Salam, A. R. Hari, M. Pronk, M. C. M. van Loosdrecht, and P. E. Saikaly, *Importance of species sorting and immigration on the*

bacterial assembly of different-sized aggregates in a full-scale Aerobic granular sludge plant, Environ. Sci. Technol. **53**, 8291 (2019).

[26] E. Morgenroth, T. Sherden, M. C. M. van Loosdrecht, J. J. Heijnen, and P. A. Wilderer, *Aerobic granular sludge in a sequencing batch reactor,* Water Res. **31**, 3191 (1997).

[27] L. Qin, J. H. Tay, and Y. Liu, *Selection pressure is a driving force of aerobic granulation in sequencing batch reactors,* Process Biochem. **39**, 579 (2004).

[28] J. J. Heijnen and M. C. M. van Loosdrecht, *Method for acquiring grain-shaped growth of a microorganism in a reactor,* (1998).

[29] M. Pronk, M. K. de Kreuk, L. M. M. de Bruin, P. Kamminga, R. Kleerebezem, and M. C. M. van Loosdrecht, *Full scale performance of the aerobic granular sludge process for sewage treatment,* Water Res. **84**, 207 (2015).

[30] M. Layer, K. Bock, F. Ranzinger, H. Horn, E. Morgenroth, and N. Derlon, *Particulate substrate retention in plug-flow and fully-mixed conditions during operation of aerobic granular sludge systems,* Water Res. X **9**, 100075 (2020).

[31] Y.-Q. Q. Y. Liu, Z.-W. W. Wang, Y.-Q. Q. Y. Liu, L. Qin, and J.-H. H. Tay, *A generalized model for settling velocity of aerobic granular sludge,* Biotechnol. Prog. **21**, 621 (2005).

[32] E. Arvin and P. Harremoes, *Biofilm Reactor Performance,* Water Sci. Technol. **22**, 171 (1990).

[33] M. K. de Kreuk, N. Kishida, and M. C. M. van Loosdrecht, *Aerobic granular sludge – state of the art,* Water Sci. Technol. **55**, 75 (2007).

[34] S. P. Wei, H. D. Stensel, B. Nguyen Quoc, D. A. Stahl, X. Huang, P. H. Lee, and M. K. H. Winkler, *Flocs in disguise? High granule abundance found in continuous-flow activated sludge treatment plants,* Water Res. **179**, 115865 (2020).

[35] D. R. de Graaff, E. J. H. van Dijk, M. C. M. van Loosdrecht, and M. Pronk, *Strength characterization of full-scale aerobic granular sludge,* Environ. Technol. **41**, 1637 (2020).

[36] J. E. Baeten, D. J. Batstone, O. J. Schraa, M. C. M. van Loosdrecht, and E. I. P. Volcke, *Modelling anaerobic, aerobic and partial nitritation-anammox granular sludge reactors - A review,* Water Res. **149**, 322 (2019).

[37] S. F. Yang, Q. S. Liu, J. H. Tay, and Y. Liu, *Growth kinetics of aerobic granules developed in sequencing batch reactors,* Lett. Appl. Microbiol. **38**, 106 (2004).

[38] B. J. Ni, G. P. Sheng, X. Y. Li, and H. Q. Yu, *Quantitative Simulation of the Granulation Process of Activated Sludge for Wastewater Treatment,* Ind. Eng. Chem. Res. **49**, 2864 (2010).

[39] M. K. de Kreuk, C. Picioreanu, M. Hosseini, J. B. Xavier, and M. C. M. van Loosdrecht, *Kinetic model of a granular sludge SBR: Influences on nutrient removal,* Biotechnol. Bioeng. **97**, 801 (2007).

[40] J. B. Xavier, M. K. de Kreuk, C. Picioreanu, and M. C. M. van Loosdrecht, *Multi-scale individual-based model of microbial and byconversion dynamics in aerobic granular sludge,* Environ. Sci. Technol. **41**, 6410 (2007).

[41] P. Dold, B. Alexander, G. Burger, M. Fairlamb, D. Conidi, C. Bye, and W. Du, *Modeling full-scale granular sludge sequencing tank performance,* in *91st Annu. Water Environ. Fed. Tech. Exhib. Conf. WEFTEC 2018* (2019) pp. 3813–3826.

[42] A. J. Li and X. Y. Li, *Selective sludge discharge as the determining factor in SBR aerobic granulation: Numerical modelling and experimental verification,* Water Res. **43**, 3387 (2009).

[43] A. Giesen, L. M. M. de Bruin, R. P. Niermans, and H. F. van der Roest, *Advancements in the application of aerobic granular biomass technology for sustainable treatment of wastewater,* Water Pract. Technol. **8**, 47 (2013).

[44] C. Picioreanu, M. C. M. van Loosdrecht, and J. J. Heijnen, *A theoretical study on the effect of surface roughness on mass transport and transformation in biofilms,* Biotechnol Bioeng **68**, 355 (2000).

[45] C. Picioreanu, M. C. M. van Loosdrecht, and J. J. Heijnen, *Effect of Diffusive and Convective Substrate Transport on Biofilm Structure Formation: A Two-Dimensional Modeling Study,* Biotechnol. Bioeng. **69**, 504 (2000).

[46] M. K. de Kreuk, M. Pronk, and M. C. M. van Loosdrecht, *Formation of aerobic granules and conversion processes in an aerobic granular sludge reactor at moderate and low temperatures,* Water Res. **39**, 4476 (2005).

[47] M. K. H. Winkler, R. Kleerebezem, L. M. M. de Bruin, P. J. T. Verheijen, B. Abbas, J. Habermacher, and M. C. M. van Loosdrecht, *Microbial diversity differences within aerobic granular sludge and activated sludge flocs,* Appl. Microbiol. Biotechnol. **97**, 7447 (2013).

[48] M. Henze, *Characterization of Wastewater for Modelling of Activated Sludge Processes,* Water Sci. Technol. **25**, 1 (1992).

[49] M. Henze, W. Gujer, T. Mino, T. Matsuo, M. C. Wentzel, G. R. Marais, and M. C. M. van Loosdrecht, *Activated Sludge Model No.2d, ASM2D,* Water Sci. Technol. **39**, 165 (1999).

[50] E. J. H. van Dijk, M. Pronk, and M. C. M. van Loosdrecht, *Controlling effluent suspended solids in the aerobic granular sludge process,* Water Res. **147**, 50 (2018).

[51] S. Degaleesan and M. P. Dudukovic, *Liquid backmixing in bubble columns and the axial dispersion coefficient,* AIChE J. **44**, 2369 (1998).

[52] E. L. Cussler, *Diffusion: Mass Transfer in Fluid Systems*, 3rd ed., Cambridge Series in Chemical Engineering (Cambridge University Press, Cambridge, 2009).

[53] L. T. Fan, Y. C. Yang, and C. Y. Wen, *Mass transfer in semifluidized beds for solid-liquid system,* AIChE J. **6**, 482 (1960).

[54] M. Andalib, J. Zhu, and G. Nakhla, *A new definition of bed expansion index and voidage for fluidized biofilm-coated particles,* Chem. Eng. J. **189-190**, 244 (2012).

[55] O. Wanner and P. Reichert, *Mathematical modeling of mixed-culture biofilms,* Biotechnol. Bioeng. **49**, 172 (1996).

[56] L. van den Berg, M. C. M. van Loosdrecht, and M. K. de Kreuk, *How to measure diffusion coefficients in biofilms: A critical analysis,* Biotechnol. Bioeng. **118**, 1273 (2021).

[57] C. Gini, *Variabilita e mutabilita contributo allo studio delle distribuzioni e delle relazioni statistiche.* (Tipogr. di P. Cuppini, Bologna, 1912).

[58] M. O. Lorenz, *Methods of Measuring the Concentration of Wealth,* Publ. Am. Stat. Assoc. **9**, 209 (1905).

[59] T. Rocktäschel, C. Klarmann, J. Ochoa, P. Boisson, K. Sørensen, and H. Horn, *Influence of the granulation grade on the concentration of suspended solids in the effluent of a pilot scale sequencing batch reactor operated with aerobic granular sludge,* Sep. Purif. Technol. **142**, 234 (2015).

[60] S. Toja Ortega, M. Pronk, and M. K. de Kreuk, *Anaerobic hydrolysis of complex substrates in full-scale aerobic granular sludge: enzymatic activity determined in different sludge fractions,* Appl. Microbiol. Biotechnol. **105**, 6073 (2021).

[61] M. Pijuan, U. Werner, and Z. Yuan, *Reducing the startup time of aerobic granular sludge reactors through seeding floccular sludge with crushed aerobic granules,* Water Res. **45**, 5075 (2011).

6

Outlook

All our knowledge has its origin in our perceptions

Leonardo da Vinci

6.1. Arrival of a technology

Almost 25 years of AGS research has brought us many insights in the technology. Although still young compared to activated sludge, which was invented well over 100 years ago, with the arrival of the 100th full-scale Nereda® installation in the very near future AGS technology can by no means be considered a novel technology anymore. Nevertheless, we are only starting to discover the full potential of the technology. A deeper understanding of the mechanisms at work in an AGS reactor, will help to unleash its full capacity. In this dissertation I aimed to add to this deeper understanding and hopefully I transferred some of the insights I gained during my PhD research to the reader.

6.2. Degasification control

Degasification of nitrogen gas in AGS reactors remains an elusive problem. The main reason for this is that the occurrence of degasification depends on many factors, like temperature, both current batch size and previous batch size, nitrite/nitrate effluent quality, residual COD from the previous batch (or endogenous respiration), aeration and mixing intensity in the main aeration, granule size, biomass concentration, and probably a few more. As a result, occurrence of degasification problems, resulting in elevated levels of biomass in the effluent, can be quite erratic. Although the silk-like appearance of a degasification scum layer should be easily recognized by the operator, because it is quite distinct from other scum layers that can occur in wastewater treatment plants, identification remains a problem. We showed in chapter 2 how the process of degasification works, but

translating knowledge into a simple process control to prevent degasification, is less straightforward. The main obstacle is the fact we cannot easily measure the dissolved nitrogen concentration in the liquid to control the nitrogen deficit in the stripping phase. In practice this means the stripping phase needs to be carefully balanced between long enough to always strip enough nitrogen to be safe under all conditions and short enough to not limit the treatment capacity of the AGS reactor.

The major obstacle to having a proper process control for the stripping phase is the fact that we cannot measure the nitrogen concentration in the water phase. We can measure ammonia, nitrite and nitrate, but there is no adequate sensor for measuring pure nitrogen (N_2). A possible solution could be to create a soft-sensor, based on measurements of ammonia and nitrite, combined with the mathematical model described in chapter 2 extended with a more elaborate description of the biological processes involved. It should be possible to get a fairly accurate estimation of the nitrogen gas concentration after the reaction phase and adapt the process control of the stripping phase (and the settling and feeding phase) accordingly. This should minimize the problems with degasification scum layers and prevent it in most cases.

6.3. Process optimization

The AGS system can appear complex, when compared to conventional activated sludge plants. In a CAS plant the sludge flocs experience changing process conditions while traversing from tank to tank, but on average all sludge flocs are exposed to these process conditions in a similar manner. On average, all flocs receive the same amount of influent, are exposed to same amount of oxygen, and have a similar chance of being spilled. Of course, we must emphasize the words *on average* here, because the reader will quickly notice that it is common practice to increase floc loading rates by use of contact tanks, where only part of the return sludge is mixed with all of the influent. Also, because of residence time distribution in aerated tanks, some flocs will have shorter exposure to oxygen then others. But *on average* the process conditions for all flocs can be considered similar within the duration of the solid retention time. For aerobic granular sludge the process conditions are not similar for the different granule size fractions. As we have seen in chapter 3 different granule sizes have very different settling properties (with terminal velocities that can be 25 times higher when comparing the largest and the smallest granule fractions). An important effect of these different settling velocities is the process called *selective feeding* (see chapter 5). This means that the substrate loading rate is extremely skewed towards the largest granules and on average the largest granules receive the most substrate and as a result will grow more. The wasting of sludge is skewed towards the smallest granules, by a process called *selective wasting*. The AGS process is engineered to selectively waste the worst settling fraction and to retain the best settling granules. As a result, there is a clear Granule Residence Time Distribution (GRTD). The large granules can have an age of more than 50 d, while proto-granules can be spilled within hours or just a few days. Also, on a micro-scale AGS adds complexity compared to activated sludge flocs. SND is a process that occurs in AGS because aerobic and anoxic

conditions can co-exist within a large enough granule. The anoxic zones within a granule are a great benefit of AGS, because it decreases or totally removes the need for a separate denitrification phase. In a sense the aerobic and anoxic zones within a granule make an AGS reactor behave as if it were an aerated reactor and a denitrification reactor simultaneously.

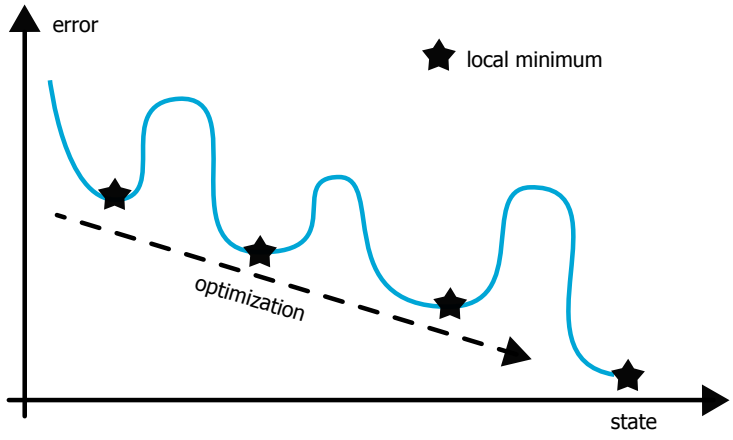

Figure 6.1: Optimization process in an AGS reactor.

So, we have different circumstances between granules (loading, SRT, selection) and different circumstances within granules (redox circumstances, loading). As a result, there can be multiple steady-states for an AGS reactor. We have shown in chapter 3 that multiple granule size distributions with the same amount of biomass can be stable under the same selection pressure. The same counts for biomass population distribution, conversion rates and in the end effluent quality. Baeten *et al.* showed in their research [1] that it takes hundreds of days to reach a steady state for the population within a granule. In this research (chapter 5) we showed it can take up to a year to get a stable granule size distribution. At the same time the age of the aggregates in an AGS reactor can range from a few days to several months [2] simultaneously. In my opinion this means we never reach a steady state in an AGS reactor, because the time to reach a steady state is (much) longer than the age of a large part of the granules. So, although from a process performance point of view the AGS process is generally very stable, we should always approach the AGS process as a system in a semi steady-state, with a mixed population, where granules are constantly growing and developing into larger particles.

When designing/researching/operating/modelling a AGS reactor, one must be aware of these semi steady-states, as illustrated in figure 6.1. This figure is an abstract representation of the optimization process of an AGS reactor. On the x-axis we have the *state* of the reactor and the y-axis represents the error regarding the performance of the reactor. One can see the latter as the *actual performance* minus the *desired performance*. Optimization can be seen as traversing towards the desired performance. Sometimes during the optimization process we need to move away from the desired state, to break out of the semi steady-state. For example,

lowering the selection pressure, decreasing the load, worsening the effluent quality can be necessary to come to a better performance of the reactor. It is important to be at least aware of this when making designs, deploying start-up strategies or troubleshooting a AGS reactor.

6.4. Mathematical models

We tend to use many models in design, operation and research of wastewater treatment plants (figure 6.2). Design models are generally less complex than models used for operation and models used in research can be very complex, with a clear example in chapter 5. Design models can be simple, because processes can be lumped into simple parameters, and some safety margins are added to the model to deal with the uncertainty caused by lumped parameters. Because of the batch-wise operation, some dynamics are generally added to AGS design models, adding complexity. There is always a trade-off when adding complexity to a model: more complexity means more effort to calibrate and validate the model.

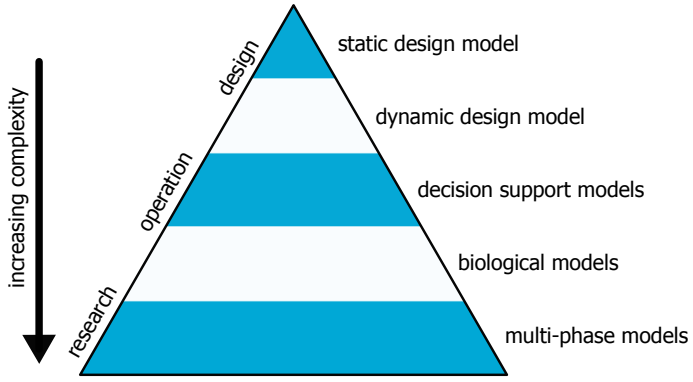

Figure 6.2: Modelling pyramid, showing different levels of modelling complexity with different applications.

In wastewater treatment there is a special role for the Activated Sludge Model (ASM). ASMs are widely used to model CAS systems, an also some attempts are made to model AGS systems with ASM type of models [3–6]. These models generally miss the essence of the AGS process, because they miss the complexity as described in the previous paragraph. They lump essential parameters, such as the GRTD, in average values, missing the dynamic behaviour of the AGS reactor. Somewhere in the near future an effort should be made to develop an ASM suited for AGS modelling. This could help greatly in the further development of the technology.

6.5. Alternative process control

Process control in the full-scale AGS process in essence is quite simple: in the feeding phase a batch of fresh influent is fed to the reactor, in the reaction phase

the reactor is aerated, until the COD, ammonium and phosphate requirements are met (possible combined with pre-denitrification, intermediate denitrification or post-denitrification), then the sludge bed is allowed to settle, and the selective wasting is done. On the other hand, process control can become difficult rapidly, when one realizes that the optimal oxygen concentration does not exist or at least depends on the granule size distribution. Larger granules need higher oxygen concentrations, to get the maximum reaction rates inside the granule. During aeration a concentration gradient exists inside the granule, and the oxygen concentration can drop to zero in large granules. Increasing the bulk oxygen concentration will increase conversion rates for oxygen dependent processes in the large granules. For the smaller granules and flocs this effect will be limited, because oxygen will completely penetrate the biofilm. Also, during the reaction phase the anoxic zone within an aerobic granule will shift inward while the COD on the outside of the granule is depleted (see figure 6.3). Small granules will reach a state of full oxygen penetration much faster than large granules. Large granules might remain partially anoxic throughout the whole reaction phase. As a result, a mature granular bed with mainly large granules will produce a better effluent quality regarding nitrate compared to a granular bed with only small granules. The process control needs to be adapted accordingly. Realizing these dynamic conditions in the granules during the reaction phase, it is a small step to a more adaptive process control, where the oxygen concentration is varied over the cycle. First steps to create such a process control have already been made [6, 7], but there is still a lot to gain.

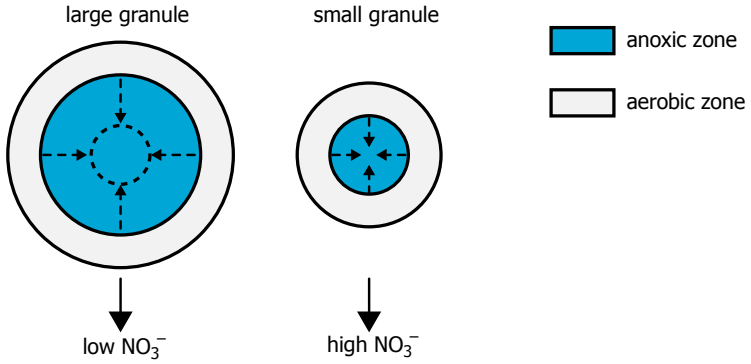

Figure 6.3: Effect granule size on denitrification.

Process control is mainly targeted at effluent requirements. The research on N_2O emissions described in chapter 4 showed that there are opportunities to minimize the N_2O emission from AGS reactors. There was a clear effect of the change of process control at the end of the measurement campaign at the wastewater treatment plant of Dinxperlo. We showed the dynamics of the N_2O emission during the cycle: periods of increasing production of N_2O were alternated by periods of reduction of N_2O by denitrification. Because N_2O concentrations can be measured in both the water phase and the off-gas, it should be possible to minimize N_2O emissions by controlling the dissolved oxygen concentration in the reactor and

adding denitrification phases when N_2O concentrations become too high. Such a process control could minimize the 'environmental' impact of the wastewater treatment plant. An optimum between *the best effluent quality* and *the least greenhouse gas emission* should be the focus. The latter would probably not be a trivial optimization, not only from a process control point of view, but even more from a regulatory perspective.

The N_2O trial in Dinxperlo also showed the potential for process control based on off-gas measurements. The current process control of Nereda® reactors relies on measurements in the water phase (ammonia, nitrate, phosphate, oxygen) for the installations with the most stringent effluent requirements. These sensors are expensive and need regular maintenance. In contrast, the off-gas unit we used in Dinxperlo did not need much maintenance, because it was measuring only the clean off-gas. The unit can be used to get respiration rates, biomass growth and other relevant parameters [3]. Possibly in combination with a simple sensor like a pH probe, this off-gas measurement could provide a whole new approach for process control of aerobic granular sludge.

In the wastewater treatment plant of Zutphen a new control strategy is developed. At this location the first Kaumera extraction is built, producing biopolymers from aerobic granular sludge. The AGS is grown on dairy wastewater, which is one of the streams treated at this wastewater treatment plant. Because the product here is biopolymers and not clean effluent (the Nereda® effluent is polished by the CAS system that treats the domestic wastewater from the municipality of Zutphen), totally different goals arise for the process control. It is much more about amount and quality of biopolymers produced and about the stability of the sludge production. In the case of Zutphen, these goals are relatively clear, because the sole purpose of the plant is to produce biopolymers. For future AGS plants, this goal could, similar to minimization of the greenhouse gas emission, be a secondary goal of the process control: to produce good effluent quality, but also to deliver the optimal properties of biopolymers.

6.6. Continuous aerobic granular sludge

The current full-scale application of AGS is based on a batch system. During my PhD research I have been closely involved in the PhD research of Viktor Haaksman, who is one of researchers looking for a continuously fed application of AGS. It seems it is not a question *if* continuous AGS system will be developed but more the question *when* this technology will arrive. There appear to be some benefits to continuously fed AGS systems, the largest one maybe being the fact that retrofitting existing CAS systems into the AGS process could be a straightforward method for increasing the treatment capacity, without many investments. These benefits might in many cases outweigh the downsides of a continuously fed system - for example loss of concentration gradients, loss of flexibility in the process control. The mechanisms for aerobic granulation (chapter 5) are closely related to the batch system in which the AGS process was originally developed. In a continuously fed system, the presence of these mechanisms is not per se evident, and I believe it will always remain more difficult to grow aerobic granules in a continuously fed system,

compared to a batch system.

6.7. Process knowledge versus big data techniques

In a batch system much more process information is generated than in a continuous flow through process. In CAS systems the sensors measure (more or less) a constant value because process conditions are kept constant over time. In a batch system all cycle measurements are done under varying process conditions. As a result, in a batch system for every reactor a vast amount of data is generated. This data can be put to good use. We could, for example, use artificial intelligence techniques to predict process failure or to minimize energy usage. The possibilities seem endless. But also from a more 'old school' perspective, a batch system gives a lot of process information. Every cycle gives nitrification and denitrification rates, phosphorus release and uptake rates, endogenous respiration and so on. On a daily basis, process engineers and operators can monitor these rates and act upon them. Based on knowledge rules, we can provide early warnings about the process performance. But the many degrees of freedom in the system - as discussed earlier, size distribution and GRTD make the process more complex - and the abundance of process information ask for machine learning techniques and other artificial intelligence applications.

This all starts with the collection of valid measurements. Data collection sometimes struggles with common issues familiar to anybody working in wastewater, like rags, fouling and lack of maintenance. These all influence the validity of the measurements. We can setup fancy process control or give early warnings based on historical and current process behaviour, but if measurements are incorrect, it will malfunction. Data validation and reconciliation techniques could help greatly with this. There is some redundancy in the system: different reactors under the same process conditions should mimic each other, allowing for comparison of sensors. Redox sensors should make sense if we compare with oxygen and nitrate, and vice versa. Nitrate production cannot be (much) higher than ammonia concentrations and so forth. Using modern data validation and reconciliation techniques could improve process reliability.

6.8. Microbial control

Understanding the mechanisms for aerobic granulation gives us new possibilities. These mechanisms, especially the mechanisms of selective feeding and selective wasting, give us some control on the microbial populations which grow in the AGS system. Over the past few years, we learned that different microbial communities exist in different granule sizes. Analysis of the metagenome and, more recently, of the proteome provide insights in the behaviour of different species resulting from the GRTD. We could use this knowledge to reverse the process: influence the GRTD to get the microbial communities we prefer. For example, we could favour PAO over GAO to improve phosphorus removal. We could enrich for nitrifiers to increase nitrification rates. But we could also try to influence the desired product characteristics of the Kaumera produced from the AGS waste sludge. Soon online

measurement of the metagenome will bring us a new tool to directly monitor and influence the microbial communities. This will bring new opportunities to minimize the footprint of our wastewater treatment plants, to enhance the effluent quality and to generate new products from the waste AGS.

6.9. Not the end

The future of the aerobic granular sludge process is bright. When compared with CAS systems, with AGS one can save both on investment costs (decrease of total reactor volume) and operational costs (less energy consumption and less chemical usage). On top of this, recovery of potentially high-end biopolymers, but also recovery of for example phosphorus make the technology well suited for the current day demands of modern wastewater treatment. There are still so many opportunities to increase the treatment capacity of the AGS process, so many discoveries to be made: the journey only just started, and we will see where we go from here.

Bibliography

[1] J. E. Baeten, M. C. M. van Loosdrecht, and E. I. P. Volcke, *Modelling aerobic granular sludge reactors through apparent half-saturation coefficients,* Water Res. **146**, 134 (2018).

[2] M. Ali, Z. Wang, K. W. Salam, A. R. Hari, M. Pronk, M. C. M. van Loosdrecht, and P. E. Saikaly, *Importance of species sorting and immigration on the bacterial assembly of different-sized aggregates in a full-scale Aerobic granular sludge plant,* Environ. Sci. Technol. **53**, 8291 (2019).

[3] J. E. Baeten, E. J. H. van Dijk, M. Pronk, M. C. M. van Loosdrecht, and E. I. P. Volcke, *Potential of off-gas analyses for sequentially operated reactors demonstrated on full-scale aerobic granular sludge technology,* Sci. Total Environ. **787**, 147651 (2021).

[4] P. Dold, B. Alexander, G. Burger, M. Fairlamb, D. Conidi, C. Bye, and W. Du, *Modeling full-scale granular sludge sequencing tank performance,* in *91st Annu. Water Environ. Fed. Tech. Exhib. Conf. WEFTEC 2018* (2019) pp. 3813–3826.

[5] M. K. de Kreuk, C. Picioreanu, M. Hosseini, J. B. Xavier, and M. C. M. van Loosdrecht, *Kinetic model of a granular sludge SBR: Influences on nutrient removal,* Biotechnol. Bioeng. **97**, 801 (2007).

[6] M. Layer, M. G. Villodres, A. Hernandez, E. Reynaert, E. Morgenroth, and N. Derlon, *Limited simultaneous nitrification-denitrification (SND) in aerobic granular sludge systems treating municipal wastewater: Mechanisms and practical implications,* Water Res. X **7**, 100048 (2020).

[7] E. J. H. van Dijk, K. M. van Schagen, and A. T. Oosterhoff, *Controlled Simultaneous Nitrification and Denitrification in Wastewater Treatment,* (2020).

Epilogue

Somewhere during my PhD research I learned that there is a special Dutch word for what I was doing: *buitenpromoveren*. It means you are doing a part-time PhD research while having a (busy) job outside the university. The fact that there is a special word for it, must mean it is different from a normal PhD research, right? The majority of the PhD students nowadays starts shortly after obtaining their master's degree. When I started, I already had 20 years of experience as a consultant. That made me very different from the other PhD candidates. To start with, I was less interested in drinking beers in the evening. Furthermore, my experience made me more efficient in planning my research and writing my papers. On the other hand, I had much less time available to ponder about what I was doing in Delft. My experience made me also less open minded than the regular PhD candidates, who still approach everything with the (naive) enthusiasm of the youngsters. So, which one is better, or... is there no difference after all?

In my opinion there is no difference. Doing your PhD research gives you the unique possibility to work on innovation, and to follow your instincts. For me the most valuable part of my PhD research was working with similar minds, in a knowledge driven organisation. Having the discussions with my room mates, hours spent in the coffee corner, while debating topics I did not even know existed. In the end it is all about the journey, to grow as a person, exploring the unknown. And that makes it all very much worthwhile.

Acknowledgements

This PhD research would not have happened without the help of many people, but by far the most important for me was *Mario Pronk*. Friend, colleague, co-promotor, Mario mixed all these roles in a mixture of inspirational debates and discussions. We spent hours and hours discussing the observations in our research (or what is better, road cycling or mountain biking). When we first met in 2014, I presented a model, which now can be seen as the first prototype of the granulation model from chapter 5. Afterwards Mario came to me, a little bit surprised, saying he thought these types of models were only made at the university. From then on, we had a mutual understanding - as similar minds. Together we have set up the R&D for Nereda® at Royal HaskoningDHV and it was Mario in the end convincing me to start with my PhD research. Many, many, many thanks for all of this.

I learned that intuition is important in scientific research. Most research starts with a feeling that something might be interesting. I think *Mark van Loosdrecht* combines a well-developed intuition with a broad experience in the field, which makes Mark a unique person. There is a bit of a rebel in Mark, ignoring authority and decorum, always going the route he thinks is best. I recognize that 'stubbornness' in myself and that made we had a good mutual understanding from the start. From every meeting I had with Mark there was a takeaway, and I really learned a lot from working with Mark. I am very grateful to have had Mark as a promotor.

There is one person, that has been very important to this research, although he did not contribute anything to the research itself. *Helle van de Roest* was awakening the interest in science in me, in the years before I started my PhD research. I worked closely together with Helle, and he constantly challenged me to deeper understand the Nereda® process and to avoid 'superficial knowledge'. Although Helle retired in the year I started my PhD research, his legacy echoed into it constantly. So, Helle, many thanks for the all the valuable lessons.

My PhD research was a unique opportunity for me, with great support from RHDHV. It was the 'Nereda director' *René Noppeney*, who initiated the whole thing and supported me along the way. During the 5 years of this research, I had two bosses at RHDHV, *Hugo van Gool* and *João Tiago de Almeida*. Both were 100 % supportive and helped me through the more difficult episodes of this research. Thank you both for your support and dedication to my journey.

There are more (former) colleagues at RHDHV that were important for me in this research, especially the colleagues in the R&D team. In de first years, *Tim van Erp* was my go-to, when I needed something built for my research at the PNU. With his practical skills he could make anything happen. *Valerie Sels* already contributed during her bachelor thesis to this research, looking at the bulk settling behaviour of AGS. After this thesis, Valerie kept connected to AGS research and after her graduation she became a valuable colleague. Especially

her contribution to the research on the settling properties of AGS (chapter 3) was invaluable. *Pascalle Vermeulen* started with an internship, looking at granulation in the PNU. We recognized talent and after her graduation she became our colleague in the R&D team, helping us greatly in all the ongoing research projects. The internal review of my four papers was done by *Andreas Giesen*. He helped greatly by spending many hours reviewing and correcting my papers.

Our research facility in Utrecht, the PNU played an important role in this PhD research. Two operators, *Jan Cloo* and *Mark Stevens* from HDSR supported us with the daily operations. Already in 2014 it was Mark, doing the official sampling of the PNU, noticing that elevated levels of effluent suspended solids were going to be a problem for AGS technology, thus triggering the research presented in chapter 2, helping to overcome this problem. The level of dedication of Jan and Mark was unique and very much appreciated. Several other people for Dutch district water authorities helped me along the way: by sampling, helping with experiments, discussion and in many other ways. Special thanks go to *Erik Rekswinkel*, *Philip Schyns*, *Henri Scheurs* and *Meinard Eekhof*.

One of the greatest benefits of my PhD research was being on the university, discussing with knowledge driven people. I especially enjoyed the discussions with my room mates: *Viktor Haaksman*, *Jure Zlopasa* and *Morez Jafari*. Many afternoons were filled with drawing on the whiteboard, having fierce discussions. I learned that having an open mindset is the only thing you need to have a fruitful discussion on any topic. The three of you really helped me to feel part of the team at the university.

Over the years I supervised many students, contributing in some way to this PhD research. Some these students later became my colleagues at RHDHV. Special thanks go to *Struan Robertson*, *Jimmy van Opijnen*, *Suellen Espindola*, *Eline van der Knaap*, *Pieter Brorens*, *Jelle Langedijk*, *Isabelle Schroeten*, *Amanda Vierwind* and *Lindsey Carver*. Working with students helped me to focus on specific research topics, forcing me to take a break from the daily routine at the office.

Finally, I want to thank my family, Ankie, Julius and Maurits. You always fully supported this journey I started, and especially in the more difficult moments you helped me in so many ways. We celebrated together when a new paper was published, but there was also the sometimes-necessary distraction to get my mind of my work. We made this journey together and I could not have done it without you!

Thank you all!

Curriculum Vitæ

Edward van Dijk

7 Oct 1976	Born in Amersfoort, the Netherlands

Education

1980–1988	OBS De Hoeve, Hoevelaken
1988–1994	Gymnasium at Eemland College, Amersfoort
1994–1999	Milieuhygiëne (cum laude) Landbouwuniversiteit Wageningen
2017-2022	PhD Technische Universiteit Delft *Thesis:* Principles of the full-scale aerobic granular sludge process *Promotor:* prof. dr. ir. M.C.M. van Loosdrecht

Employment

1999–present	Royal HaskoningDHV Engineer/project leader in Hydraulics department (1999–2013) Process engineer in Wastewater department (2013–2020) Senior researcher in Nereda® R&D department (2015–present)
2013-2020	Teacher at Stichting Wateropleidingen

List of Publications

1. **E. J .H. van Dijk**, M. Pronk, and M. C. M. van Loosdrecht, *Controlling effluent suspended solids in the aerobic granular sludge process*, Water Res. **147**, 50 (2018).

2. **E. J. H. van Dijk**, M. Pronk, and M. C. M. van Loosdrecht, *A settling model for full-scale aerobic granular sludge*, Water Res. **186**, 116135 (2020).

3. **E. J. H. van Dijk**, M. C. M. van Loosdrecht, and M. Pronk, *Nitrous oxide emission from fullscale municipal aerobic granular sludge*, Water Res. **198**, 117159 (2021).

4. **E. J. H. van Dijk**, V. A. Haaksman, M. C. M van Loosdrecht, and M. Pronk, *On the mechanisms for aerobic granulation model based evaluation*, Water Res. **216**,118365 (2022).

5. M. Pronk, **E. J. H. van Dijk**, and M. C. M. van Loosdrecht, *Aerobic granular sludge*, in Biol. Wastewater Treat. Princ. Model. Des., edited by G. Chen, G.A. Ekama, M. C. M. van Loosdrecht, and D. Brdjanovic (IWA Publishing, 2020) Chap. 11, pp. 497-516.

6. D. R. de Graaff, **E. J. H. van Dijk**, M. C. M. van Loosdrecht, and M. Pronk, *Strength characterization of fullscale aerobic granular sludge*, Environ. Technol. **41**, 1637 (2020).

7. J. E. Baeten, **E. J. H. van Dijk**, M. Pronk, M. C. M. van Loosdrecht, and E. I. Volcke, *Potential of offgas analyses for sequentially operated reactors demonstrated on fullscale aerobic granular sludge technology*, Sci. Total Environ. **787**, 147651 (2021).

Nomenclature

Symbols

A	area (m^2)
a	interfacial area of bubbles/granules (m^{-1})
Ar	Archimedes number (-)
c	concentration ($kg\,m^{-3}$)
C_D	drag coefficient (-)
D	diffusion or dispersion coefficient (m^2/s)
d	diameter (m)
EF	emission factor (-)
F	fouling factor (-)
f	fraction (-)
G	number of granules in a cluster (-)
g	gravitational acceleration ($m\,s^{-2}$)
H	height of the reactor (m)
K	monod constant ($kg\,m^{-3}$)
M	molar mass ($g\,mol^{-1}$)
m	mass (kg)
N	number of clusters in a set a set (-)
n	expansion index (-)
P	breaking chance of granule clusters (-)
p	pressure (Pa)
q	biomass specific substrate uptake rate ($kg\,kg^{-1}\,s^{-1}$)
R	volumetric reaction rate ($kg\,m^{-3}\,s^{-1}$)
r	radial position (m)

Re	Reynolds number (-)
T	temperature (K)
t	time (s)
V	volume (m^3)
v	velocity ($m\,s^{-1}$)
x	position from the bottom of the reactor (m)
Y	yield coefficient ($kg\,kg^{-1}$)

Greek symbols

α	MTR correction factor (-)
ϵ	voidage fraction (-)
μ	dynamic viscosity of water ($kg\,m^{-1}\,s^{-1}$)
ν	kinematic viscosity of bulk-liquid ($m^2\,s^{-1}$)
ρ	density ($kg\,m^{-3}$)
θ	volumetric concentration (-)

Subscripts

0	start or reference value
AN	anaerobic
ax	axial direction
B	biofilm phase
d	deficit
e	effluent
G	gas phase
GFS	granule forming substrate
i	index of set of biomass clusters
in	influent
j	index of biomass cluster or class
L	bulk-liquid phase
N	nitrogen

O oxygen

PHA polyhydroxyalkanoates

R reactor

s solubility

t fluidizing (velocity)

t terminal (velocity)

TN total nitrogen

X biomass

Constants

k correction factor for wall effects (-)

k_{HC} Henry correction factor (K)

k_H Henry coefficient ($mol\,m^{-3}\,Pa^{-1}$)

k_{LB} mass transfer coefficient for bulk-liquid/biofilm interface ($m\,s^{-1}$)

Acronyms

AGS Aerobic Granular Sludge.

ASM Activated Sludge Model.

CAS Conventional Activated Sludge.

DWF Dry Weather Flow.

EBPR Enhanced Biological Phosphorus Removal.

EF Emission Factor.

GAO Glycogen Accumulating Organisms.

GFS Granule Forming Substrate.

GRTD Granule Residence Time Distribution.

HDSR Hoogheemraadschap de Stichtse Rijnlanden.

MLSS Mixed Liquor Suspended Solids.

mUCT modified University of Capetown process.

n-GFS non-Granule Forming Substrate.

PAO Phosphorus Accumulating Organisms.

PBM Population Balance Model.

PNU Prototype Nereda Utrecht.

RHDHV Royal HaskoningDHV.

RWF Rainy Weather Flow.

SBR Sequencing Batch Reactor.

SND Simultaneous Nitrification and Denitrification.

UASB Upflow Anaerobic Sludge Blanket reactor.

VER Volumetric Exchange Ratio.

VFA Volatile Fatty Acids.

A

Full-scale settling experiment

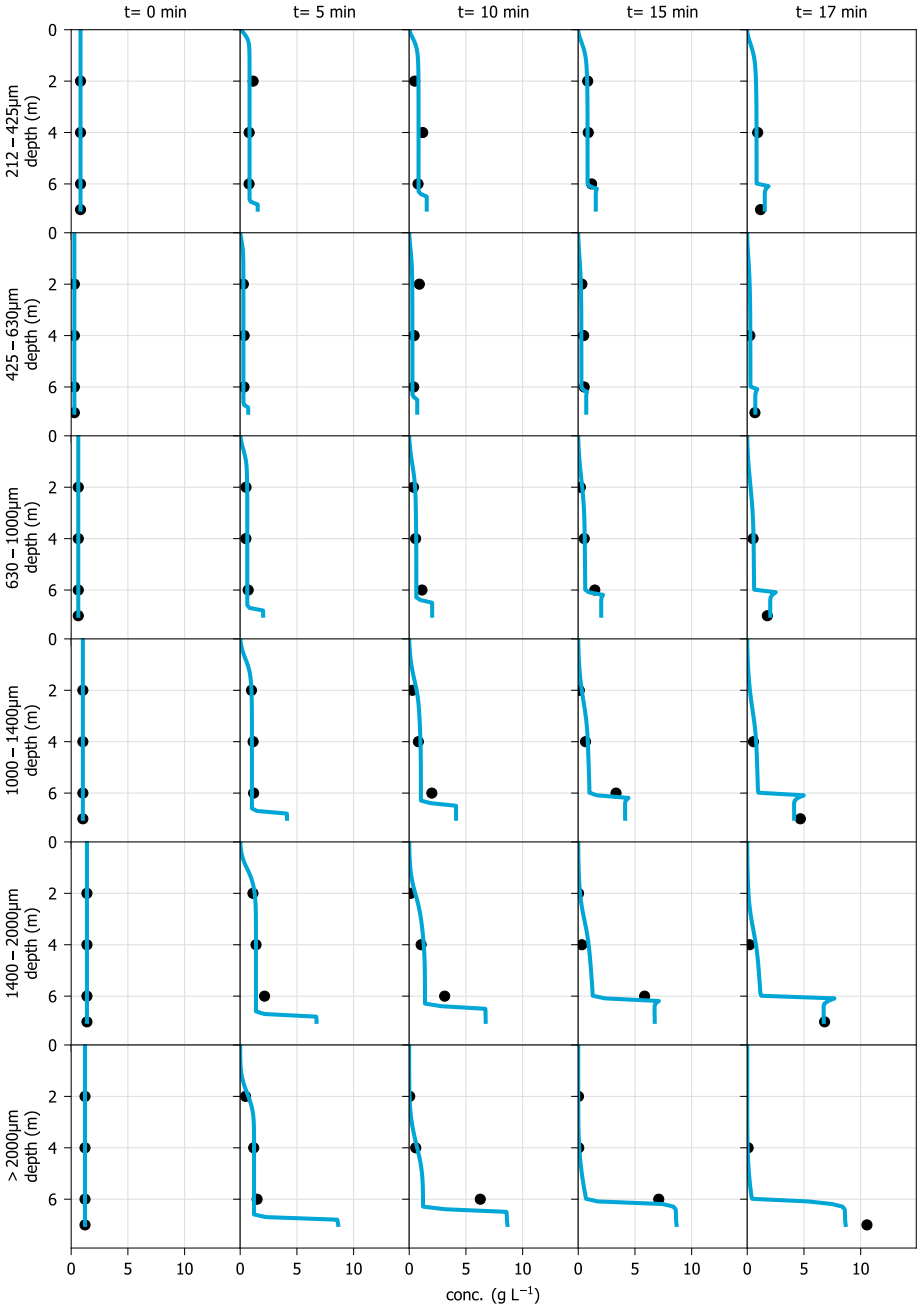

Figure A.1: Settling of granules in a full-scale Nereda® reactor in Utrecht; model results (line) and measurements (dots) at settling times between 0 min and 17 min.

B

Segregation of sludge bed

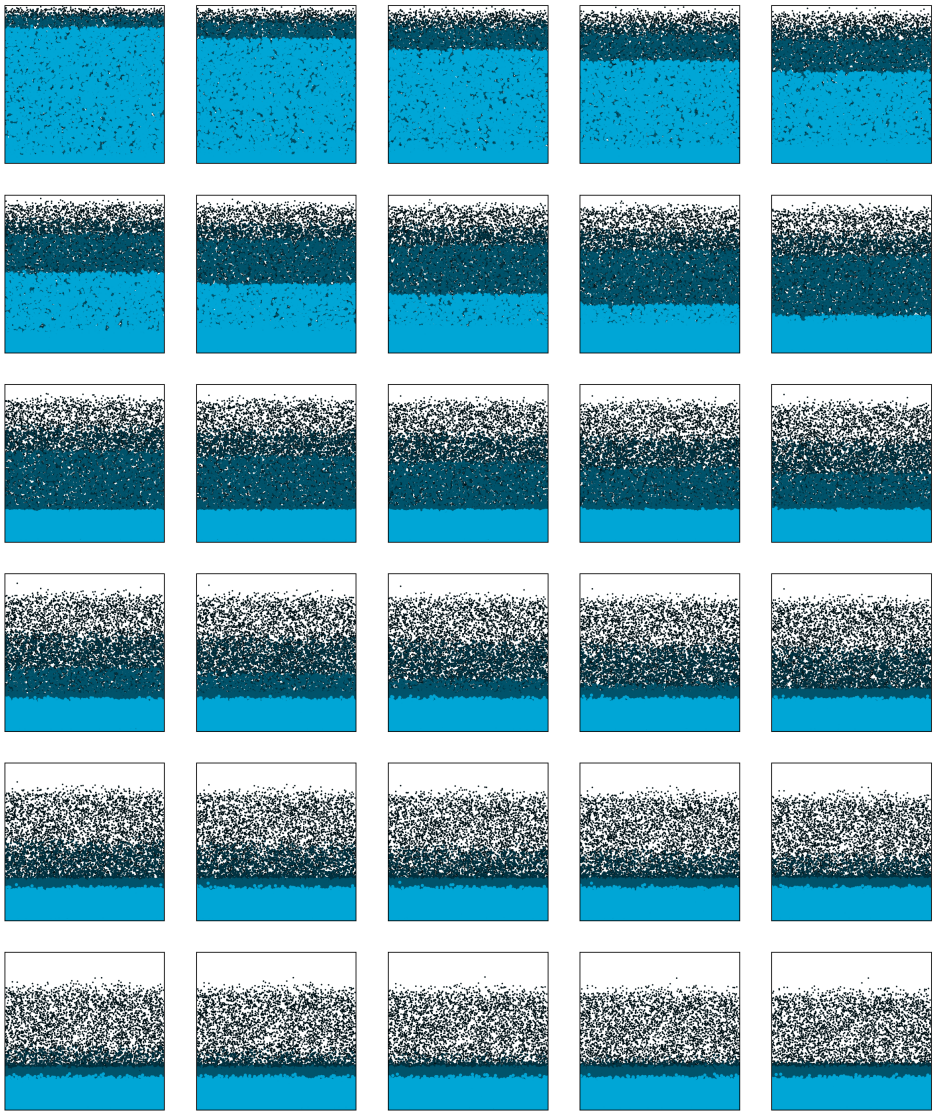

Figure B.1: Settling of granules in the population model of chapter 5 in a reactor of 6 m water depth. Sludge bed consisting of granules of 200 µm, 600 µm, 1000 µm and 2000 µm each of a biomass concentration of 2 kg m^{-3}. Output 30 minutes with 1 frame per minute. The largest granules are already stacked on top of each other on the bottom of the reactor after a few minutes, while the smallest fraction is still settling after 30 minutes.